DEVELOPMENT OF BACTERIOPHAGE NANOPARTICLES FOR GLYCOMICS ANALYSIS BY GENETIC ENGINEERING

GLİKOMİKS ANALİZİNE YÖNELİK BAKTERİYOFAJ NANOPARTİKÜLLERİNİN GENETİK MÜHENDİSLİĞİ İLE GELİŞTİRİLMESİ

GÖKSU GÜR

ASST.PROF. DR. EDA ÇELİK AKDUR
Supervisor

Submitted to Institute of Sciences of Hacettepe University
as a Partial Fulfillment to the Requirements
for the Award of the Master's Degree
in Bioengineering

2014

This work named **"Development of Bacteriophage Nanoparticles for Glycomics Analysis by Genetic Engineering"** by **Göksu Gür** has been approved as a thesis of Degree of **MASTER OF PHILOSOPHY IN BIOENGINEERING** by the below mentioned Examining Committee Members.

Prof. Dr. Erhan Bişkin
Head : .....

Asst. Prof. Dr. Eda Çelik Akdur
Supervisor : .....

Prof. Dr. Mehmet Mutlu
Member : .....

Assoc. Prof. Dr. Halil M. Aydın
Member : .....

Assoc. Prof. Dr. Çağdaş Son
Member : .....

This thesis has been approved as a thesis for the Degree of **MASTER OF PHILOSOPHY IN BIOENGINEERING** by board of Directors of Institute for Graduate Studies in Science and Engineering.

Prof. Dr. Fatma SEVİN DÜZ

Graduate School of Science
and Engineering

To my family…

ETHICS

In this thesis study, prepared in accordance with the spelling rules of Institute of Graduate Studies in Science of Hacettepe University,

I declare that

- all the information and documents have been obtained in the base of the academic rules
- all audio-visual and written information and results have been presented according to the rules of scientific ethics
- in case of using others works, related studies have been cited in accordance with scientific standards
- all cited studies have been fully referenced
- I did not do any distortion in the data set
- and any part of this thesis has not been presented as another thesis study at this or any other university.

24/12/2014

Göksu Gür

ABSTRACT

DEVELOPMENT OF BACTERIOPHAGE NANOPARTICLES FOR GLYCOMICS ANALYSIS BY GENETIC ENGINEERING

Göksu Gür

Master of Philosophy, Department of Bioengineering

Supervisor: Asst. Prof. Dr. Eda ÇELİK AKDUR

December 2014, 84 Pages

Complex carbohydrates (glycans) are attached to proteins and lipids by the process of glycosylation and play important roles in many biological processes. Altered glycosylation is known to cause diseases including cancer and retroviral infection. Carbohydratebased arrays, or “glycoarrays,” have emerged in the last decade as a powerful tool in glycomics, especially in glycosylation-based diagnosis of diseases; however, to fully exploit the potential of glycans arrays, it is necessary to increase the diversity of glycans and to develop reliable and reproducible chemistries for immobilization of the carbohydrate probes onto solid support. Recently, the protein glycosylation locus (Pgl) discovered in *Campylobacter jejuni* was functionally transferred to *Escherichia coli*, conferring ability to glycosylate proteins. Additionally, our research group has recently demonstrated for the first time, *N*-glycosylation of phage particles (glycophages), simply by infecting the glycosylation competent *E. coli* with M13 phage displaying a glycan-acceptor protein. Considering that phage-patterned microarrays are a standard art in proteomics, the hypothesis of this study is that the glycophage particles can be exploited for the development of “glycophage arrays”, to be used in pathogen or cancer diagnosis in the future.

In this study, host cell engineering and six new bicistronic phagemids construction and design were planned (pBAD-MBP^{DQNAT}-g3p::PglB, pBAD-MBP^{DQNAT}-g3p::PglB$_{mut,}$ pBAD-MBP^{4xAQNAT}-g3p::PglB, pBAD-MBP^{4xDQNAT}-g3p::PglB$_{mut}$, pBAD-MBP^{4xDQNAT}-g3p$_{tr}$::PglB, pBAD-MBP^{4xDQNAT}-g3p$_{tr}$::PglB$_{mut}$), and the designed phagemids were constructed using standard genetic engineering techniques. The sequence of the constructed phagemids were confirmed with restriction digestion and DNA sequencing analysis. Next, because glycosylation potential of phage particles are increased if the waaL gene is deleted from *E. coli* TG1 host cell, the deletion of waaL gene was verified with flourescence-activated cell sorting (FACS) analysis. Thereafter, in order to increase the glycophage production efficiency and stability of phagemids, different parameters were tested; and (i) the truncated-g3p in the phagemid enabled better display of glycans on the phage compared to full-length g3p, (ii) different purification conditions were tested to get spesific signals and the higher anti-glycan signal was obtained from sarkosyl treated samples, (iii) effect of induction conditions on cell growth and phage production capacity were compared with nine different parameters and best results were detected in the case where, OD_{600}=0.6 at the time of infection, 8x10^9 CFU/mL of helper phage is used for infection and induction period is 16 h. Finally, “glycophage-ELISA” method was developed for the first time, as a new tool in glycomics analysis. Indirect ELISA method was choosen as the suitable ELISA type; and %2 BSA-PBS (bovine serum albumine) buffer gave a more specific anti-glycan signal compared to other blocking buffers tested.

The study is significant because it has overcome the current bottlenecks in glycan array construction and provide a relatively inexpensive, specific and stable glycan representation method, as well as introduce a simplified and universal purification technique that is not dependent on the carbohydrate. With the development of new glycosylation pathway encoding plasmids, the variety of glycophages can be extended in the future. The basis of glycophage array technology described here should help to expand the diversity of glycan libraries and provide a complement to the existing toolkit for high-throughput analysis of glycan–protein interactions.

Key Words: Genetic Engineering, Microarrays, Glycomics, GlycoPhage Display

ÖZET

GLİKOMİKS ANALİZİNE YÖNELİK BAKTERİYOFAJ NANOPARTİKÜLLERİNİN GENETİK MÜHENDİSLİĞİ İLE GELİŞTİRİLMESİ

Göksu Gür
Yüksek Lisans Biyomühendislik Bölümü
Tez Danışmanı: Yrd. Doç. Dr. Eda ÇELİK AKDUR
Aralık 2014, 84 sayfa

Kompleks karbonhidratlar (glikanlar) glikozilasyon prosesi sonucunda lipid ve proteinlere bağlanırlar ve hücre-hücre tanıması, metabolik alışveriş, patojen-konakçı ilişkisi de dahil olmak üzere birçok biyolojik süreçte önemli roller oynarlar. Değişim geçiren glikozilasyonun, kanser ve retroviral enfeksiyonlar gibi hastalıkların nedeni olduğu bilinmektedir. Karbonhidrat tabanlı dizinler (arrays), ya da "glikodizinler," glikomiks çalışmalarında güçlü bir araç olarak son on yılda ortaya çıkmıştır. Ancak bu dizinlerin potansiyelini arttırmak için, glikanların çeşitliliğini arttırmak ve katı destek üzerine karbonhidrat problarının immobilizasyonunu güvenilir ve tekrarlanabilir olacak şekilde geliştirmek gerekli olacaktır. Yakın zamanda, *Campylobacter jejuni* bakterisinde keşfedilen protein glikozilasyon gen bölgesi (Pgl), *Escherichia coli* bakterisine aktarılarak, bu bakteriye proteinleri glikozilleme yeteneği kazandırmıştır. Ayrıca, araştırma grubumuz, glikozilasyon genini taşıyan *E. coli*'yi enfekte eden, ve bir "alıcı proteini" taşıyan M13 bakteriyofaj parçacıklarının N-glikozillenebildiğini göstermiştir. Faj desenli mikrodizinlerin proteomik çalışmalarında artık kabul görmüş bir metod olduğu göz önüne alındığında, gelecekte GlikoFaj parçacıklarının mikrodizin kütüphanelerine eklenerek patojenlerin ve kanser teşhisinde kullanılması mümkün olacaktır.

Bu çalışmada, konak hücre mühendisliği ve altı yeni bisistronik fajmid tasarımı ve üretimi planlanmış (pBAD-MBP^{DQNAT}-g3p::PglB, pBAD-MBP^{DQNAT}-g3p::PglB$_{mut,}$

pBAD-MBP^{4xAQNAT}-g3p::PglB, pBAD-MBP^{4xDQNAT}-g3p::PglB$_{mut}$, pBAD-MBP^{4xDQNAT}-g3p$_{tr}$::PglB, pBAD-MBP^{4xDQNAT}-g3p$_{tr}$::PglB$_{mut}$) ve tasarlanan fajmidlerin üretimi standart genetik mühendisliği teknikleri ile gerçekleştirilmiştir. Üretilen fajmidlerin restriksiyon enzimleri ile kesildikten sonra jel elektroforezinde boyut kontrolü ve ayrıca DNA dizin analizi ile doğrulaması yapılmıştır. Hücre içi glikan havuzunun arttırılarak faj parçacıklarının glikozillenme potensiyelinin arttırılması için, *E. coli* TG1 konak hücresinde bulunan waaL geninin silinmesi flüoresan aktif hücre ayırma (FACS) analizi ile doğrulanmıştır. Ardından glikofaj üretim kapasitesi ve faj stabilitesini arttırabilmek için farklı parametreler test edilmiş; (i) fajmidde kodlanan kısaltılmış-g3p, normal-g3p ile kıyaslandığında, glikanların faj üzerindeki gösteriminin daha etkin ve stabil olduğu saptanmış; (ii) daha spesifik sinyaller alabilmek için farklı saflaştırma koşulları araştırılarak, sarkosyl ile muamele edilen örneklerden daha yüksek anti-glikan sinyali alındığı görülmüş; (iii) indükleme koşullarının hücre çoğalması ve faj üretimindeki etkisini kıyaslamak için dokuz farklı parametre sınanmış; OD_{600}=0.6 hücre derişiminde, 8x10^9 cfu/mL hacminde yardımcı faj ile enfekte edilen hücrelerden ve 16 saatlik indükleme sonrasında en yüksek glikofaj derişimi elde edilmiştir. Son olarak glikomik analizlemede yeni bir yöntem olan “glikofaj-ELISA metodu” ilk kez geliştirilmiştir. Dolaylı-ELISA metodu en uygun ELISA çeşidi seçilmiş; sınanan farklı bloklama tamponlarından %2 BSA-PBS (bovin serum albümin) tamponu ile anti-glikan antikoru ile daha spesifik bir sinyal elde edilmiştir.

Bu çalışma, karbonhidrat temelli olmayan, basitleştirilmiş ve evrensel bir glikan saflaştırma tekniği sunması; nispeten daha ekonomik ve kararlı bir glikan temsil metodu olması sebepleriyle önem taşımaktadır. Farklı glikozilasyon yolaklarını kodlayan yeni plazmidlerin geliştirilmesiyle, glikofajların çeşitliliği gelecekte arttırılabilir. Sonuç olarak, bu çalışmada tanımlanan “glikofaj dizin teknolojisi”, glikan kütüphanelerinin genişletilmesine fayda sağlayacağı gibi, glikan-protein etkileşimlerinin yüksek-verimli analizinde kullanılan ekipmanların geliştirilmesinde tamamlayıcı bir özellik gösterecektir.

Anahtar Kelimeler: Genetik Mühendisliği, Mikrodizinler, Glikomiks, Gliko-Faj Gösterimi

ACKNOWLEDGMENTS

I would like to thank first and foremost my thesis advisor, Asst. Prof. Dr. Eda Çelik-Akdur, for her support and guidance throughout this research. I am grateful for freedom she has given in the lab and her launching me on the path to becoming an independent researcher and for taking me with her to Cornell University for three months summer research.

I would like to thank members of thesis examining committee; Prof. Dr. Erhan Bişkin, Prof. Dr. Mehmet Mutlu, Assoc. Prof. Dr. Halil M. Aydın and Assoc. Prof. Dr. Çağdaş Son, for their time, invaluable suggestions and comments which make the final version of the thesis better.

I am really indebted to current labmates; Zehra Tatlı, İlkay Koçer for sharing their knowledge and motivating. Being with them was great pleasure to me.

I would like to acknowledge, scholarship from FP7 (FP7-PEOPLE-2012-CIG-322096) and Hacettepe University Research Funds (Project No: 014 D01 602 006).

I would like to thank Prof. Dr. Matthew P. Delisa at Cornell University and his research group; for all their help during initial phase of this project where I spent three monhts.

I would like to thank Prof. Dr. Pınar Çalık from Middle East Technical University and her research group members especially Özge Ata for letting me use their gel documentation system and Prof. Dr. Emir Baki Denktaş Lab. from Hacettepe University for letting me use their Nanodrop.

I wish to express my deep appreciation to my dearest friends Gizem Geçmez, Başak Tatar, Kübra Ünal, Elmas Soyak.

I am sure that I cannot find any appropriate words to express my gratitude to my parents Ali Murat and Gülay Gür and Batuhan Gökçe for their never ending support and caring even as I followed my ambitions. They are always with me only to encourage, cheer up and love. When I have to cope with any difficulties, talking to them and even thinking of them are enough for me. I hope I make them proud at the end.

TABLE OF CONTENTS

Page

ABSTRACT i
ÖZET ..... İİİ
ACKNOWLEDGMENTS V
LIST OF TABLES ..... İX
LIST OF FIGURES x
LIST OF ABBREVIATIONS AND SYMBOLS xii
1. INTRODUCTION 1
2. LITERATURE SURVEY 4
2.1. Glycans and Glycosylation of Proteins 4
2.1.1. O-antigen 6
2.2. Glycomics 8
2.2.1. Carbohydrate (Glycan) Arrays 8
2.3. Bacteriophages and Phage Display Technology 12
2.3.1. Phage Biology 12
2.3.2. Phage Display Technology 19
2.3.3. GlycoPhage Display 21
2.3.4. Bacteriophages in Biosensor and Microarray Technologies 22
3. MATERIALS AND METHODS 24
3.1. Buffers and Stock Solutıons 24
3.2. Strains, Plasmids and Maintenance of Microorganisms 24
3.3. Genetic Engıneering Techniques 24
3.3.1. Plasmid DNA Isolation from *E. coli* 24
3.3.2. Agarose Gel Electrophoresis 27
3.3.3. DNA Extraction from Agarose Gels 27
3.3.4. Primer Design 27
3.3.5. Polymerase Chain Reaction (PCR) 28
3.3.5.1. DNA Purification After PCR 29
3.3.6. Digestion of DNA Using Restriction Endonucleases 29
3.3.6.1. DNA Purification after Digestion 29
3.3.7. Ligation 30
3.3.8. Transformation of *E. coli* 30

3.3.9. DNA Sequencing 30
3.4. Production of Phages and Phage Purification 31
3.4.1. Production of Helper Phage 31
3.4.2. Production of Phages Displaying Glycans (GlycoPhage) 31
3.4.3. Phage Purification 32
3.5. Analyses 32
3.5.1. Cell Concentration 32
3.5.2. Total Protein Concentration 32
3.5.3. Phage Concentration 32
3.5.4. SDS-Polyacrylamide Gel Electrophoresis (SDS-PAGE) 33
3.5.5. Western Blotting 33
3.5.6. Phage ELISA 33
4. RESULTS AND DISCUSSION 35
4.1. Design of Phagemids 35
4.1.1 Propagation and Purification of the Backbone for pBAD24 Based New Phagemids 35
4.1.2. PCR Amplification of Gene Cassettes 35
4.1.3 Digestion and Ligation Reactions 38
4.1.4. Transformation of *E. coli* 41
4.1.5. Restriction Digestion and DNA Sequencing to Select the True Transformants 41
4.2. Host Cell Engineering 43
4.3. Production of Helper Phage and Glycophage Nanoparticles 43
4.3.1. Effect of the Size of G3p on Glycophage Production 43
4.3.2 Purification of Glycophage Samples 45
4.3.3. Effect of Induction Conditions on Cell Growth and Phage Production Capacity 46
4.4 Analysis of Glycophages for Glycomics Analysis 50
4.4.1 Comparision of ELISA Methods for GlycoPhages 50
4.4.2 Effect of Blocking Buffer Type on GlycoPhage ELISA Analysis 52
5. CONCLUSION 53
REFERENCES 56

APPENDIX A. BUFFERS AND STOCK SOLUTIONS 71
APPENDIX B. GROWTH MEDIA 74
APPENDIX C. BACKBONE PLASMID MAP 76
APPENDIX D. MOLECULAR WEIGHT MARKERS 77
APPENDIX E. PROPERTIES OF DESIGNED PRIMERS 78
APPENDIX F. CALIBRATION OF PROTEIN CONCENTRATION 79
APPENDIX G. SDS-PAGE AND WESTERN BLOTTING PROTOCOLS 80

CURRICULUM VITAE 83

LIST OF TABLES

Table 3.1. Strains and plasmids used in the study 25
Table 3.2 Primers used in this study and their sequences 28
Table 4.1. PCR components and product description 37
Table 4.2. Digestion reactions 38
Table 4.3. Ligation reactions 40
Table 4.4 Phage production capacity for different phage production strategies. .. 46
Table E.1. Properties of the designed primers. 78

LIST OF FIGURES

Figure 2.1. (A) Genetic organization of protein *N*-glycosylation locus (pgl) of *C. jejuni*. (B) Functional transfer of the *C. jejuni* protein glycosylation pathway on plasmid pACYCpgl (pgl) into *E. coli*..... 5
Figure 2.2. General structure of Gram-negative LPS 7
Figure 2.3. Current applications for glyco arrays 10
Figure 2.4. Schematic representation of the M13 virion 14
Figure 4.1. Display of new designed phagemids. 36
Figure 4.2. Agarose gel electrophoresis results of amplified gene cassette. 37
Figure 4.3. Agarose gel electrophoresis of products of digestion reactions. 39
Figure 4.4. Agarose gel electrophoresis of plasmid and gene (insert) digested with restriction enzymes 39
Figure 4.5. Agarose gel electrophoresis of plasmid and gene (insert) digested with restriction enzymes 40
Figure 4.6. Agarose gel electrophoresis of digested recombinant phagemids after ligation 41
Figure 4.7. Agarose gel electrophoresis of digested recombinant phagemids. 42
Figure 4.8. Agarose gel electrophoresis of digested recombinant phagemids. 42
Figure 4.10. Western blot analysis of $4x10^{10}$ phage particles produced from *E. coli* TG1 Δ*waaL* carrying pPglΔB plasmid and the phagemid, pMG_4GP_{mut}, pMG_4GP, $pMG_4G_SP_{mut}$ or pMG_4G_SP.. 44
Figure 4.11. ELISA analysis of glycophage samples purified by six different strategies. 45
Figure 4.12. Final cell concentration ($OD_{600,final}$) in nine different glycophage production strategies. 47
Figure 4.13 Phage production capacity (total CFU) for nine different glycophage production strategies. 47
Figure 4.14 Phage production capacity per cell (CFU/OD_{600}) for nine different glycophage production strategies. 48
Figure 4.15 Phage particles produced (CFU_{Total}) at different phage production (induction) periods. 48
Figure 4.16. Final cell concentration (OD_{600}) at different phage production (induction) periods. 49

Figure 4.17. Final cell concentration (OD_{600}) based on different cell concentrations at the point of phage infection 49
Figure 4.18. Final phage particles concentration (CFU_{Total}) based on different cell concentrations at the point of phage infection 50
Figure 4.19 Comparison of glycophage-ELISA based on three diffrent methods. 51
Figure. 4.20 Glycophage-ELISA analysis of glycophage (produced from *E. coli* TG1ΔwaaL host carrying pPglΔB plasmid and pMG4GsP phagemid) and wild-type phage (VCSM13) samples. 52
Figure C1. Plasmid map of pBAD24..... 76
Figure D1. (a) 1 kb DNA Ladder, NEB (b) 100 bp DNA ladder, NEB (c) Precision Plus Protein™ Standards, BioRad. 77
Figure F.1. Standard curve for Bradford Assay 79

LIST OF ABBREVIATIONS AND SYMBOLS

Amp : Ampicillin
Bac : Bacillosamine
Bp : Base pair
BSA : Bovine serum albumine
CFU : Cell forming unit
CIAP : Calf intestinal alkaline phosphate
Cm : Chloramphenicol
CT : Carboxyl terminal
dH_2O : Distilled water
DNA : Deoxyribonucleic asid
dNTP : Deoxyribonucleotide triphosphate
EB : Elution Buffer
EDTA : Ethylenediaminetetraacetic acid
ELISA : Enzyme-linked immuno sorbent assay
G : Glycine
GalNAc : N-acetylgalactoseamine
GBP : Glycan-binding-protein
GlcNAc : N-acetyglucoseamine
GT : Glycosylation tag
FACS : Fluorescene activated cell sorting
HRP : Horse radish peroxidase
Kan : Kanamycin
Kb : Kilo base
LB-Broth : Luria Bertani broth
LPS : Lipopolysaccharide
MBP : Maltose Binding Protein
MS : Mass spectrometry
M9 : Minimal medium
OD : Optical density
OPD : o-Phenylenediamine dihydrochloride
OST : Oligosaccharryl transferase

PBS : Phosphate buffer saline

PCR : Polymeraze chain reaction

PEG : Polyethylene glycol

PFU : Phage forming unit

Pgl : Protein glycosylation locus

RBS : Ribosome binding site

RT : Room temperature

SBA : Soybean agglutinin

SDS-PAGE : Sodium dodecylsulfate-polyacrylamide gel electrophoresis

SOB : Super optimal broth

SOC : SOB with added glucose

SPR : Surface plasmon resonance

wt : Wild-type

T : Tween

TBE : Tris borat EDTA

Tet : Tetracycline

Thi : Thiamine

Tp : Trimethoprim

YE : Yeast extract

YENB : Yeast extract nutrient broth

2TY : 2x Tryptone and Yeast extract

1. INTRODUCTION

Similar to the genetic code for DNA/RNA/proteins, there is a 'sugar code' in biological structures that relates to both health and disease. Complex carbohydrates (glycans) are attached to proteins and lipids by the process of glycosylation and play important roles in many biological processes including cell-cell recognition, metabolic trafficking and host-pathogen interactions. Abnormalities in the glycosylation pattern of a cellular protein can often lead to functional changes that are associated with cancer [1-3] neurodegenerative disorders [4, 5] retrovirus infection [6, 7] disorders of the heart, lung and blood [8] and other diseases [9, 10]. However, progress toward deciphering the 'sugar code' has been relatively slow compared to that of nucleic acids and proteins. High-throughput glycomic methods for characterizing protein-carbohydrate interactions have been relatively lacking, mainly because biosynthesis of glycans is not template-driven unlike other biopolymers, and the information content of glycans is enormous. Nevertheless, carbohydrate microarray technology was introduced in 2002 [11] and is at the frontier of glycomics in the post-genomic era.

The key steps in the establishment of carbohydrate microarrays is to (i) increase the quantity and diversity of carbohydrate structures and (ii) develop reliable and reproducible chemistries for the immobilization of chemically and structurally diverse carbohydrate probes onto the solid support with retention of their functionality. In general, the glycan substrates for most glycoarrays are either synthesized via chemical, enzymatic and/or chemo-enzymatic routes, which can be expensive; or isolated from natural sources such as cells, tissues, pathogens, milk or urine [12] which yields low amounts of glycan and requires several purification steps. These carefully crafted carbohydrates are then immobilized in a spatially defined manner on a solid support. While most glyco-array studies use a small fraction of the total structural diversity found in nature, this has been sufficient to obtain useful results in a variety of applications [13-15, 11]. Still, improved control of the assortment of carbohydrates on arrays remains in high demand. In this study, immobilizing *N*-glycosylated proteins and O-antigens displayed on phage particles is proposed as an alternative in glycan array construction.

The lack of glycosylation pathways in bacteria has greatly restricted the utility of prokaryotic expression hosts for biosynthesis of diagnostic and therapeutic proteins. Recently however, the protein glycosylation locus (Pgl) discovered in *Campylobacter jejuni* was functionally transferred to *E. coli*, conferring ability to glycosylate proteins [16, 17]. Later, groundbreaking work by Aebi and colleagues has shown that protein *N*-glycosylation and lipopolysaccharide (LPS) biosynthesis pathways converge in *E. coli* [18]. This convergence occurs at the step in which PglB transfers LPS O-polysaccharide (or O-antigen) from a lipid carrier (undecaprenylpyrophosphate, UndP) to an acceptor protein. Inactivation of WaaL in *E. coli* results in the accumulation of UndP-linked O-polysaccharides, which PglB can transfer to protein acceptors. PglB is the only protein of the bacterial *N*-glycosylation machinery required for the transfer of O-antigen polysaccharides. Along these lines, various O-antigens (encoded by plasmids containing the entire O-antigen biosynthetic locus) can be transferred by PglB to the acceptor protein displayed on phage particles. Additionally, our group has recently demonstrated glycosylation of phage particles (bacterial viruses) simply by infecting the glycosylation competent *E. coli* with M13 phage displaying an acceptor protein [19]. The hypothesis of this study was based on our ability for presentation of *N*-glycosylated proteins on phage particles and similarly O-antigen (polysaccharides) display were exploited for the development of glycan arrays.

Thus, the significance of this study lies in overcoming the current bottlenecks in glycan array construction and providing a relatively inexpensive, specific and stable glycan representation. A key advantage of our approach is that the use of glycans expressed on the surface of phage particles requires no tedious purification of any expressed ligand. Thus, a simplified and universal purification method that is not dependent on the carbohydrate structure will have been introduced. Furthermore, the use of glycophage as a scaffold for displayed glycans is advantageous because (i) there are no native glycan structures on phage, (ii) phage are released into the media eliminating the requirement for cell lysis (iii) a chemical synthesis step will not be required, and (iv) it will be a modular design that permits easy incorporation of desired glycans.

The utility of a glyco-array is correlated directly with the diversity of polysaccharides incorporated. Thus, to expand the diversity of our glycophage array, in this study, the ability of *E. coli* to incorporate O-antigen polysaccharides just as *N*-glycans was used as an advantage and the starting hypothesis. An array displaying O-antigens, would be significant not only for expanding the array size, but also for identifying human receptors utilized by a pathogen or in understanding the immune response to an infection in the future.

Using the Glycophage technology recently developed [19], recombinant phage particles that display new glycoforms were generated and immobilized on the first generation of array surfaces, nitrocellulose membranes and 96- well microtiter plates. And also verified by western blot and dot blot analysis.The end results will be (i) obtaining a primitive glycan 'bar code' that is specific to the interaction between the terminal glycan (for instance with *N*-acetyl galactosamine and SBA) (ii) a proof of concept that diverse antigens for glycophage-arrayed glycans can be detected from heterogeneous solutions.

2. LITERATURE SURVEY

2.1. Glycans and Glycosylation of Proteins

Glycosylation is one of the major ways in which proteins are post-translationally modified and involves linking of monosaccharides via glycosidic bonds to form a glycan that is covalently attached to a biomolecule, such as a protein or a lipid. Over 50% of eukaryotic proteins are predicted to be glycosylated [20] although yeasts have fewer total glycoproteins than multicellular eukaryotes [21]. The significance of glycosylation is further illuminated by the fact that approximately 70% of therapeutic proteins that are either approved by European and US regulatory agencies or are in clinical and preclinical development are glycoproteins [22].

Glycosylation can occur at several amino acid residues, most commonly through asparagine (*N*-linked) and serine or threonine (*O*-linked). Although there are currently no established rules for predicting the effect of glycosylation on protein folding or function, empirical evidence reveals numerous roles for this protein modification. For example, glycans can influence folding, stability, molecular interactions, and quality control [23]. Extracellular display of glycans plays a role in cell–cell recognition, adhesion, and host immune responses to pathogens [24], Intentionally changing protein-associated carbohydrates can be used to tailor the pharmacokinetic properties of a protein, leading to drugs with enhanced *in vivo* activity, half-life, and resistance to proteolysis [23]. Glycosylation can also be used to target therapeutic proteins to specific cells or tissues [25] and to modulate their biological activities through interactions with specific receptors [26]. Conversely, the incorrect structure or position (on a protein backbone) of glycans can negatively affect pharmacokinetics, and in some cases trigger immunogenic responses [27].

Although long established in eukaryotes, *N*-linked protein glycosylation in bacteria is a relatively recent discovery. The pathogenic e-proteobacterium *Campylobacter jejuni* was the first bacterium found to have an *N*-linked glycosylation pathway [16] encoded by the protein glycosylation locus (pgl) (Fig 2.1. A). This locus encodes all of the necessary enzymes for *N*-linked protein glycosylation with a heptasaccharide consisting of GalNAc–1,4-GalNAc –1,4 (Glc-1,3)-GalNAc–1,4–GalNAc–1,4-GalNAc-1,3-Bac ($GalNAc_5GlcBac$, Bac is

bacillosamine). Functional analysis of the genes from the pgl locus has revealed that the heptasaccharide is synthesized by five glycosyltransferases encoded by the pglA, pglC, pglH, pglI, and pglJ genes [28-31].

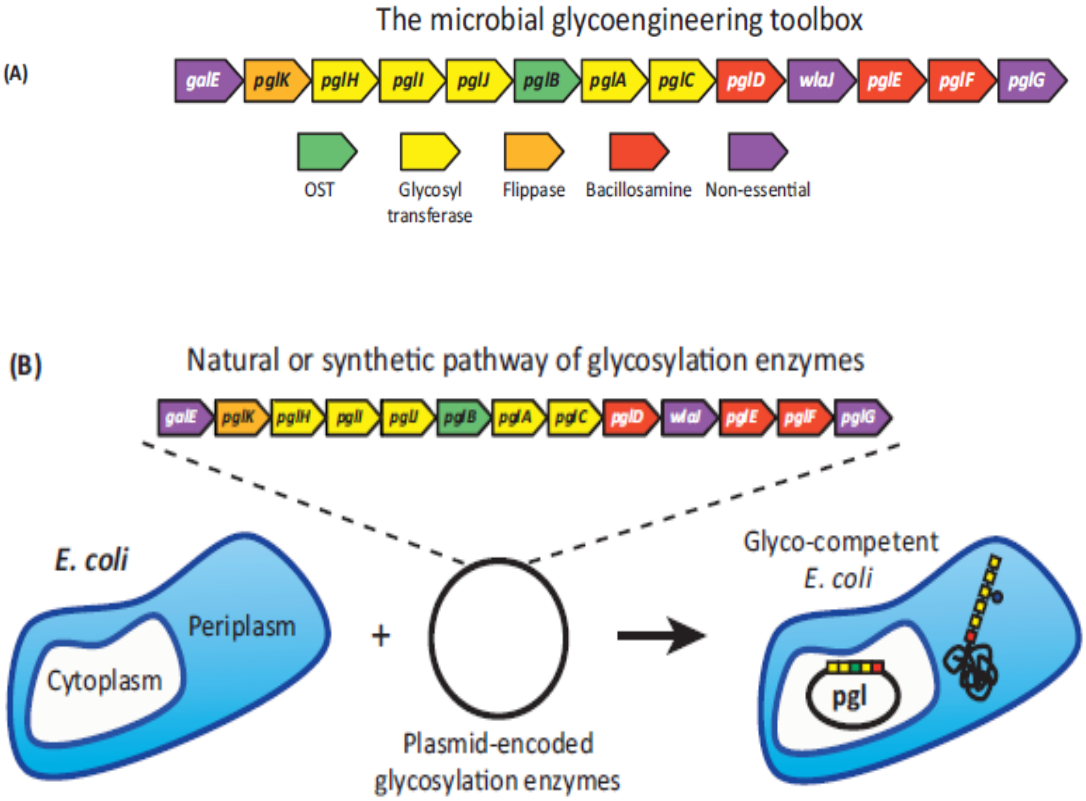

Figure 2.1. (A) Genetic organization of protein *N*-glycosylation locus (pgl) of *C. jejuni*. Yellow, genes encoding glycosyl-transferases that are involved in assembly of the oligosaccharide; red, genes encoding enzymes involved in biosynthesis of DATDH; orange, pglK encoding an ABC transporter; green, pglB that encodes the oTase. **(B)** Functional transfer of the *C. jejuni* protein glycosylation pathway on plasmid pACYCpgl (pgl) into *E. coli* (Modified from [23]).

A growing number of similar protein modification systems have been discovered in other ε- and δ-proteobacteria bacteria but the *C. jejuni N*-glycosylation pathway remains the most extensively characterized [32, 33]. To date, more than 60 periplasmic and membrane *N*-glycoproteins have been identified in *C. jejuni* [34]. It has been predicted that up to 150 proteins of various functions in this bacterium are *N*-glycosylated [35]. Bacterial glycan is synthesized by sequential addition of nucleotide-activated sugars on a lipid carrier on the cytoplasmic side of the inner

membrane and, once assembled, is transferred across the membrane by a flippase enzyme called WlaB (PglK) where it is covalently linked to asparagine residues [36, 37].

Shortly after its discovery, the *C. jejuni* glycosylation pathway that is encoded by single 17 kb locus (pgl) was, functionally transferred in to *Escherichia coli*, bestowing on the latter organism the ability to produce *N*-linked glycoproteins [17, 34]. Transfer of the glycan to substrate proteins occurs in the periplasm and is catalyzed by an oligosaccharyltransferase (OST) called PglB, a single, integral membrane protein with significant sequence similarity to the STT3 catalytic subunit of the eukaryotic OST complex [34] (Fig 2.1.B). This transfer in to a genetically tractable system made it possible to study the basic mechanism of bacterial *N*-linked protein glycosylation in a defined system. PglB attaches the glycan to asparagine in the motif D/E-X1-N-X2-S/T where X1 and X2 are any residues except proline [38]. With this system, proteins can be glycosylated at authentic sites or can be modified for glycosylation by the introduction of short glycosylation tags (GlycTags) containing a preferred *C. jejuni N*-glycosylation consensus sequence, D-Q-N-A-T [39]. When expressed in glycosylation-competent *E. coli*, recombinant proteins engineered with GlycTags are efficiently glycosylated [19, 39]. This glycosylation is compatible with transport mechanisms that deliver the proteins to environments beyond the periplasm, such as the outer membrane, membrane vesicles, and the extracellular medium [39].

N-Linked glycoproteins have also been displayed on filamentous phage particles [40, 41], opening up the route for glycophage display and its application to the engineering of glyco-phenotypes.

2.1.1. O-antigen

Lipopolysaccharide (LPS) is a surface glycoconjugate unique to Gram-negative bacteria and a key elicitor of innate immune responses, ranging from local inflammation to disseminated sepsis. Gram-negative bacteria have two membrane layers separated by a periplasmic space: an inner or plasma membrane and the outer membrane. LPS is a major component of the outer leaflet of the outer membrane [42] and consists of lipid A, core oligosaccharide (OS), and O-specific polysaccharide or O-antigen (Fig 2.2) [42, 43].

O-antigens are present only in smooth type Gram-negative bacteria. They consist of repetitive subunits which make polysaccharides extending out from the bacteria. The O-antigen is extremely variable between species and is an important component of the outer membrane of Gram-negative bacteria. It acts as a receptor for bacteriophages and is also important in the host immune response. In pathogens, these O-chains are in direct contact with the host during infection. Since they are antigenic, they form the basis for serotype classification among the various bacterial families [44].

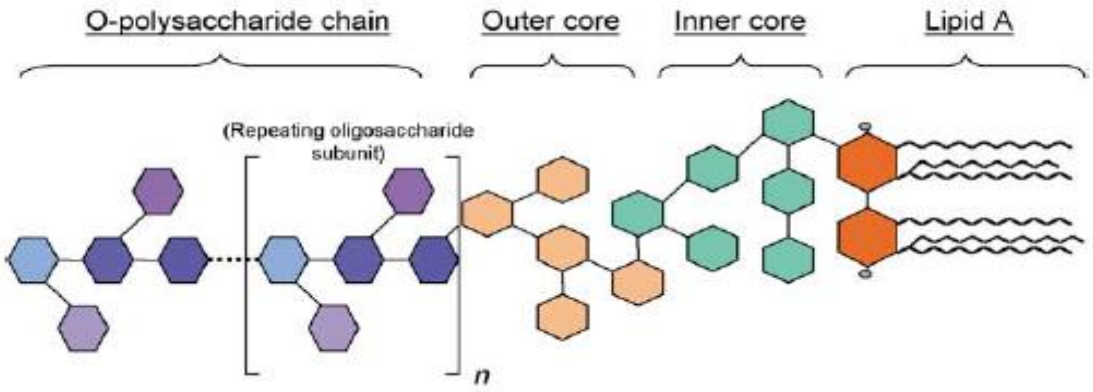

Figure 2.2. General structure of Gram-negative LPS [45].

The O-chains determine the specificity of each bacterial serotype, a kind of fingerprint for bacteria. A combination of monosaccharide diversity, the numerous possibilities of glycosidic linkage, substitution and configuration of sugars, and the genetic capacities of the diverse organisms, have all contributed to the uniqueness of the great majority of O-chain structures.

O-chain structures, like any polysaccharide structures, can be linear or branched and substituted by many different aglycones. The most common substituents are O- and N-acetyl, phosphate, and phosphorylethanolamine groups [46]. Amino acids in amide linkages, acetamidino groups as well as formal groups, and glyceric acid are often found as nonstoichiometric substituents [47].

Each subunit comprises one to eight sugar units and there may be up to 50 identical subunits in an O-chain. During biosynthesis, subunits are polymerized into blocks of varying length and then added to the core. The resulting diversity of chain lengths on different LPS molecules in a culture is responsible for the well-

known ladder-like pattern of LPS molecules on SDS-electrophoretic gels [48]. The nature of the O-chain may, in some cases, be directly related to the pathogenic effects of the bacteria [44].

2.2. Glycomics

Glycomics, the comprehensive study of glycomes (all glycan structures of a given cell type or organism), including genetic, physiologic, pathologic, and other aspects [49, 50] is emerging as a frontier research field in the post-genomic era.

The structural aspects of glycomics are being extensively addressed with the development of advanced profiling and structural characterization strategies, e.g., high-resolution chromatography methods coupled with exoglycosidase digestions [51] and modern mass spectrometry (MS) analyses [52] and NMR [53]. However, understanding the involvements of carbohydrates in diverse recognition systems (often through their interactions with effector proteins) that participate in cell-cell communication and signaling still remain challenging [54].

Detailed analyses of carbohydrate-protein interactions present difficulties at all levels. First, only limited amounts of oligosaccharides (at submicromol levels) can typically be isolated from natural sources when released from proteins or lipids, and these are often highly heterogeneous. Second, the structural diversity of oligosaccharides leads to difficulties in their structural characterization; currently, there is a lack of an efficient means of automated assignment and the characterization is mainly reliant on expert interpretation by MS analyses. Third, the biosynthesis of oligosaccharides is not template driven, as for nucleic acids and proteins, and the diverse repertoire of oligosaccharides is difficult to access by chemical synthesis. Fourth, most carbohydrate-protein interactions are of low affinity, and there is a requirement of multivalent presentation of carbohydrate ligands for detection of binding in microscale screening analysis. Several aspects of these challenges are now being addressed with the advent of carbohydrate arrays in the last decade.

2.2.1. Carbohydrate (Glycan) Arrays

Carbohydrates are composed of polyhydroxy units known as monosaccharides, of which some of the more common monosaccharides are glucose, galactose, mannose, fucose, sialic acid, *N*-acetylgalactosamine (GalNAc), and *N*-acetylglucosamine (GlcNAc). These units are joined together via a glycosidic

bond between the ‘anomeric’ hydroxyl group of one monosaccharide and any of the hydroxyl functions of the second monosaccharide, with loss of a molecule of water. In contrast to proteins in which their sequences are unique, oligosaccharides and polysaccharides are typically composed of the same monosaccharide unit repeated over and over, such as in cellulose and starch [55].

In the last 20–30 years, the role of carbohydrates in cellular recognition and function has started to be thoroughly recognized and understood [56]. Carbohydrates play key roles in mediating interactions among cells and between cells and other elements in the cellular environment, and can operate at cell surfaces.

Carbohydrate arrays (glycoarrays) consist of sugars that are bound, covalently or noncovalently, to a solid surface in a spatially defined and miniaturized fashion. To prepare glycoarrays, pure carbohydrates have to be attached to appropriate chip surfaces. Glycoarray technology has been applied most extensively to the high-throughput analysis of carbohydrate–protein interactions. The proteins are incubated on the microarrays to allow for binding to the exposed carbohydrates before unbound proteins are washed away from the surface. In the next step, bound proteins are detected. Fluorescence-based methods are the most widely used because of high sensitivity and availability of high resolution fluorescence scanner. When fluorescent-labelled proteins are used, microarrays are directly read out and the fluorescence intensities indicate the amount of ligand bound to the chip. It should be noted that protein labelling with fluorescent tags may cause protein denaturation or modification of the sugar-binding domain. Therefore, an alternative approach involves the use of an antibody that specifically recognizes proteins bound to glycoarrays. The antibody can be directly detected if it contains a fluorescent tag. A typical sandwich procedure involving fluorescently labelled secondary antibodies has also been extensively used. However, specific antibodies can only be applied in some cases due to their limited availability [57].

In the past few years, glycoarrays have become a standard tool to screen large number of sugar–biomolecule interactions and investigate the role of carbohydrates in biological systems (Fig 2.3); mostly because characterization of the strength, stoichiometry, and specificity of carbohydrate–protein interactions is

fundamental to many practical applications including profiling cell surface carbohydrate and lectin expression, clinical diagnostics of infectious diseases, and environmental as well as food safety monitoring for bacterial outbreak.

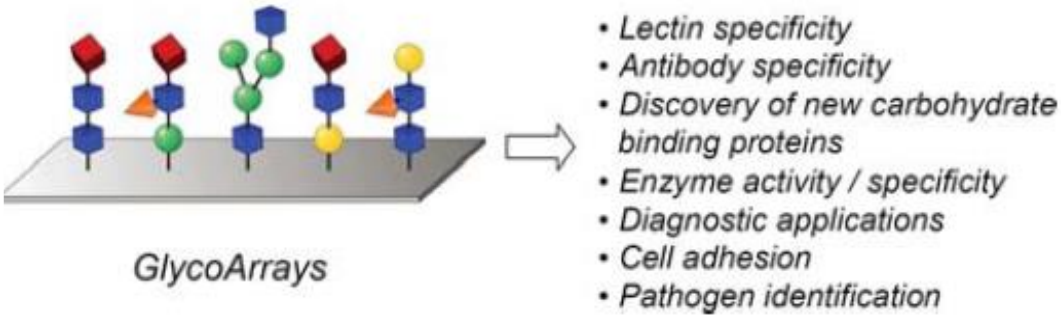

Figure 2.3. Current applications for glyco arrays [58]

The most important advantages of glycoarray technology over conventional approaches, such as enzyme-linked lectin assay, surface plasmon resonance (SPR), or isothermal titration calorimetry (ITC), are the ability to screen several thousand binding events on a single slide and the miniscule amounts of both analyte and ligand required for one experiment. Additionally, glycoarrays are ideal platforms to detect interactions that involve carbohydrates, because the multivalent display of ligands on a surface overcomes the relative weakness of these interactions by mimicking cell–cell interfaces [57].

A number of experimental approaches have been developed to construct carbohydrate-based microarrays to facilitate the exploration of sugar chain diversity and its biomedical significance [59]. These carbohydrate microarrays are all solid-phase binding assays for carbohydrates and their interaction with other biological molecules. In spite of their technological differences, they share a number of common characteristics and technical advantages. First, they have the capacity to display a large panel of carbohydrates in a limited chip space. Second, the amount needed to spot each carbohydrate is drastically smaller than that required for a conventional molecular or immunological assay. Third, the microarray-based assays have higher detection sensitivity than most conventional molecular and immunological assays; this increased sensitivity is due to the fact that the binding of a molecule in solution phase to an immobilized

microspot of ligand in the solid phase minimally reduces the molar concentration of the molecule in solution [60]. Therefore, it is much easier to have a binding equilibrium take place in a microarray assay and result in a high sensitivity.

Glycoconjugates have been immobilized on silica plates [61], synthesized on beads [62] or immobilized in different wells of ELISA (enzyme-linked immunosorbent analysis) plates [63]. Regardless of the immobilization technique, glycan array technology has been used in various applications, mostly for the analysis of binding specificity of lectins and antibodies.

The Consortium for Functional Glycomics (CFG) has developed one of the largest glycan arrays in the world and has provided routine screening for many investigators. Some recent examples include the screening of galectin 8 [64], human ficolin [65] and *Candida glabrata* adhesion [66]. Some other labs have developed and utilized glycan array technology for lectin and antibody screening. Feizi and coworkers used a carbohydrate microarray to reveal the structure of the preferred ligand for a novel protein, malectin [67]. Gildersleeve and coworkers used a carbohydrate microarray to evaluate the specificities of a set of lectins and antibodies used as reagents to detect the tumor-associated Tn antigen [68-70]. One of the growing applications of glycan array technology is serum antibody profiling. Human serum contains a wide variety of carbohydrate-binding antibodies, and the populations of these antibodies change as a result of disease, exposure to pathogens, and vaccination. Several recent examples illustrate the utility of carbohydrate antigen arrays for high-throughput profiling of serum antibodies. Glycan arrays have also been developed for the detection of pathogen specific antibodies for the serodiagnosis of infectious agents. Seeberger and coworkers reported preparation of a microarray comprising synthetic *P. falciparum* glycosylphosphatidylinositol (GPI) glycans [71]. Other recent examples include profiling of mellidosis patients and animals vaccinated or infected with anthrax or tularemia- causing bacteria [72, 73], salmonellosis patients [74] and *Schistosoma mansoni* infected individuals [75]. Microarrays have also seen many applications in cancer research. One recent report highlights the utility and sensitivity of a glycan microarray to measure antibody levels to a tumor-associated carbohydrate antigen, Globo-H, and related structures [76].

These preliminary studies show great promise for glycan microarray technology. However, to fully exploit the potential of arrays, it will be necessary to (i) increase the quantity and diversity of carbohydrate structures and (ii) develop reliable and reproducible chemistries for the immobilization of the carbohydrate probes onto solid support. In general, the glycan substrates for most glycoarrays are either synthesized via chemical, enzymatic and/or chemo-enzymatic routes, which can be expensive; or isolated from natural sources such as cells, tissues, pathogens, milk or urine [12], which yields low amounts of glycan and requires several purification steps. While most glyco-array studies only sample a small fraction of the total structural diversity found in nature, this has been sufficient to obtain useful results in a variety of applications [13-15, 11]. Still, improved control of the assortment of carbohydrates on arrays remains in high demand.

In this context, in the present study, immobilizing *N*-glycosylated proteins and *O*-antigens displayed on phage particles is proposed as an alternative in glycan array construction. Future developments and automation will expand the possibilities of carbohydrate and lectin analysis in the clinical sciences, biosensor fields for various applications such as bioterrorism defense, environmental pollutant monitoring, forensic analysis, food safety, biological research, and routine clinical tests in laboratory medicine [77, 78].

2.3. Bacteriophages and Phage Display Technology

Bacteriophages are viruses that infect bacterial cells. Much of the acquired knowledge about phage replication and structure has been exploited in phage display technology since the 1990's. Because of their nanoscale size, the small genome size enclosed in the capsid and relative ease of their genetic manipulation, bacteriophages are nowadays also being adapted for the fabrication of nanotechnological materials.

2.3.1. Phage Biology

Phages may have single- or double-stranded DNA or RNA genomes, protected by filamentous or icosahedral capsids. The most common bacteriophages used in phage display is fd (M13 and f1) filamentous phage, though T4, T7, and λ phage have also been used [79-81]. Filamentous (Ff) phages constitute a large family of bacterial viruses that infect many gram-negative bacteria. In total around 60 different filamentous phage have been described to date (International

Committee on Taxonomy of Viruses., 2005). Filamentous bacteriophage, long and thin filaments that are secreted from the host cells without killing them, have been an antithesis to the standard view of head-and-tail bacterial killing machines. The filamentous phage of *Escherichia coli* are the most productive phage in Nature, giving rise to titers of up to 10^{13} per mL of culture. Among *E. coli* filamentous phage, the best studied and most-exploited group are the F pilus-specific phage or Ff, known as f1 and M13, 98.5% identical in their DNA sequence [82, 83].

Certain characteristics of M13 make it useful for phage display, among other molecular genetic manipulations. Ff phage replication and assembly is tolerated by infected bacterial wall. Infected cells continue to grow but at a lowered rate of division. Therefore, infected *E. coli* cells producing M13 phages appear as turbid plaques resulting from lytic or temperate phages, respectively, are formed when infected bacteria die. The non-lytic nature of the M13 phage-host interactions means that infected *E. coli* strains can be grown and propagated for some time. Second, the replicative form of the M13 phage genome is a double-stranded circular DNA molecule, essentially a plasmid. Therefore, it is possible to purify the replicative form from infected cells and perform DNA manipulations that one typically performs on a plasmid. In fact, some of the earliest cloning vectors were derivatives of M13 [84]. The ability to manipulate the phage genome is also a critical aspect of this system. Finally, because the phage genome is simply bound by coat protein, as opposed to filling a phage head structure, there is not a strict limit on the size of the packaged DNA. This enables flexibility in the size of recombinant tools.

The phage used in this study is M13 filamentous bacteriophage from the family Inoviridae (Fig 2.4). The general appearance of bacteriophage M13 is that of a flexible filament, about 900 nm long and 6 to 10 nm thick, with a molecular weight of 12×10^6 [85-87].

The M13 phage consists of a circular single-stranded DNA genome complexed with a major coat protein (pVIII) and a few minor structural proteins (pIII, pVI, pVII, pIX) at either end. The 6.4-kb genome encodes 11 genes, five of which contribute to particle structure (Fig 2.4).

The major coat protein pVIII is an integral inner membrane protein prior to assembly into the virion and contains a signal sequence. The pIII protein found at one end of the particle is present in about five copies and is responsible for binding of the phage to the F-pilus receptor. It also has a role in release of the phage particles from infected E. coli cells. Thousands of pVIII subunits are held together through hydrophobic interactions, in a helical arrangement that is reminiscent of snake-skin scales (Fig 2.4).

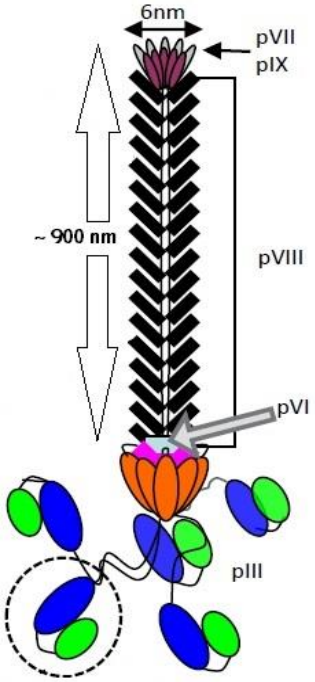

Figure 2.4. Schematic representation of the M13 virion (modified from, [88])

The cap is composed a few copies of the pVII and pIX proteins. It contains no lipid or carbohydrate. In contrast to the detailed knowledge of pVIII structure and packing along the filament, no structural information is available for the two caps. Proteins pVII and pIX are incorporated into the virion at the initiation step of assembly and are the first to be extruded from the cell [89, 90]. Both are small hydrophobic proteins of only 32 (pVII) and 33 (pIX) amino acids; they are inner membrane proteins prior to assembly, but in Ff phage they do not contain a signal sequence and are thought to spontaneously insert into the membrane [89]. The structure of these two proteins has not been solved and their arrangement in the virion has not been determined. Genetic analysis showed that the residues near

the C-terminus are involved in interactions with the packaging signal, a DNA hairpin that targets phage genome for packaging [91]. The sole clue about the accessibility of these two proteins is their ability to display peptides and proteins fused to their N-termini. For both proteins, once an addition to the N-terminus has been made, a signal sequence is required for successful incorporation of these chimeric proteins into the virion and display on the surface of the virion [92-94].

Proteins pIII and pVI are added to the virion at the end of assembly. They form a distal"cap" of the filament and at the same time release the virion from the cell [95, 96]. These two proteins are required for the structural stability of the virion and also for termination of assembly. In addition, pIII mediates entry of the phage into the host cell (Fig 2.5). Both pIII and pVI are integral membrane proteins [97, 89]. At 406 amino acids in length (424 residues including signal sequence), pIII is distinctly larger than the other four virion proteins. PIII is composed of three domains (N1, N2 and C) separated by long glycine-rich. PVI is mostly hydrophobic integral membrane protein prior to assembly into the virion to contain three transmembrane α helices, with the N terminus in the periplasm and the C-terminus in the cytoplasm [89].

The N1 and N2 domains of pIII interact with the host receptors; the structure of these two domains has been determined using X-ray crystallography and NMR [98, 99]. The three-dimensional structure of the C-domain, which is required for termination of phage assembly, formation of a detergent-resistant virion cap and for late steps in phage infection, is yet to be determined [100, 95]. An antibody specific for the C-terminal 10 residues of pIII cannot bind to pIII when it is in the virion. Therefore, this C-terminus must be buried within the virion cap, which is composed of the pIII C-domain and pVI. The largest virion protein, pIII, mediates infection of the host (Fig 2.5). Its two N-terminal domains bind to the primary and secondary receptors and its C-domain is involved in virion uncoating and DNA entry into the host cell cytoplasm [100]. PIII is the most diverse virion protein among filamentous phage, often with no significant homology between the counterparts from distant phage. Functional pIII C-domain covalently linked to the "N1, N2" domains, are absolutely required for phage infection, which ultimately results in entry of the phage ssDNA into the cytoplasm and integration of the major coat protein into the inner membrane [100]. C-domain of pIII is predicted to

be α-helical; three C-terminal helices (two amphipathic and the third, hydrophobic anchor) are required for phage entry [101].

N1 and N2 domains of pIII are required for infectivity of the particles, if truncated pIII is used for display, a wild-type (full length) pIII must be provided in order to allow easy amplification of phage. As with pVIII, the inserted sequence must be in frame with the upstream signal sequence and downstream mature (or truncated) pIII. The pIII fusions are most commonly expressed from phagemid vectors, which carry both plasmid and f1 origins of replication, the f1 packaging signal and an antibiotic resistance gene [102]. The phagemid vectors carry a cloning restriction site between sequences encoding the signal sequence and mature full length or truncated pIII. This allows proteins encoded by the inserts to be displayed on the surface of the phage as a fusion with pIII. Phagemid DNA into which inserts have been cloned are introduced into F+ cells, and upon helper phage infection, the phagemids replicate from the f1 origin, resulting in production of ssDNA that is assembled into the virions displaying the proteins encoded by the phagemids (Fig 2.6). To amplify a phagemid, the particles are mixed with F+ host cells. The phagemid DNA is introduced into the cell by infection, resulting in expression of the antibiotic resistance encoded by the phagemid. In the absence of the helper phage, the phagemid replicates from the plasmid origin of replication [103, 84, 87].

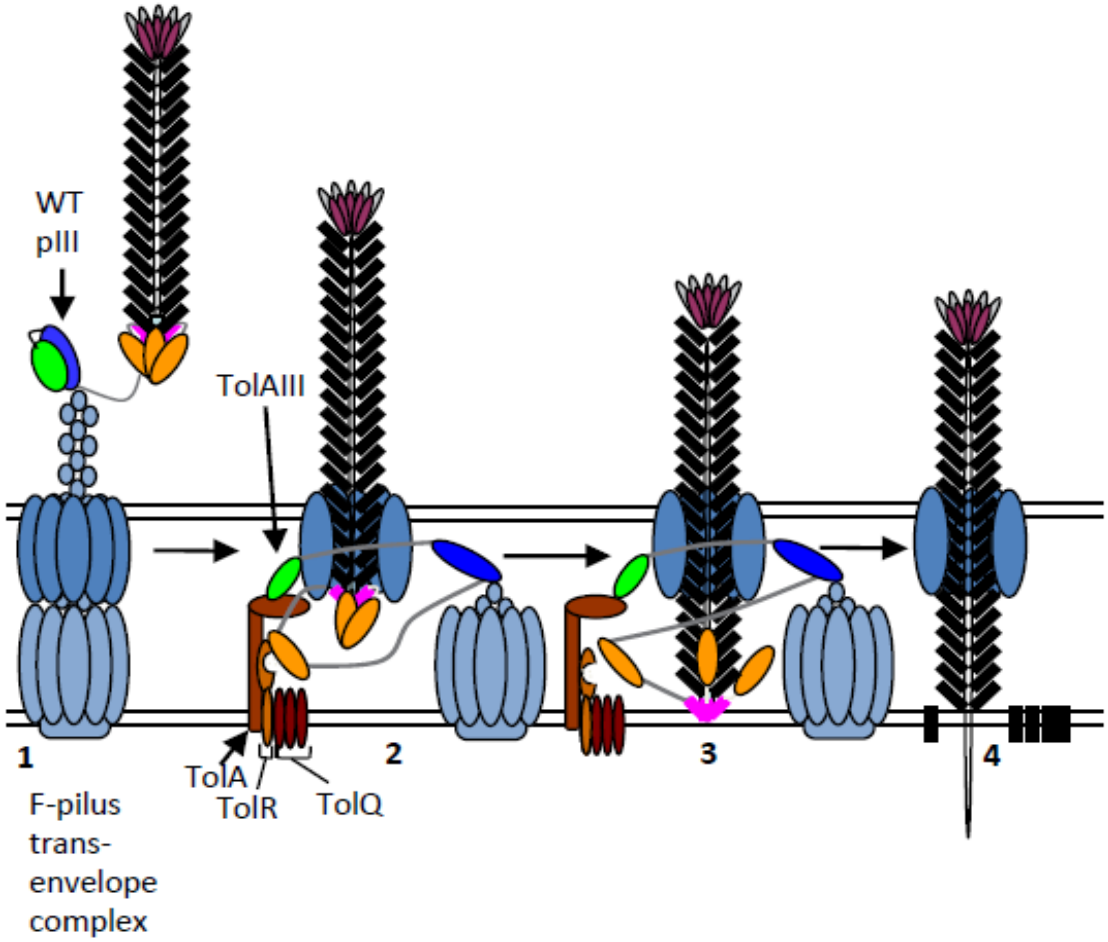

Figure 2.5. Model of Ff phage infection. (1) Binding of N2 domain (dark-blue oval) to the tip of the F-pilus (light-blue circles)and pilus retraction. (2) Binding of N1 domain (bright-green oval) to TolA III domain (brown oval). (3) "Opening" of the C-domain and insertion of the C-terminal hydrophobic helix into the inner membrane. (4) Entry of phage DNA into the cytoplasm and integration of the major coat protein pVIII into the inner membrane. Steps 1 and 4 are based on published findings, whereas steps 2 and 3 are speculative. Symbols: OM, outer membrane; IM, inner membrane. pIII N1 domain, dark-blue oval; pIII N2 domain, bright-green oval; pIII C domain, orange oval; pIII C-terminal hydrophobic helix (membrane anchor), pink rectangle; pIII glycine linkers, gray lines; major coat protein pVIII, black rectangles; pVII, gray ovals, pIX, purple ovals; TolA and TolRQ,brown shapes; F-pilus, and the trans-envelope pilus assembly/retraction system, light-blue. The phage contains 5 copies of pIII, but for simplicity only one full-length pIII is shown. However, this is consistent with experimental data: N1, N2 and C domain operate "*in cis*" and fewer than five functional copies are sufficient for infection [100].

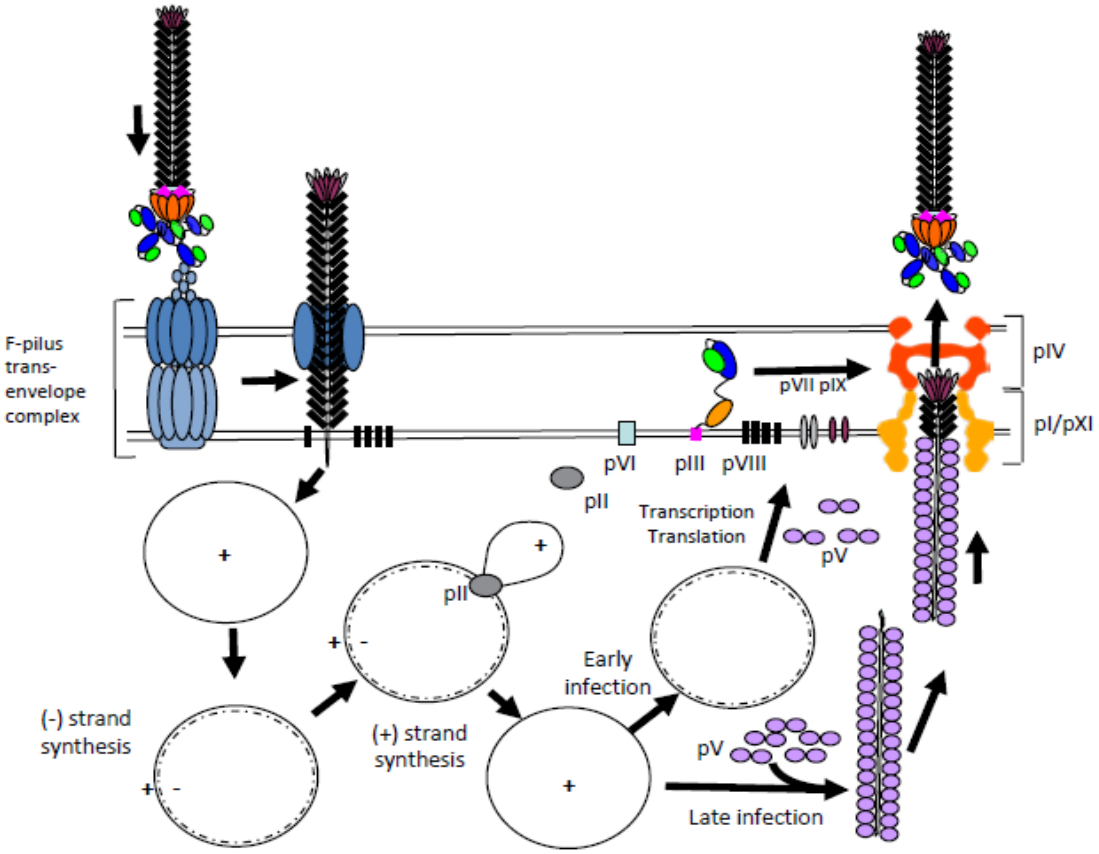

Figure 2.6. The Ff phage life cycle [88]. Upon infection, the ssDNA enters into the cytoplasm, while the pVIII major coat protein integrates into the inner membrane. Synthesis of the negative (-) strand is initiated at the negative strand origin of replication by RNA polymerase, which generates an RNA primer and is then released from the template [104]. Host DNA polymerase III uses this primer to replicate the complete negative strand. Positive strand synthesis is initiated by pII (gray circle), which creates a nick in the + strand of the dsDNA replicative for at the positive origin of replication. Supercoiling and formation of a stem-loop structure of the positive (+) origin of replication is required for this step (not shown in the figure). Rolling circle replication then ensues, one strand at a time. During the initial period of viral infection, new positive strands are used as templates for synthesis of negative strands, resulting in an increase in copy number of the dsDNA replicative form (RF). The RF serves as a template for production of phage proteins. Phage proteins II, V and X remain in cytoplasm and mediate genome replication and formation of the packaging substrate. Proteins pI, pIV and pXI form a transport complex spanning the inner and outer membrane (yellow and orange, respectively). Virion proteins pVII, pIX, pVIII, pVI, pIII are inserted into the membrane prior to their assembly into phage particles. Later in the infection, positive strands are coated by dimers of the phage encoded single-stranded DNA binding protein pV to form the packaging substrate and brought to the cell membrane assembly/export complex (pI/pXI and pIV) for assembly and export. The pIV silhouette is derived from determined cryo-EM structure [105]. The structure of the inner membrane complex (yellow silhouette) has not been determined; it is drawn based on the cryo-EM structure of the type III secretion system [86].

Phages and phagemids are the most common vectors used in phage display, while phagemids are used more widely than phages due to the reasons summarized below [106, 107]. First, genomes of phagemids are smaller and can accommodate a larger foreign DNA fragment. Second, the phagemids are more efficient in transformation that allows obtaining a phage display library with high diversity. Third, a variety of restriction enzyme recognition sites are available in the genome of phagemids convenient for DNA recombination and gene manipulation. Fourth, the expression level of fusion proteins can be controlled and modulated easily. Finally, phagemids usually are genetically more stable than recombinant phages under multiple propagations.

The basic components of a phagemid mainly include the replication origin of a plasmid, the selective marker, the intergenic region, a gene of a phage coat protein, restriction enzyme recognition sites, a promoter and a DNA segment encoding a signal peptide. Additionally, a molecular tag can be included to facilitate screening of phagemid-based library. Phagemids can be converted to filamentous phage particles with the same morphology as Ff phage [108] by co-infection with the helper phages [109] such as R408, [110] M13KO7 [111] and VCSM13. As with other filamentous phages, the length of progeny phage particles would be varied along with the length of phagemid DNA [112].

2.3.2. Phage Display Technology

Using bacteriophages in nanotechnology has been done using filamentous bacteriophages, principally bacteriophage M13-related phages. These phages are employed in a technology termed phage display [113]. In phage display, peptides or proteins are displayed on the surface of filamentous bacteriophage particles which contain the encoding DNA, thus giving a physical link between the phenotype of the displayed polypeptide and the corresponding genotype. The method for displaying polypeptides on phage particles was first described by Smith, G.P. (1985) [81]. Since then, phage display technology has proved to be a powerful tool for screening libraries of proteins and peptides for selection of molecules with desired properties and it is still the dominating method for construction of protein libraries and selection of affinity proteins. Phage display was first developed for the M13 filamentous phage and even though several

alternative phage systems have been explored, M13 still remains the most extensively studied and most commonly used phage [114].

In phage display, a library of peptides is typically inserted into the pIII receptor-binding protein or into the pVIII major capsid protein. A population of phages bearing a library of display peptides (commonly 7–14 amino acids) is exposed to the target material. This target can be a protein, a cell, or an inorganic material. Phages whose display peptides bind to some feature of the target will adhere and the remainder of the phages can be washed away. The bound phages are then released (using a wash with different pH or salt concentrations) and used to grow a new sublibrary stock. This process is often described as biopanning. Generally, three to five rounds of biopanning are effective at identifying a small number (<25) of peptide-binding sequences from an initial library [115]. For a library of 10^{10} variants, representation of every variant demands that, depending on the expected affinity of interaction, a larger number of particles be screened. This is not a problem, because Ff used in phage display technology are produced at concentrations (or titers) of up to 10^{13} per mL of culture. Increasing the culture volume and concentrating the phage particles further increases this number. The peptide-binding sequences derived via phage display can be used in one of two ways: as peptides or remaining as phage sequences. In the former, the peptide-coding sequences are added to other, non-phage genes to provide proteins with the same target-binding capacity or the peptides are made independently and attached to non-protein molecules for the same purpose. This method has been used to synthesize a variety of nanoparticles that can be used for other applications [116]. The second way leaves the peptide-binding sequence attached to the phage using both the phage's physical properties and the ability to bind the target molecules for the application [113].

Peptide-displaying phage technology may also provide carbohydrate-mimetic peptides, which are equivalent to amplifiable carbohydrates [117-120]. Carbohydrate-mimetic peptides can be used as immunogens to raise anti-carbohydrate antibodies for cancer therapy [121-123] and infectious diseases [124-129]. In addition, phage display technology provides peptide sequences that bind to carbohydrates, enabling us to produce recombinant humanized

monoclonal anti-carbohydrate IgG antibodies against cancer cells [130] and infectious agents [131, 132].

Phage display technology has also been used to detect bacterial pathogens, mostly through screening of random peptide libraries. Goldman et al. (2000) [133] used the NEB 12-mer library to isolate peptides with affinity for SEB, a toxin associated with food poisoning. Stratmann et al., 2002 [134] used the NEB 12-mer library to isolate peptides that recognized *Mycobacterium avium* subspecies *paratuberculosis* (*M. Paratuberculosis*), and acid fast pathogen found in milk that is associated with a chronic inflammatory bowel disease of animals called Johne's disease. Turnbough and colleagues [135, 136] used the NEB 7- and 12-mer libraries to isolate phage clones that recognize spores of a variety of species of *Bacillus*, most importantly *B. anthracis* of relevance for bioterrorism. Ide et al., 2003 [137] used the NEB 12-mer library to identify peptides that recognize the H7 flagella of *E. coli* O157:H7, otherwise known as enterohemorrhagic *E. coli* (EHEC). EHEC is pathogenic *E. coli* that causes hemorrhagic colitis and fatal kidney damage. Kim et al., 2005 [138] used the NEB 7-mer Ph.D. system to isolate peptides that recognized lipopolysaccharide (LPS) from a variety of gram-negative bacteria. Bishop-Hurley et al., 2005 [139] used a 15-mer random peptide phage display library made by G.P. Smith to isolate phages recognizing non-typeable *Haemophilus influenzae* (NTHI), a gram-negative bacterium that causes respiratory disease. Gasanov et al., 2006 [140], used the NEB random 12-mer library to pan on whole *Listeria monocytogenes* cells, where *L. monocytogenes* is a gram-positive food-borne bacterial pathogen.

2.3.3. GlycoPhage Display

The power of phage display has recently been combined with the bacterial glycosylation machinery to expand the microbial glycoengineering toolbox, allowing the production and selective enrichment of phages that display *N*-linked glycoproteins [19]. This involved fusing the minor phage coat protein g3p with a target glycoprotein, such as the maltose-binding protein modified with a *C*-terminal GlycTag. The resulting fusion protein was efficiently glycosylated in *E. coli* cells equipped with the *C. jejuni N*-glycosylation machinery. Moreover, by virtue of the g3p protein, the glycosylated fusion protein became displayed on the head of filamentous phage particles. The glyco epitope displayed on the phage

is the product of biosynthetic enzymes encoded by genes of the *C. jejuni* pgl pathway and minimally requires three essential factors: a pathway for oligosaccharide biosynthesis, a functional OST, and an acceptor protein with a bacterial D/E-X1-N-X2-S/T acceptor motif. Phage display of *N*-linked glycoproteins creates a genotype-to-phenotype link between the phage-associated glyco-epitope and the phagemid-encoded genes, allowing screening, optimization, and engineering of the acceptor protein as described previously [23, 19].

The significant potential of this novel glycoprotein display technique was similarly demonstrated through the use of an acceptor protein natively glycosylated by *C. jejuni* (AcrA) [41], instead of an engineered maltose-binding protein (MBP) variant appended with a GlycTag. In both studies, an enrichment factor for the glycosylated phages of approximately 10^5-fold was achievable.

Thus, the high-throughput glycophage display system should provide an invaluable tool for genetic analysis of protein glycosylation and for glycoengineering studies in *E. coli* cells [23]. In this study the above glycophage display system was used to describe a facile alternative for glycan array fabrication using engineered phages that display defined glycan epitopes, so-called “glycophages” [19, 41].

2.3.4. Bacteriophages in Biosensor and Microarray Technologies

Phage can be used as a recognition element in biosensors by using physical adsorption to immobilize phage on the sensor surface, as well as in an array format, in a spatially defined arrangement. The phage selected for binding β-galactosidase exemplifies the ability to use phage in biosensor technology for selective and specific recognition of relatively large protein molecules [141]. The combination of the phage-displayed protein chip and the SPR technique has been proved to be fit for proteomics research. Balasubramanian et al., 2007 [142] detected *Staphylococcus aureus* by using lytic phages as the probes on an SPR platform.

Landscape phages have been shown to serve as bioprobes for various biological targets [143-147]. These phage probes have been used in ELISA and quartz crystal microbalance (QCM) to detect bacterial and mammalian targets [148]. The QCM acoustic wave sensor has proven to be an excellent analytical tool for the

study of specific molecular interactions at the solid–liquid interface [149-153, 141, 154, 155].

Phage-patterned microarrays are a standard art in proteomics and have been used as carriers to display small peptides for the diagnosis of the immune response in cancer patients [156, 157] or HIV patients [158], cDNA libraries to diagnose non-small cell lung cancer [159] and antibody clones for the detection of leukocyte surface antigens [160]. Antibodies can also be designed against phage coat proteins to assist in proper alignment, as was demonstrated by [161] in their development of patterned lithographic microarrays of antibody–M13 phage complexes. In all of these cases, phage particles were entirely compatible with the microarray patterning process and the displayed molecules (e.g., proteins, peptides) were accessible for subsequent protein-protein interaction analysis using standard microarray scanners. A key advantage conferred by the use of recombinant phage is that it obviates the need for protein purification and thus saves considerable time and cost.

Various methods have been employed to immobilize phages on surfaces for biosensor or array development. Physical absorption for ELISA, covalent binding and molecular recognition were proposed for a variety of applications. Phages have been immobilized by peptide bond between amino and carboxyl terminal (CT) groups on solid platforms. Other proposed approaches for immobilization of phages are through disulfide bonds and thiol groups, or by specific recognition between hexa-histidine tags on the phage and nickel coated surface [162-168].

Building on these ideas, immobilization compatibility of phage particles combined with recent demonstration of glycan display on filamentous phage [169, 19] to create a novel glycan array technology for detecting GBP interactions. Specifically, our research group aimed to show that glycophages are compatible with surface immobilization procedures, can be modified with different glycan structures, and retain the ability following immobilization to be recognized by different GBPs (e.g. antibodies and lectins) that recognize the displayed oligosaccharides [169]. Hence, glycophage ELISA technique was developed within the scope of this thesis study.

3. MATERIALS AND METHODS

3.1. Buffers and Stock Solutions

All buffers and stock solutions listed in Appendix A were prepared with distilled water. The sterilization of solutions was performed either by autoclaving at 121°C for 20 min or by filter sterilization through 0.20 µm filters (Sartorius AG, Gottingen, Germany).

3.2. Strains, Plasmids and Maintenance of Microorganisms

E. coli strain DH5α was used for cloning of phagemids, while strain TG1 Δ*waaL* was used for glycophage production and strain TG1 was used for helper phage production and titering experiments. *E. coli* strains were grown in Luria Bertani (LB) medium at 37°C or 2xTY medium at 30°C (induction phase). Culture medium was supplemented with 50 mM glucose or 30 mM arabinose (induction phase), and with the appropriate antibiotics at the following concentrations: 100 µg/mL ampicillin, 20 µg/mL chloroamphenicol, 50 µg/mL kanamycin and 100 µg/mL trimethoprim. M9 minimal medium was used to select for the presence of F' plasmid when needed. VCSM13 (Stratagene) was used as the helper phage.

For long-term storage of microorganisms, *E. coli* strains were suspended in 1 mL LB medium containing 15% glycerol and stored at -80°C. The compositions and preparation protocols of all the media used are given in Appendix B.

The strains and plasmids used in this study are summarized in Table 3.1. The sequences and schematic representation of the backbone plasmid is given in Appendix C.

3.3. Genetic Engineering Techniques

Moleculer genetics methods were performed according to standart protocols [170] and are summarized in Figure 3.1.

3.3.1. Plasmid DNA Isolation from *E. coli*

Plasmid DNA from *E. coli* cells was extracted using QIAGEN Mini-Prep Kit, (Qiagen, Valencia, CA, USA) according to manufacturer's instructions. For this purpose, a single colony from selective solid medium was inoculated into 5 mL selective liquid medium and grown overnight at 37˚C and 200 rpm. At the end of the protocol, 50 µL of elution buffer (EB) was used to elute DNA from QIAprep spin column and the extracted plasmid was stored at -20˚C.

Table 3.1. Strains and plasmids used in the study

Strains	Relevant genotype or description	Reference or source
E. coli DH5α	F⁻ Φ80*lac*ZΔM15 Δ(*lac*ZYA-*arg*F) U169 *rec*A1 *end*A1 *hsd*R17 (rK–, mK+) *pho*A *sup*E44 λ– *thi*-1 *gyr*A96 *rel*A1	Invitrogen
TG1	K-12 supE thi-1 Δ(lac-proAB) Δ(mcrB-hsdSM)5, (rK^-mK^-)	Stratagene
TG1 Δ*waaL*	K-12 supE thi-1 Δ(lac-proAB) Δ(mcrB-hsdSM)5, (rK^-mK^-) Δ*waaL*	[169]
Plasmids		
pBAD24	Cloning vector, arabinose-inducible, Amp^r	[171]
pPglΔB	pMW07 containing the *C. jejuni pgl* locus without pglB	[169]
pBAH2B	pBAD24 based plasmid containing MBP cassette.	Laboratory stock
pBAH2Bmut	pBAD24 based plasmid containing MBP cassette, were pglB has been inactivated.	Laboratory stock (Guarino)
pMWO78	pMW07-O78 for *E. coli* O78 O-antigen polysaccharide (Ec-OAg (O78); laboratory stock)	[172]
pMGG	pBAH2B based plasmid encoding MBP-GT-G3P	[19]
pMGGP	pMGG based phagemid containing pglB.	This study
pMG_4GP	pMGGP based phagemid four tandem repeats of GT (Glyc Tag).	This study and [169]
pMG_4G_sP	pMG_4GP based phamid containing truncated g3p	This study and [169]
$pMGGP_{mut}$	pMGG based phagemid containing inactivated pglB (PglBmut).	This study
pMG_4GP_{mut}	$pMGGP_{mut}$ based phagemid containing four tandem repeats of GT and PglBmut .	This study and [169]
$pMG_4G_sP_{mut}$	pMG_4GP_{mut} based phamid containing truncated g3p.	This study and [169]

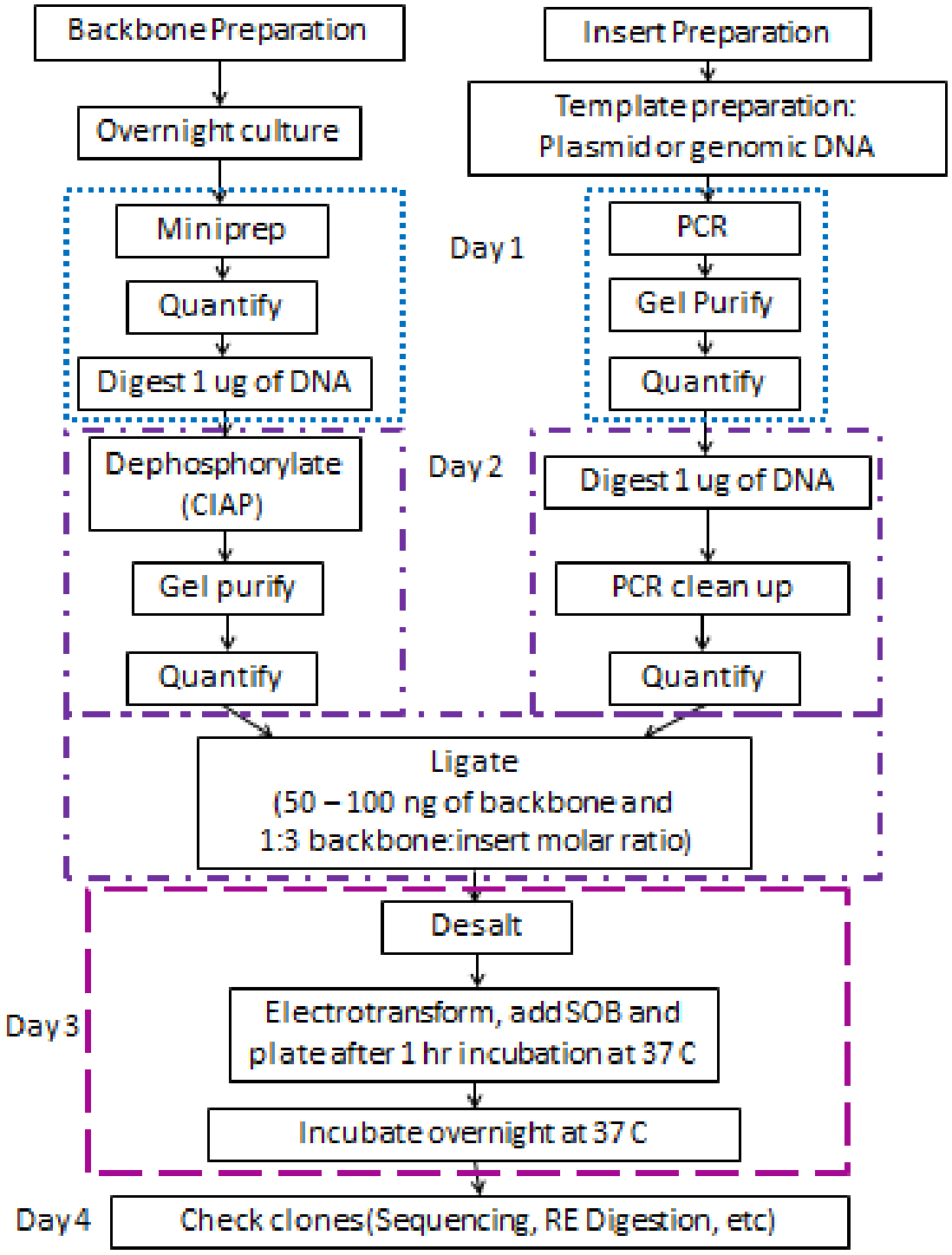

Figure 3.1. Schematic representation of the general cloning procedure

3.3.2. Agarose Gel Electrophoresis

Gel electrophoresis was used to separate and visualize DNA strands. 1 g of agarose was dissolved in 100 mL 1xTBE and heated until boiling point. After cooling to approximately 50°C, 0.5 µg/mL of ethidium bromide was added and the gel was poured into a gel tray. An appropriate comb was inserted and the gel was allowed to cool. The gel tank was filled with 1xTBE buffer. DNA samples mixed with loading buffer were loaded into the wells, together with the DNA ladder (Appendix D) for size estimation. Electrophoresis was performed at 100 V for 45-60 min. The bands were visualized under UV illumination and photographed.

3.3.3. DNA Extraction from Agarose Gels

In the case where a single band of DNA is to be purified from agarose gel after electrophoresis, QIAquick Gel Extraction Kit (Qiagen) was used according to manufacturer's instructions. The procedure is designed to purify DNA from agarose and salts. For this aim, the DNA fragment as visualized above UV illuminating board, was excised from the gel with a clean, sharp scalpel and weighed in an microcentrifuge tube, to be approximately 400 mg of gel. At the end of the protocol, 50 µL of EB was used to elute DNA from QIAquick spin column (Qiagen) and the extracted DNA was stored at -20˚C till further use.

3.3.4. Primer Design

General recommendations for PCR primer design were followed as outlined below:

a. Primer is preferentially 16-60 nucleotides long.
b. One or two G or C at the 3'-end of the primer should be preferred, avoiding more than three G or C nucleotides at the 3'-end, to lower the risk of nonspecific priming.
c. Optimal GC content of the primer is 40-60%.
d. Primer self-complementarities should be avoided, complementarities between the primers and direct repeats in a primer to prevent hairpin formation and primer dimerization.
e. Differences in melting temperatures (Tm) of the two primers should not exceed 5°C for conventional PCR.

The primers used in this study are given in Table 3.2. The sequences for restriction enzyme recognition sites are underlined. Extra nucleotides were added to the 5' end of restriction enzyme recognition sites, since site recognition by the enzyme close to the end of DNA fragment could otherwise be problematic. The priming sites for sequence verification are given in Appendix E. Formation of primer dimmer and self-complementation are not desired, therefore were controlled by the program Oligo 2.0. The result of this program, together with thermodynamic properties of the designed primers are given in Appendix E.

Table 3.2 Primers used in this study and their sequences

Name	**Sequence (5'-> 3')**
MBPss-for-EcoRI	CACCGAATTCATGAAAATAAAAACAGGTGCACG
G3P-XmaI-Rev	ATCATTCCCGGGTTAAGACTCCTTATTACGCAGTATGTTAGC
XmaIRBSPglB	GCGATGCCCGGGTTAAAGAGGAGAAAGCATATGTTGAAAAAAGAGTATTTAAAAAAC
PglB-stop-SphI-R1	TACTCTGCATGCCTGCAGGTTAAATTTTAAGTTTAAAAACTTTAGCATCTCTAG
PglB-stop-30bp-SphI-R2	TGCAGCATGCTAGTGATGGTGGCCACCAGAGCTCACTAGTCCTGCAGGTTAAATTTTAAG
MBP-GT-4x-Rev1	TGTGGCATTTTGGTCACCGCCGGTCGCGTTCTGATCCTCGAGCTTGGTGATACGAGTCTG
MBP-GT-4x-SalI-R2	TACTGAGTCGACTGTCGCATTCTGGTCACCGCCGGTGGCGTTTTGATCGCCACCTGTGGCATTTTGGTC
trG3P-XhoI-SalI-For	ATAAGCTCGAGGGCGGCGGCGGTAGCGATCAGAATGCGACAGTCGACGAGGGTGGTGGCTCTG

3.3.5. Polymerase Chain Reaction (PCR)

The amplification of DNA was carried out by PCR. The reaction mixture, prepared on ice, contained the following:

- 10x PCR Reaction buffer (with Mg^{2+}) : 5 µL
- dNTP (10 mM stock) : 1 µL
- Forward primer 5µM stock : 3 µL
- Reverse primer 5µM stock : 3 µL
- Template DNA : 100 ng (1-3 µL)
- Taq DNA polymerase (1U/µL) : 1 µL
- Sterile dH_2O : to 50 µL

A commonly used, representative PCR program is given below.

94°C	3 min	x 1 cycle

94°C	45 sec	x 30 cycles
60°C	45 sec	
72°C	1 min	

72°C	7 min	x 1 cycle
4°C	∞	

3.3.5.1. DNA Purification after PCR

After PCR, removal of primers, nucleotides, polymerases and salts was performed by QIAquick PCR Purification Kit (Qiagen), according to manufacturer's instructions. The purified DNA was eluted with 50 µL of EB from QIAquick spin columns.

3.3.6. Digestion of DNA using Restriction Endonucleases

Restriction enzyme digestion reaction mixture prepared in microcentrifuge tube, contained:

- DNA fragment : 0.1 to 5 µg
- 10x Reaction buffer (supplied with the enzyme) : 2 µL
- Restriction enzyme : up to 10 U/µg DNA
- Sterile dH_2O : to 20 µL

The samples were incubated at 37˚C water-bath for minimum 1 h and thereafter run on agarose gel.

3.3.6.1. DNA Purification after Digestion

After restriction endonuclease digestion, removal of primers less than 100 bases, enzymes, salts and unincorporated nucleotides was achieved by QIAquick Nucleotide Removal Kit, according to manufacturer's instructions. At the end of the protocol, purified DNA was eluted with 50 µL of EB from the QIAquick spin column.

3.3.7. Ligation

20 µL first ligation reaction mixture as an example contained the following:

- 10X ligation buffer : 2 µL
- Insert DNA : 10 µL
- Double digested vector DNA : 5 µL
- T4 DNA ligase : 1 µL
- Sterile dH_2O : 2 µL

$$100 \text{ ng vector} : \frac{\text{size of insert (bp)}}{\text{size of vector (bp)}} : \frac{3}{1} = \text{amount of insert (ng)} \qquad (3.1)$$

The amount of insert DNA to be added to the reaction mixture was calculated such that insert:vector ratio of 1:3 was achieved, as given in equation 3.1. A control reaction was also set up, containing all the reagents listed above except the insert. The reaction was carried out for 16h in 16˚C water-bath equipped with cooler. The ligation product was desalted and stored at -20˚C till required and 5 µL was used for *E. coli* transformation.

3.3.8. Transformation of *E. coli*

For propagation of plasmids, or the ligation mixture, *E. coli* DH5α chemically competent cells were used.

One 50 µL vial was thawed on ice for 5 min 5 µL of the plasmid was added and gently mixed by tapping. The vial was incubated on ice for 30 min, then in 42˚C water-bath for exactly 90 sec and immediately placed on ice for 2 min 250 µL of pre-warmed SOB medium (Appendix B) was added to the vial and the vial was incubated at 37˚C for exactly 45 min with shaking. 50-200 µL of transformation mixture was spread on prewarmed LB agar containing the appropriate antibiotics (Appendix B) and incubated at 37˚C overnight.

3.3.9. DNA Sequencing

The sequence of the constructed phagemid was sequenced using sequencing primers. 200-500 ng of purified plasmid DNA was mixed with 1 µL of 4 µM sequencing primer and the final volume was adjusted to 18 µL with sterile dH_2O. The sample was run by the Sequencing Facility (Cornell University, NY). The provided data was analyzed using the freeware ApE v.2.0.45.

3.4. Production of Phages and Phage Purification

3.4.1. Production of Helper Phage

E. coli TG1 was grown in 5 mL 2TY medium at 37°C to OD_{600}=0.5-0.6 (Cells express F-pili at this concentration). The culture was infected with 8 x 10^9 cfu/mL helper phage VCSM13, incubated at 37°C for 25 min. Phage-infected TG1 culture was diluted in 200 mL 2TY and 35 µL kanamycin. Diluted cells was grown at 30°C for over night in shaker. Next day cells were spinned down at 6,000 *g* for 10 min at 4°C. Phage particles were precipitated from supernatant by adding 1/5 volume of mixture PEG/NaCl and incubated on ice for at least 1 hour. Precipitated phage particles were collected by centrifugation at 10,000 *g* for 25 min at 4°C then the phage pellet was resuspended in 4 mL PBS and remaining cells were spinned down at 16,000 *g* for 2 min at 4°C the supernatant was completely discarded and the phage pellet was resuspended in PBS (1/100 volume of supernatant). Phages were collected by centrifugation at 16,000 *g* for 2 min at 4°C. The phage containing solution was filtered through a 0.45 µL filter and stored at -20°C. The phage concentration was determined by OD_{268}.

3.4.2. Production of Phages Displaying Glycans (GlycoPhage)

M9 agar medium containing (20 µg/mL chloramphenicol and 100 µg/mL ampicillin when needed) were inoculated with *E. coli* TG1 Δ*waaL* carrying the appropriate plasmids at 37°C. 6 mL of M9 medium containing (chloramphenicol and ampicillin when needed) were inoculated with a single colony of *E. coli* TG1 Δ*waaL* and shaken at 37°C overnight. Next day, cells were subcultured into 40 mL 2TY containing 1% glucose, 100 µg/mL ampicillin, 20 µg/mL chloramphenicol (2TY/Cm/Amp/Glc) such that the initial OD_{600}=0.05 and shaken at 37°C to OD_{600}=0.5-0.6, so that cells express the f-pili. The culture was infected with 32 x 10^{10} cfu helper phage (VCSM13, Stratagene) and were incubated for 30 min at 37°C without shaking. For recovering cells, flasks were put in to shaker for 10 min at 37°C. Then cells were centrifuged (12 min, at 3300 *g* 16°C). The medium was changed by harvesting the cells by centrifugation and the cell pellet was resuspended in 40mL 2xTY medium containing ampicillin, chloramphenicol and 35 µg/mL kanamycin. The culture was shaken at 30°C for 30 min, 30mM arabinose was added and induced for 16 h.

3.4.3. Phage Purification

The culture supernatant was separated from the cells by centrifugation (6,000 *g* for 12 min 4°C). Phage particles were precipitated from supernatant by adding 1/5 volume of mixture PEG/NaCl and were incubated on ice for at least 1 hour. Precipitated phage particles were collected by centrifugation (10,000 *g* for 25 min at 4°C) then the phage pellet was resuspended in 1 mL 2% sarkosyl in PBS. Then for purifying phage particles precipitation step was repeated and was added 1/5 volume of mixture PEG/NaCl and incubated on ice for at least 1 hour. Precipitated phage particles were collected by centrifugation (10,000 *g* for 25 min at 4°C) supernatant was completely discarded. Phage pellet was resuspended in PBS. Phages which were collected by centrifugation (16,000 *g* for 2 min at 4°C) transfered in PEG/NaCl incubated on ice for at least 1 hour. Next day the phage containing solution was recentirifuged and resusped in PBS based on pellet size. The phage concentration was determined by OD_{268}.

3.5. Analysis

3.5.1. Cell Concentration

Cell concentration was measured using a UV-Vis Spectrophotometer (Thermo Scientific) at 600 nm and 1 mL sample taken from liquid medium was diluted with dH_2O to read OD_{600} in the range 0.1 - 0.8.

3.5.2. Total Protein Concentration

Total protein concentration was determined spectrophotometrically using Bradford assay (Bradford, 1976). 20 µL of sample was mixed with 1 mL of Bradford reagent (BioRad), incubated at room temperature for 5 min and the absorbance was read at 595 nm by UV-spectrophotometer. The calibration curve was obtained using BSA in the concentration range of 0-2 mg/mL (Appendix F).

3.5.3. Phage Concentration

Phage concentration was determined spectrophotometrically at 268 nm (NanoDrop 1000, Thermo Scientific). The calibration equation used for converting absorbance to phage concentration, C_{Ph} (CFU/mL) is given in equation (3.2).

$$C_{Ph} = 5 * 10^{12} * OD_{268} * \text{Dilution Ratio} \quad (3.2)$$

3.5.4. SDS-Polyacrylamide Gel Electrophoresis (SDS-PAGE)

SDS-PAGE was performed as described by Laemmli (1970). Purified protein samples were mixed with the sample buffer and heated in boiling water for 4 min. 20 µL of the samples and 5 µL of a dual color prestained protein MW marker (Appendix D) were run simultaneously at 100 V of constant voltage. The buffers used are given in Appendix A and the detailed protocol is given in Appendix G.

3.5.5. Western Blotting

Western Blotting was performed to distinguish the phage particles by using its specific antibody. After the samples were run on SDS-PAGE gel, the gel was sandwiched between membrane, blotting paper, sponges and the blotting cassette. The membrane (PVDF) used, had been pre-wet with methanol and equilibrated with the Transfer Buffer. Blotting was performed electrophoretically (BioRad), for 3 h at 50 V. The blotted membrane was washed with TBS-T 2-3 times, then with TBS-T-Milk for 1 h, at room temperature, shaking. After 3 washes with TBS-T, the membrane was incubated overnight at 4°C, in primary antibody diluted 1:1000 with TBS-T-Milk. After 3 washes with TBS-T, the membrane was incubated for 1 h at room temperature, in secondary antibody diluted 1:10000 with TBS-T-Milk. After 3 washes, the presence of glycophage was visualized either by peroxidase-based immunocytochemical procedure using an Opti-4CN colorimetric kit (Biorad) or using a chemiluminescent substrate (BioRad), the signals of which were detected by exposing to X-ray film. Detailed protocol is given in Appendix G.

3.5.6. Phage ELISA

For glycophage enzyme-linked immunosorbent analysis (ELISA), high-binding 96-well clear half-area microtiter plates (Corning) were coated with 0.1 - 20 x 10^{10} phage particles in 25 µL of PBS buffer in replicates, and incubated for 18-24 h at 4°C. The plate was blocked with blocking buffer (PBS + 2% nonfat milk) for 2 h at RT. The wells were washed 4 times with PBST (PBS with 0.1% Tween20) and probed with 50 µL of primary antibody and shaken for 1 h at RT, and if secondary antibody was required, the washed wells were probed for 1 hour at RT. After additional washings with PBS, o-phenylenediamine dihydrochloride (OPD) substrate (Sigma) was added to each well and after 40 min the reaction was

stopped with 3 M H_2SO_4. The absorbance in each well was measured at 492 nm (Abs492).

Blots or arrays were probed with one of the following: anti-MBP antibody conjugated with horseradish peroxidase (HRP) (New England Biolabs), hR6 rabbit serum that is specific for the *C. jejuni* heptasaccharide glycan and also recognizes the *C. lari* hexasaccharide glycan (kindly provided by Markus Aebi). For non-HRP conjugated antibodies, anti-rabbit IgG-HRP (Promega) was used as the secondary antibody. HRP activity was detected using a chemiluminescent substrate (BioRad).

4. RESULTS AND DISCUSSION

4.1. Design of Phagemids

The research program is schematically summarized in Figure 3.1., for the production of new phagemids. As part of this study; six new phagemids has been developed, all based on the previously constructed pMGG [19] phagemid. These new phagemids; pMGGP, pMGGP$_{mut}$, pMG$_4$GP, pMG$_4$GP$_{mut}$, pMG$_4$G$_s$P and pMG$_4$G$_s$P$_{mut}$ are schematically summarized in Figure 4.1.

4.1.1 Propagation and Purification of the Backbone for pBAD24 Based New Phagemids

The pMGGP phagemid's insert gene cassette was obtained from pMGG phagemid, pMG$_4$GP phagemid's insert gene cassette was obtained from pMGGP phagemid and pMG$_4$G$_s$P phagemid's insert gene cassette was obtained from pMG$_4$GP phagemid. Moreover, the subscript "mut" at the end of the plasmid name, denoted the mutated PglB enzyme, which should be inactive. However, for the scope of this study, the main difference is the expression of the PglB enzyme from the phagemid. Therefore, all the new phagemids should contain the PglB gene. To add this gene to the phagemid sequence, i.e. constructing pMGGP from pMGG, there were two options: (i) the pglB gene could be amplified and inserted into the pMGG phagemid through restrion sites including a RBS; (ii) the MBP cassette could be amplified and inserted into a pBAD24 phagemid already containing the PglB cassette. Luckily, the second option was previously constructed in a previous study in our research group, and those phagemids, pBAH2B and pBAH2B$_{mut}$ (Guarino, NY) carried the suitable restriction sites to be used as the backbone. Therefore, the *E. coli* DH5α-pBAH2B strain was grown at 37°C, 200 rpm, for t=16h, to obtain the backbone plasmid DNA, which was purified with Miniprep kit (Qiagen) and its concentration was determined with Nanodrop™.

4.1.2. PCR Amplification of Gene Cassettes

Forward and reverse primers given in Table 3.2 were designed to amplify the gene cassettes in PCR, to obtain the phagemids (Fig 4.1), and coupled with the template and other primers as given in Table 4.1. The expected product sizes are also given (Table 4.1). In order to obtain pMG$_4$GP phagemids, two PCR steps were used consecutively to be able to extend the GlyTag sequence.

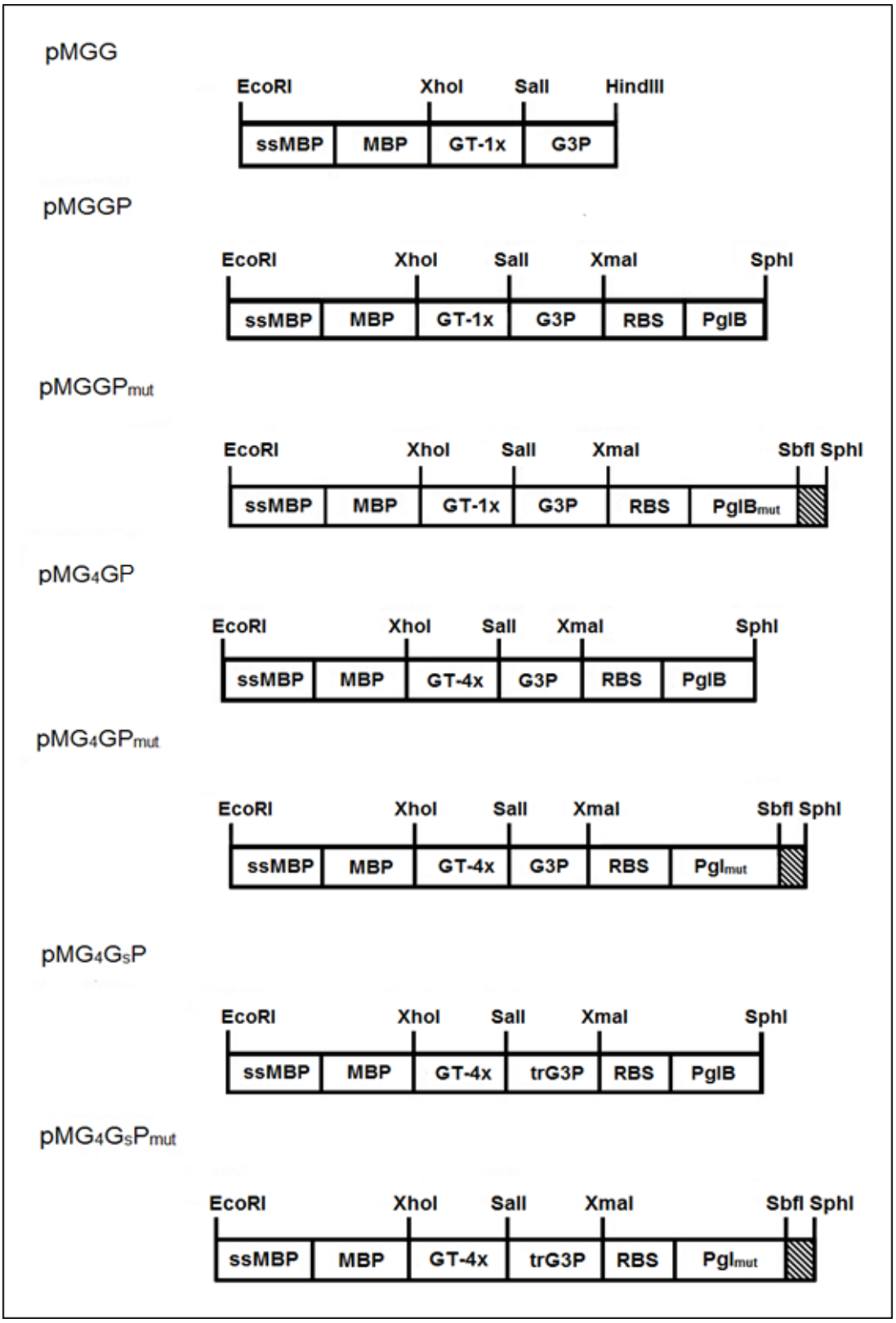

Figure 4.1. Display of new designed phagemids. pMGGP (pBAD-MBP^{DQNAT}-g3p::PglB), pMGGP$_{mut}$ (pBAD-MBP^{DQNAT}-g3p::PglB$_{mut}$), pMG$_4$GP (pBAD-MBP^{4xAQNAT}-g3p::PglB), pMG$_4$GP$_{mut}$ (pBAD-MBP^{4xDQNAT}-g3p::PglB$_{mut}$), pMG$_4$G$_s$P (pBAD-MBP^{4xDQNAT}-g3p$_{tr}$::PglB), pMG$_4$G$_s$P$_{mut}$ (pBAD-MBP^{4xDQNAT}-g3p$_{tr}$::PglB$_{mut}$).

Table 4.1. PCR components and product description

PCR	Template	Forward Primer	Reverse Primer	Product Size
PCR 1	pMGG	MBPss-for-*Eco*RI	G3P-*Xma*I-Rev	2470 bp
PCR 2	pMGGP	MBPss-for-*Eco*RI	MBP-GT-4x-Rev1	1240 bp
PCR 3	PCR2	MBPss-for-*Eco*RI	MBP-GT-4x-*Sal*I-R2	1294 bp
PCR 4	pMG_4GP	trG3P-*Xho*I-For	G3P-*Xma*I-Rev	590 bp

These expected PCR product sizes were controlled by agarose gel, run at 90 V (Fig 4.2). Then, the DNA fragments were excised from the gel and purified from the other gel components. Concentration was determined with Nanodrop (The Thermo Scientific NanoDrop 1000) and stored at 4°C until used further in digestion reactions.

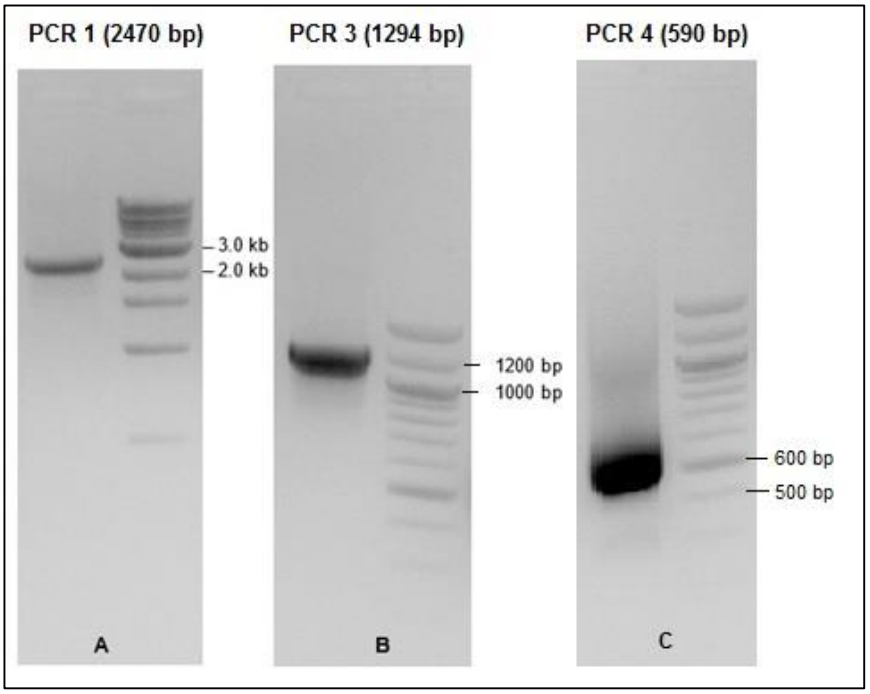

Figure 4.2. Agarose gel electrophoresis results of amplified gene cassette.

4.1.3 Digestion and Ligation Reactions

The restriction digestion enzymes used in this study, given in Table 4.2, had been selected with criteria to cut the template DNA with correct restriction sites matching the backbone plasmids. The expected DNA fragment sizes are also given in the table below.

Table 4.2. Digestion reactions

Digestions	Template	Forward RE	Reverse RE	Restriction Size
D0	pBAH2B	*Eco*RI	*Xma*I	6661 bp
D1	PCR 1	*Eco*RI	*Xma*I	2458 bp
D2	$pBAH2B_{mut}$	*Eco*RI	*Xma*I	6672 bp
D3	PCR 3	*Eco*RI	*Sal*I	1282 bp
D4	PCR 4	*Sal*I	*Xma*I	544 bp
D5	pMGGP	*Sal*I	*Eco*RI	7888 bp
D6	$pMGGP_{mut}$	*Sal*I	*Eco*RI	7926 bp
D7	pMG_4GP	*Sal*I	*Xma*I	7939 bp
D8	pMG_4GP_{mut}	*Sal*I	*Xma*I	7977 bp

DNA (1-2 µg) was digested with restriction enzymes (Table 4.1 and Table 4.2) at 37°C for 1 hour. Calf-intestinal alkaline phosphatase enzyme (CIAP, Invitrogen) was used after restriction digestion of vector DNA to remove 5'-phosphates groups to prevent recircularization of linearized vector DNA, before ligation. The expected size of the PCR products (Table 4.2) were controlled by agarose gel run at 90 V and visualized under UV light as seen from the agarose gel photos (Fig 4.3, Fig 4.4 and Fig 4.5) and the size confirmed bands were then purified from gel (Qiagen Gel Purification Kit). Vector and gene cassette's concentration were determined with Nanodrop. Afterwards, for sticky end ligation reaction, digested PCR gene products, vector DNA and ligation enzymes were put into the ligation reaction for a nightlong at 16°C.

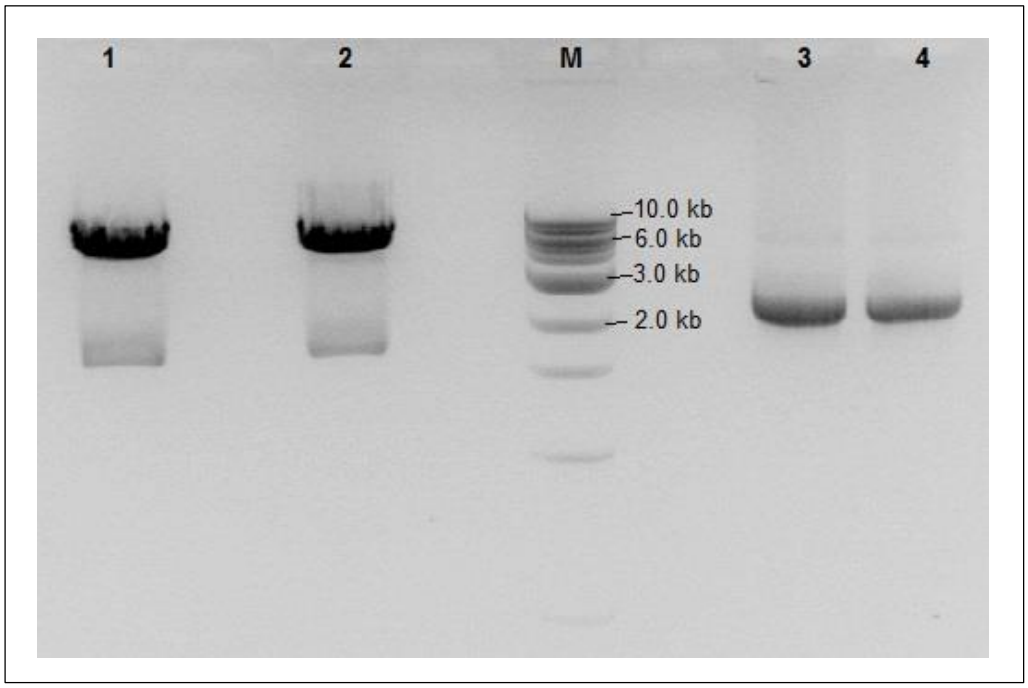

Figure 4.3. Agarose gel electrophoresis of products of digestion reactions. 1: D0 (6661bp), 2: D2 (6672 bp), 3-4: D1 (2458 bp).

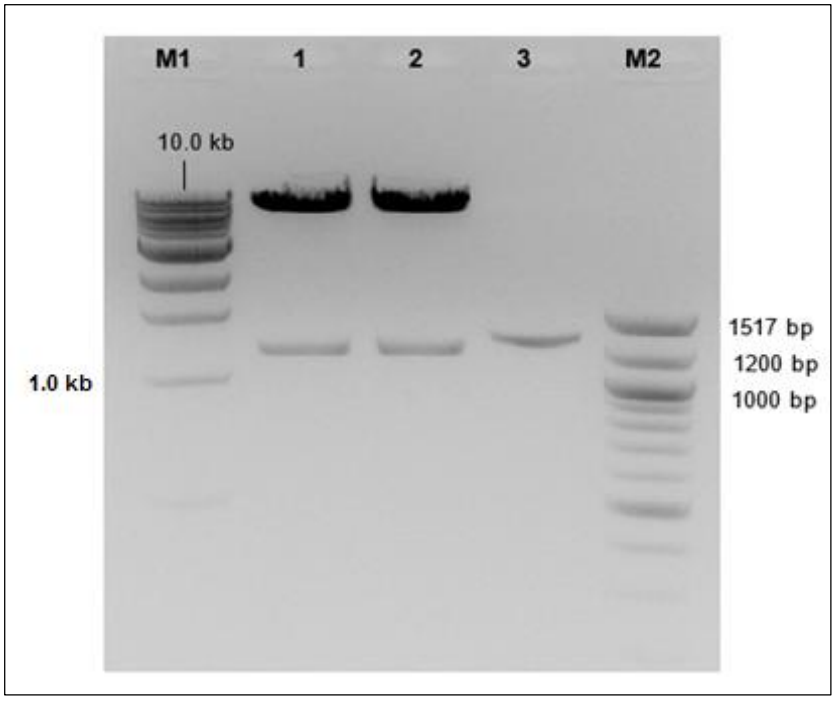

Figure 4.4. Agarose gel electrophoresis of plasmid and gene (insert) digested with restriction enzymes. 1: D5 (7888 bp), 2: D6 (7926 bp), 3: D3 (1282 bp).

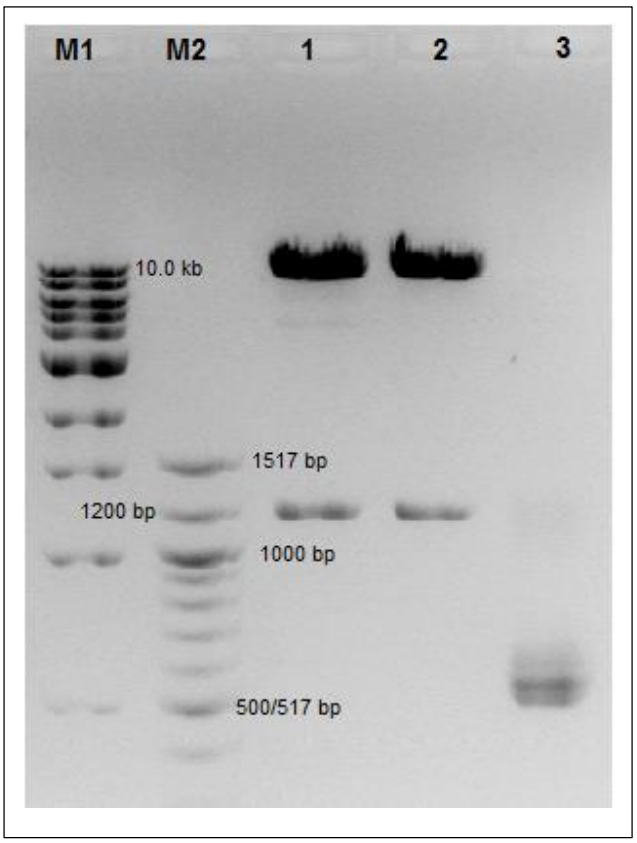

Figure 4.5. Agarose gel electrophoresis of plasmid and gene (insert) digested with restriction enzymes. 1: D7 (7939 bp), 2: D8 (7977 bp), 3: D4 (544 bp).

The ligated pieces of digestion products, the products of the ligation reactions with putative plasmids named as pMGGP, pMG$_4$GP, pMG$_4$G$_s$P, pMGGP$_{mut}$, pMG$_4$GP$_{mut}$, pMG$_4$G$_s$P$_{mut}$ phagemids, and their final sizes are given in Table 4.3. The ligation products were controlled after the transformation step.

Table 4.3. Ligation reactions

Ligation #	**L1**	**L2**	**L3**	**L4**	**L5**	**L6**
Digestions used in ligation	D0-D1	D0-D2	D5-D3	D6-D3	D7-D4	D8-D4
Product	pMGGP	pMGGP$_{mut}$	pMG$_4$GP	pMG$_4$GP$_{mut}$	pMG$_4$G$_s$P	pMG$_4$G$_s$P$_{mut}$
Product Size	9119 bp	9130 bp	9170 bp	9208 bp	8483 bp	8521 bp

4.1.4. Transformation of *E. coli*

E. coli DH5α strain were transformed using $CaCl_2$ transformation with the desalted ligation, products and the transformed cells were spread onto LB-ampicillin agar plates, for overnight growth at 37°C. Negative controls for transformation reaction included only the backbone plasmid but not the insert. Non-transformed cells were also included as negative control. Colonies from selective plates were grown in LB-ampicillin culture media overnight, and plasmids were isolated the next day. Backbone only plates compared to those includng insert contained at least 5-fold lesscolonies indicating that colonies on selective plates carried the insert. Moreover, non-transformed control cells yielded no colonies on selective plates as expected.

4.1.5. Restriction Digestion and DNA Sequencing to Select the True Transformants

The purified plasmids were digested again with restriction digestion enzymes (Table 4.2). The digestion products were run on agarose gel for verification of the size and successively visualization under UV light (Fig 4.6, Fig 4.7 and Fig 4.8). Thereafter, the plasmids with correct digestion products of pMGGP, pMG_4GP, pMG_4G_sP, $pMGGP_{mut}$, pMG_4GP_{mut} and $pMG_4G_sP_{mut}$ phagemids were sequenced for confirmation (Cornell, NY).

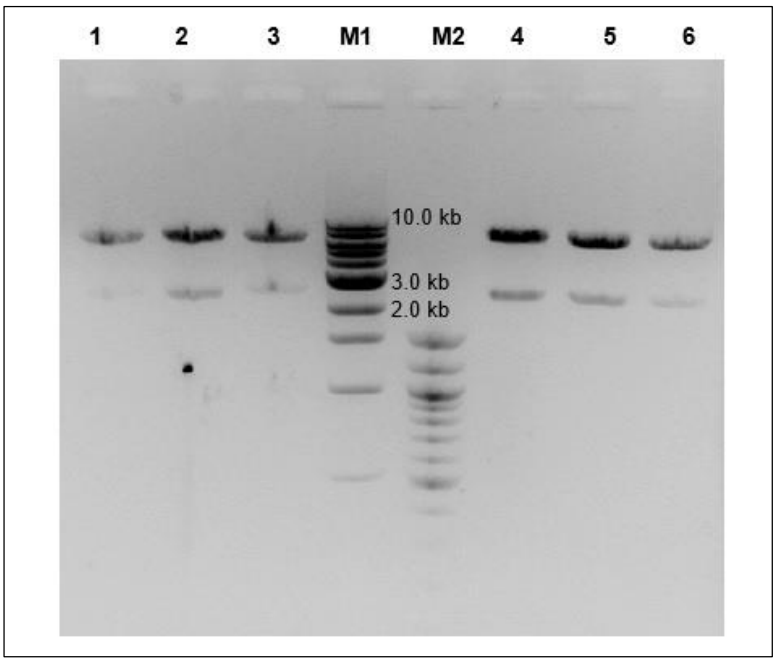

Figure 4.6. Agarose gel electrophoresis of digested recombinant phagemids after ligation. 1-2-3: L1: (6661-2458 bp), 4-5-6: L2: (6672-2458 bp).

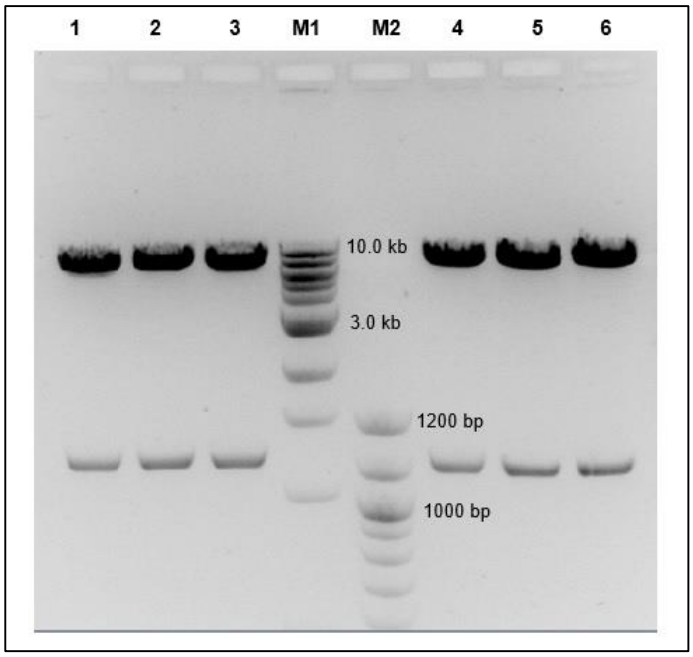

Figure 4.7. Agarose gel electrophoresis of digested recombinant phagemids. 1-2-3; L3 (7888-1282 bp), 4-5-6; L4 (7926-1282 bp)

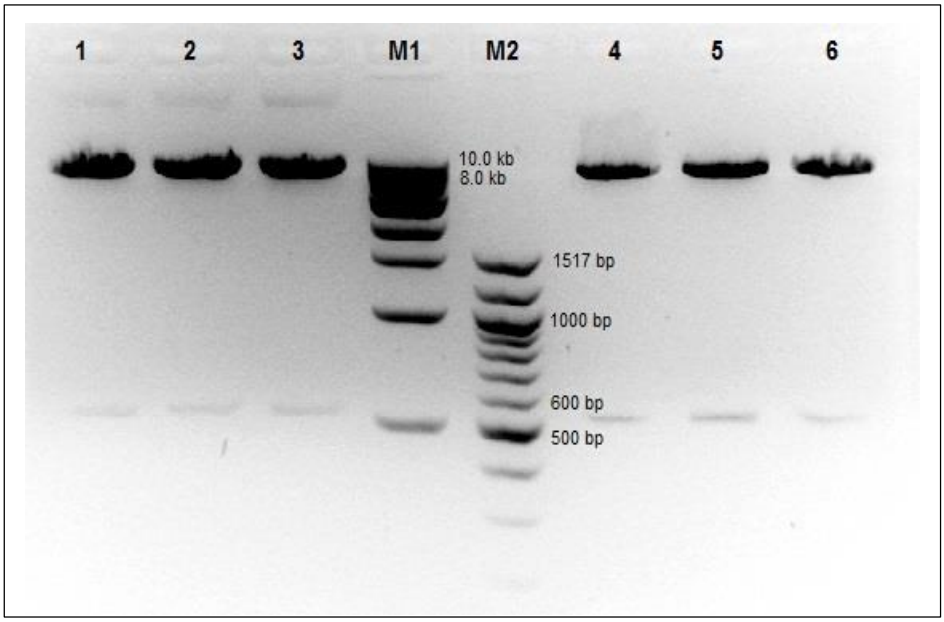

Figure 4.8. Agarose gel electrophoresis of digested recombinant phagemids. 1-2-3; L5 (7939-544 bp), 4-5-6; L6 (7977-544 bp)

4.2. Host Cell Engineering

The host cell, *E. coli* TG1 Δ*waaL* [169] , devoloped by our research group, used in glycophage production was analysed by Fluorescence-activated cell sorting (FACS, BD BioSciences) using a labeled SBA lectin (Sigma), to verify the deletion of the waaL gene. The gene encodes O-antigen ligase, which is responsible for attaching the O-antigen to lipid A-core oligosaccharide. Therefore the deletion of the gene potentially increases the pool of glycans, that are necessary for the glycosylation of the phage particles [173]. The majority of the population was non-fluorescent, showing that the waaL gene was not present (Fig 4.9). Although there was a small subpopulation of cells potentially exposing glycans on their outer membranes in cells expressing PglB (green line, Fig 4.9), rest of the population should be sufficient for producing the glycosylated phage particles.

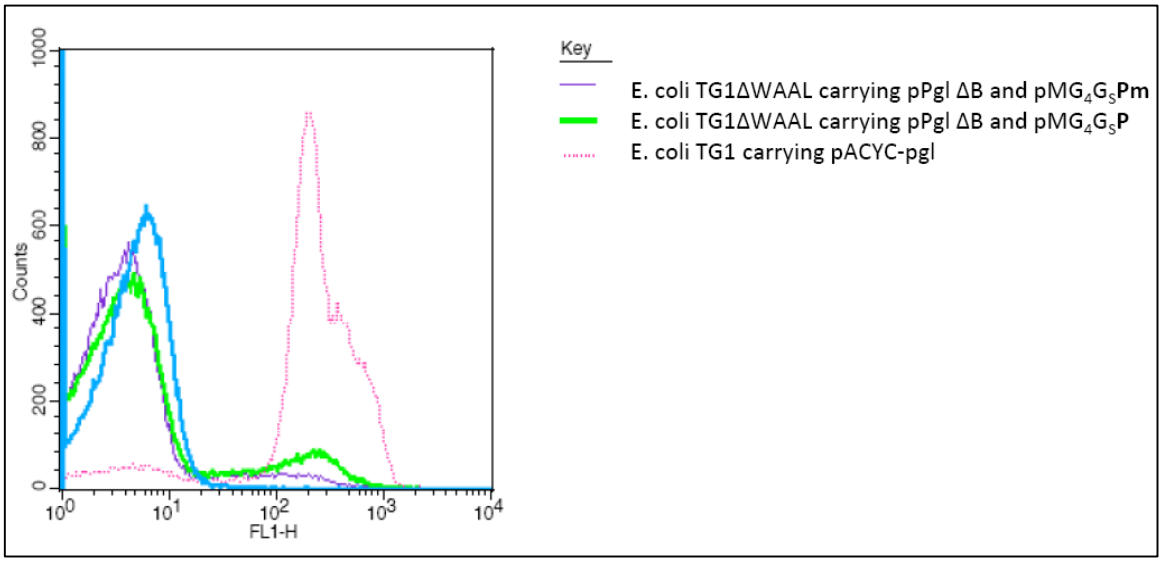

Figure 4.9 FACS analysis of different *E. coli* TG1 strains to verify waaL gene knockout.

4.3. Production of Helper Phage and GlycoPhage Nanoparticles

4.3.1. Effect of the size of g3p on glycophage production

The size of the displayed fusion protein can affect the assembly of phage particles out of the host cell [174]. Carboxyl-terminal domain of g3p is sufficient for the release of phage particle from the host cell, as well as its stability [95]. Although the N-terminal fragment of g3p is required for infectivity [175] wild type g3p is

incorporated together with recombinant g3p, and therefore the recombinant phage particles were still infectious. Fusing the protein of interest to a C-terminal fragment of g3p (CT) lowered the size of the fusion protein (Fig 4.10) by truncating g3p. This strategy was motivated by the fact that fusion to the CT can be more stable than fusion to full-length g3p [176] and also that shortened g3p enables better display of certain structures by relieving spatial constraints that occur with fulllength g3p [177], however the phage production capacity was not affected significantly by the size of the g3p.

The presence of the immunoreactive bands only for the helper phage infected cultures confirmed the display of the glycoprotein on the phage particles (Fig 4.10-a, lanes 2,3,5 and 6). The absence of anti-glycan immunoreactive bands for the phage samples produced from cells containing the non-glycosylatable phagemids,that was not infected with helper phage (Fig 4.10-b, lanes 1 and 4) and the phagemid expressing a mutated PglB, $pMG_4G_SP_{mut}$ (Fig 4.10-b, lanes 2 and 5), indicated that glycosylation of phage displayed protein was specific. On the other hand, as well as the degradation bands observed in the system with full length g3p, pMG_4GP (Fig 4.10-b, lane 3), led to conclusion that the truncated g3p fusions were superior for further glycophage studies (pMG_4G_SP) (Fig 4.10-b, lane 6).

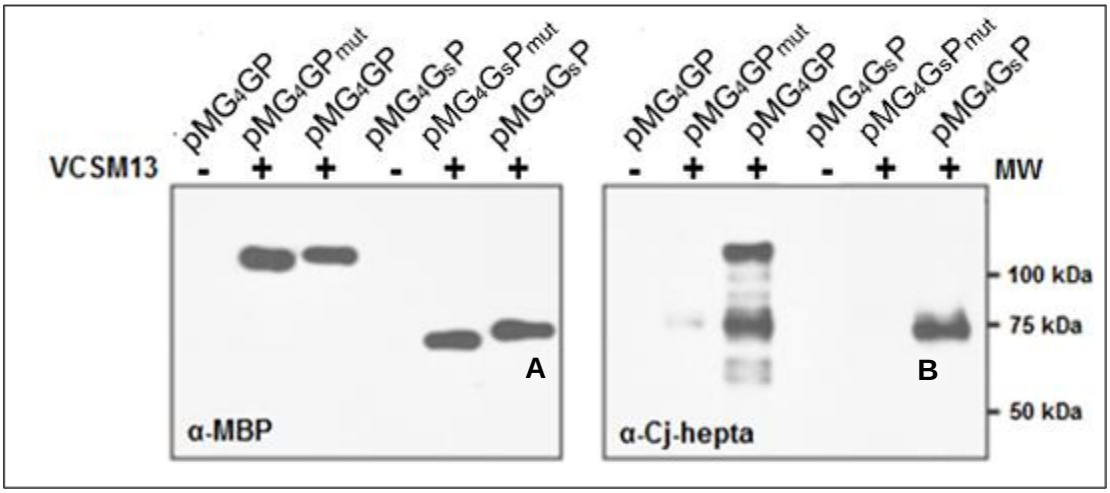

Figure 4.10. Western blot analysis of $4x10^{10}$ phage particles produced from *E. coli* TG1 Δ*waaL* carrying pPglΔB plasmid and the phagemid, pMG_4GP_{mut}, pMG_4GP, $pMG_4G_SP_{mut}$ or pMG_4G_SP. The samples from non-infected cultures were loaded based on cell concentration. Both SDS-PAGE jels were loaded the same. After blotting antibodies used are **(a)** anti-MBP **(b)** anti-glycan.

4.3.2 Purification of glycophage samples

The purification strategy is crucial to get specific but yet detectable signal. Six different purification conditions were tested (Fig. 4.11). Non-infected culture control was also included. The purified phage particles were analysed by glycophage-ELISA assays after titering the phage.

The higher anti-glycan (HR6P) signal obtained in sarkosyl treated samples in ELISA assays (Fig 4.11, lane 8) could be due to a detergent artifact, which should be washed away during the precipitation. Pgl and Pgl_{mut} containing phage particles treated two round precipitation with PEG gave almost same signal with each other and lower signal than sarkosyl treated samples (Fig 4.11, lane 4 and 6).

Samples bound differently to ELISA plates that is evident from the effect of the detergent on binding to the ELISA plates (Fig 4.11). The remaining detergent maybe effecting the glycophage samples binding to the plates, and similarly to the array targets. Thus, after the second round of precipitation with the detergent, the third round can be performed without a detergent, to wash the detergent away, which has comparabily low display-loss rates.

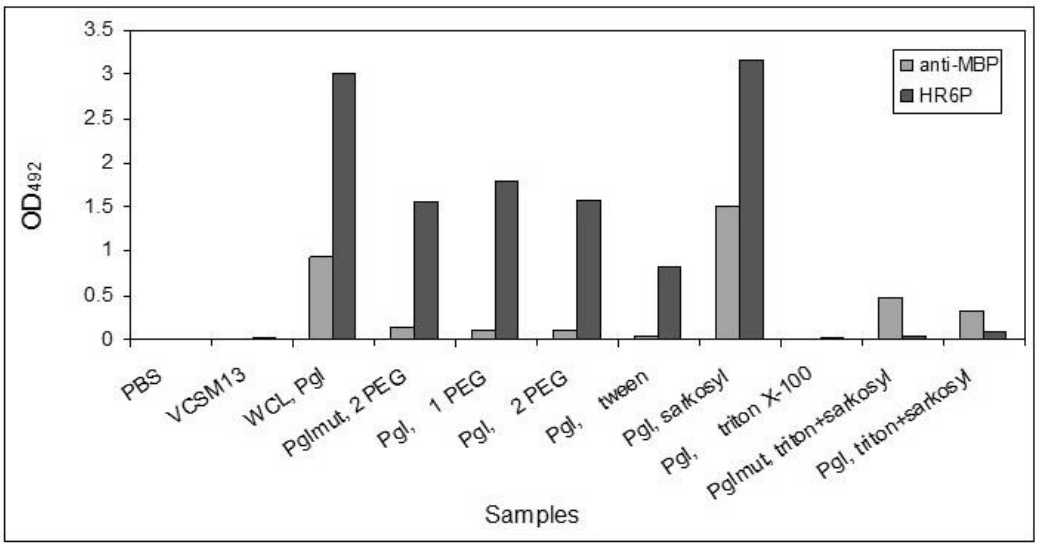

Figure 4.11. ELISA analysis of glycophage samples purified by six different strategies. PBS and helper phage (VCSM13) were included as negative controls and whole cell lysate (WCL) was included as positive control. Six strategies were (i) 1-step precipitation with PEG, (ii) 2-step precipitation with PEG, (iii) PBS-tween wash followed by PEG precipitation, (iv)PBS-sarkosyl wash followed by PEG precipitation, (v) PBS-triton X-100 wash followed by PEG precipitation, (vi) PBS+triton X-100+sarkosly wash followed by PEG precipitation.

4.3.3. Effect of induction conditions on cell growth and phage production capacity

Phage particles were produced from *E. coli* TG1 Δ*waaL* carrying pPglΔB plasmid and the phagemid pMG_4G_sP. Nine different strategies has been used for optimization of phage production capacity and cell growth by optimizing; cell concentration at the time of infection ($OD_{600,infection}$), volume of helperphage used for infection (V_{VCSM13}) and different induction hours (t_{ind}) (Table 4.4).

Table 4.4 Phage production capacity for different phage production strategies.

	Experimental Condition				Experimental Results				
#	Phagemid	OD_{600} (Infection)	V_{VCSM13}*	Hour (Ind.)	OD_{600} (Final)	OD_{268}	CFU/mL	Total CFU	CFU/cell
1	pMG_4G_sP	0.6	V	16	4.1	1.72	8.6E+12	3.4E+12	5.7E+12
2	pMG_4G_sP	0.2	V	16	3.9	1.63	8.2E+12	1.6E+12	8.2E+12
3	pMG_4G_sP	0.45	V	16	4.1	1.78	8.9E+12	2.2E+12	4,9E+12
4	pMG_4G_sP	1.2	V	16	4.1	1.47	7.4E+12	2.9E+12	2.5E+12
5	pMG_4G_sP	0.6	2V	16	4.1	1.96	9.8E+12	3.9E+12	6.5E+12
6	pMG_4G_sP	0.6	V	12	2.9	1.18	5.9E+12	1.2E+12	2.0E+12
7	pMG_4G_sP	0.6	V	20	4.0	1.73	8.7E+12	3.5E+12	5.8E+12
8	pMG_4G_sP	0.6	V	24	4.0	1.59	8.0E+12	3.2E+12	5.3E+12
9	pMG_4G_sP	0.6	V	40	4.0	1.43	7.2E+12	2.9E+12	4.8E+12

***** V= $8x10^9$ cfu/mL ; 2V= $16x10^9$ cfu/mL VCSM13 used at infection.

Most of the parameters given in Table 4.4 did not greatly influence the cell growth (Fig 4.12), except in the case where induction was carried for 12 hour, as expected. On the other hand, the phage production capacity was significantly affected (Fig 4.13, Fig 4.14). Eventually, when more VCSM13 (Helper phage) was used for infection, i.e. two times more than usual volume, %15 increase was obtained at phage final concentration (Table 4.4), instead of %50 increase expected (increase from 3.4 x 10^{15} to 3.9 x 10^{15}). Thus, more helperphage didn't trigger the production of as much glycophage in the end.

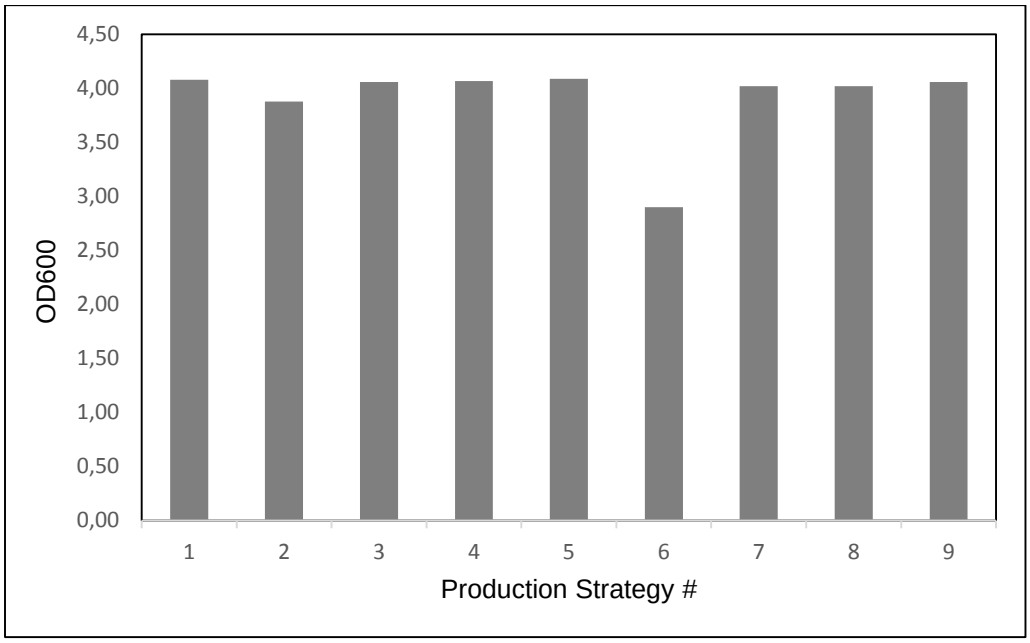

Figure 4.12. Final cell concentration ($OD_{600,final}$) in nine different glycophage production strategies.

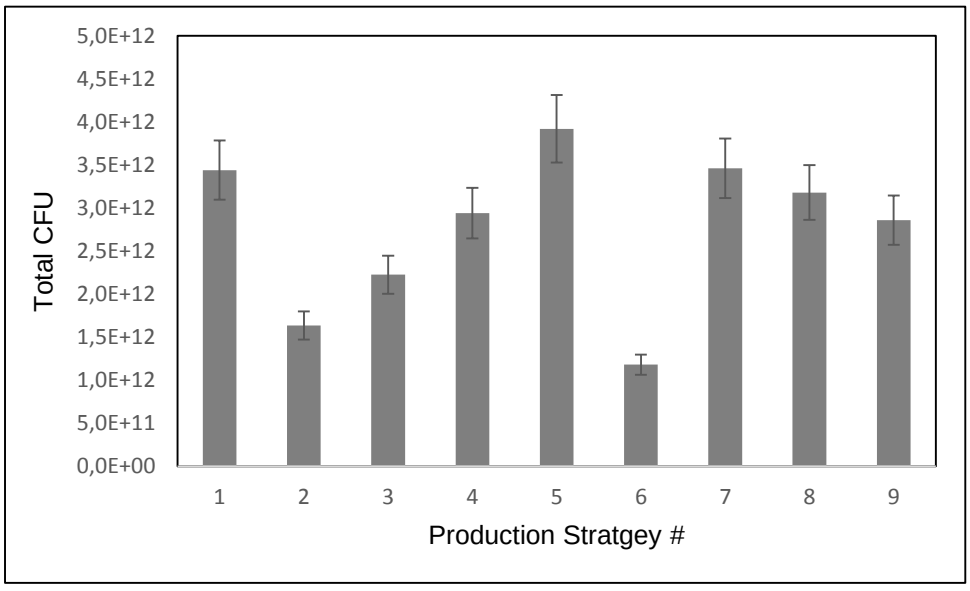

Figure 4.13 Phage production capacity (total CFU) for nine different glycophage production strategies.

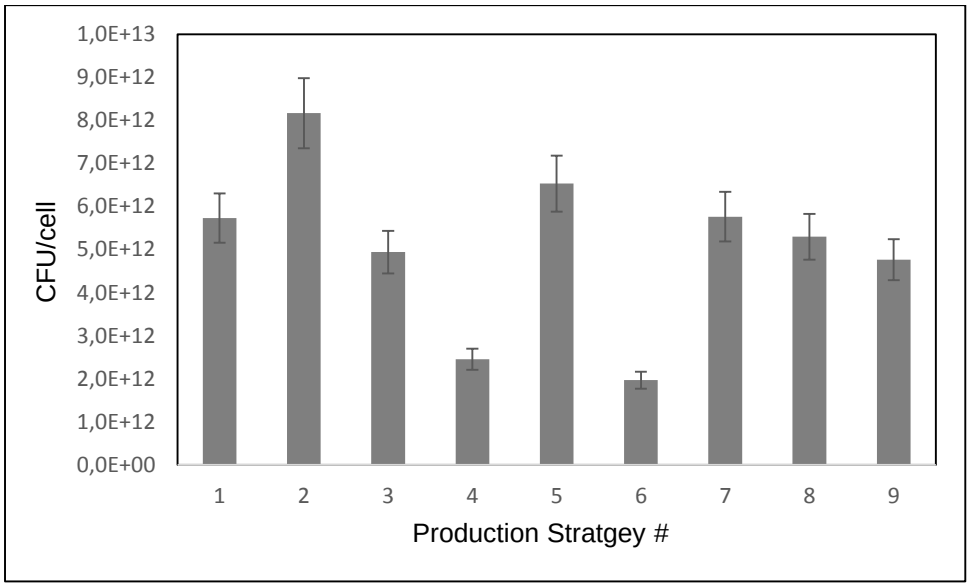

Figure 4.14 Phage production capacity per cell (CFU/OD_{600}) for nine different glycophage production strategies.

Phage production period was investigated for 12, 16, 20, 24 and 40 hours. Final phage particle concentration was obtained optimally between 16-20 hours (Fig 4.15). Similarly, cell concentration increased with induction time until 16 hour (Fig 4.16).

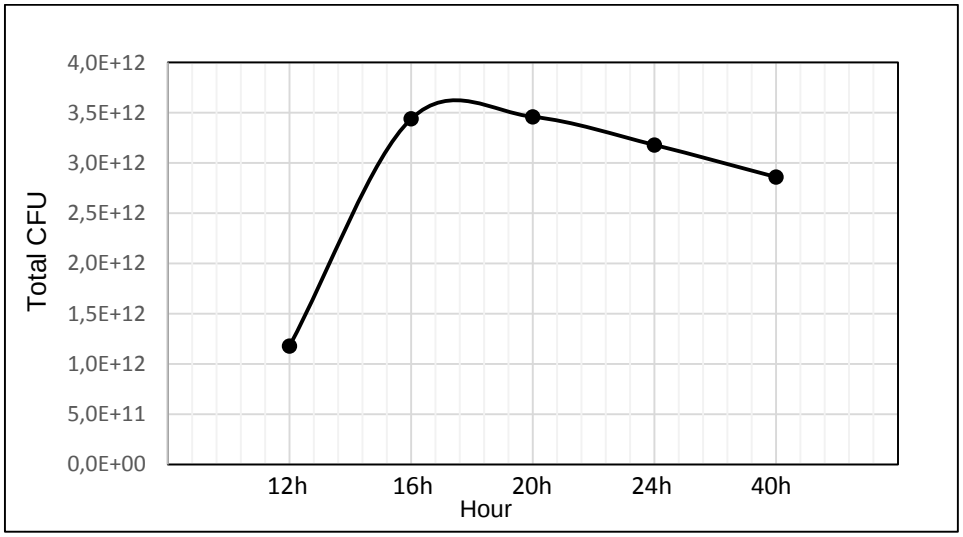

Figure 4.15 Phage particles produced (CFU_{Total}) at different phage production (induction) periods (12, 16, 20, 24 and 40 hours).

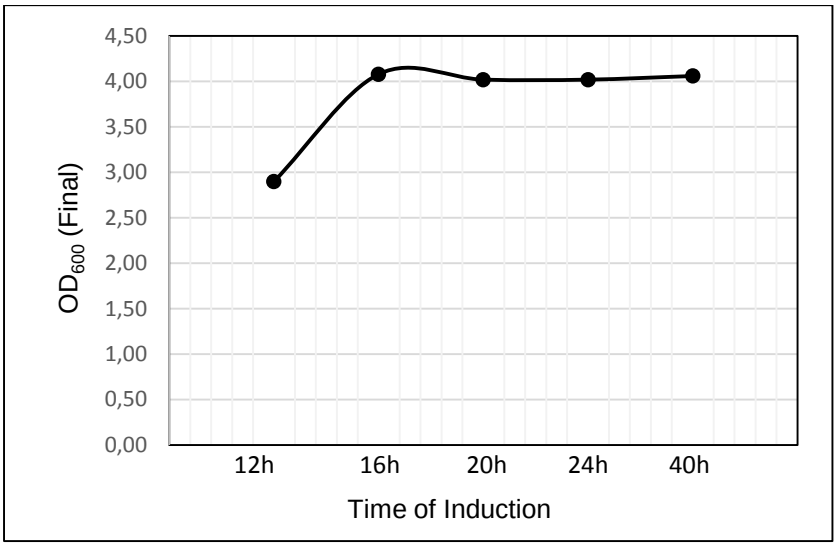

Figure 4.16. Final cell concentration (OD_{600}) at different phage production (induction) periods (12, 16, 20, 24 and 40 hours).

Shortening or postponing infection time from OD_{600}= 0.2 to OD_{600}= 1.2 have a significant effect on phage production and growth capacity. Infection time gives the best production and growth results at OD_{600}= 0.6, with infection concentrations from OD_{600}=0.2 to OD_{600}= 0.6, phage final efficiency was increased, conversely from OD_{600}= 0.6 to OD_{600}= 1.2 yield started to decrease (Fig 4.17, Fig 4.18).

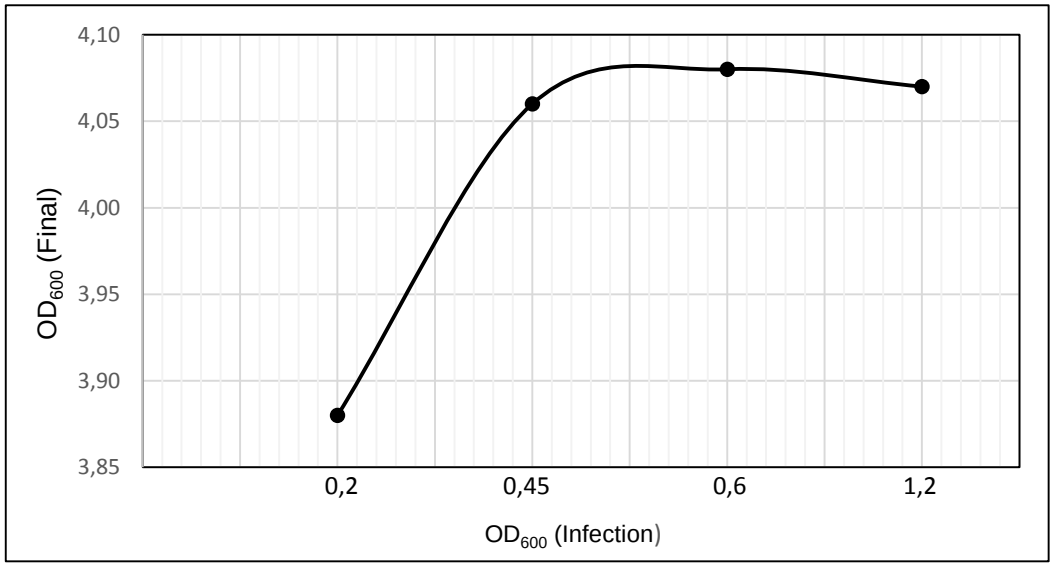

Figure 4.17. Final cell concentration (OD_{600}) based on different cell concentrations at the point of phage infection (OD_{600}= 0,2; 0.45; 0.6; 1.2).

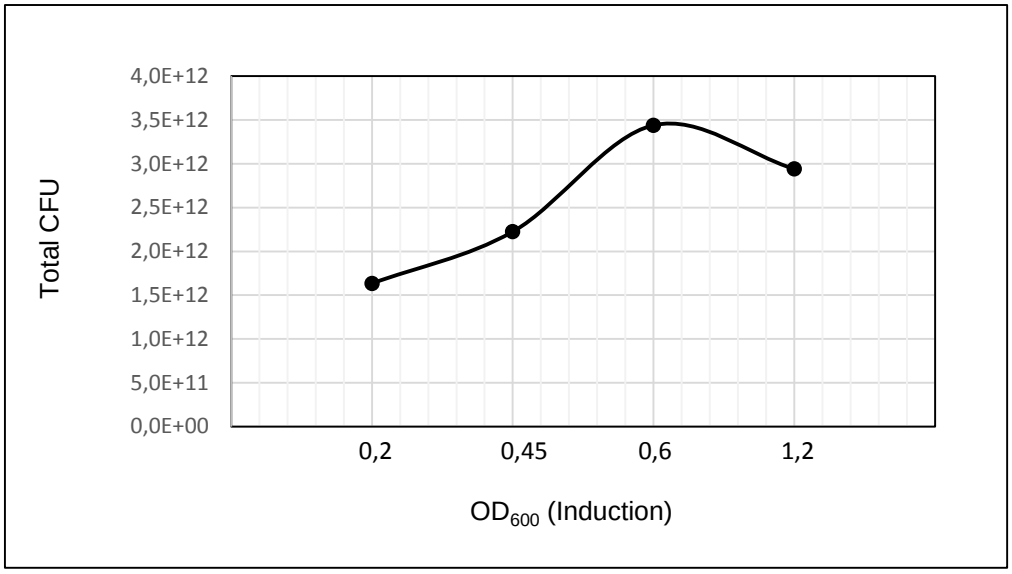

Figure 4.18. Final phage particles concentration (CFU_{Total}) based on different cell concentrations at the point of phage infection (OD_{600}= 0.2; 0.45; 0.6; 1.2).

4.4 Analysis of GlycoPhages for Glycomics Analysis

Glycophage-ELISA method, based on identifying and profiling glycans covalently bonded to phages with anti-glycans or lectins, was developed, for potential use in glycomics analysis in the future. For “proof-of-concept”, the avaiblity of the specific signal, its quantitive value and lowness of non-spesific signals are important. For this purpose, initially, the type of ELISA and one of most important method parameters, ie., type of blocking buffer, were optimized.

4.4.1 Comparision of ELISA methods for GlycoPhages

In this contex firstly, two types of sandwich ELISA (Fig 4.19, B1 and B2) and indirect ELISA (Fig 4.19, B3) methods were examined. Purified phage particles were immobilized on 96-well ELISA plates: (i) the standard glycophage produced from *E. coli* TG1ΔwaaL host carrying pPglΔB plasmid and pMG_4GsP phagemid and infected with helper phage (GT-C.j); and as control groups, (ii) buffer solution (PBS); (iii) wild-type (helper) phage (VCSM13); (iv) glycophage displaying a non-specific glycan (GT-NS), (i.e. those produced from cells carrying an O-antigen coding plasmid (pMWO78) instead of the *C. jejuni* glycan coding plasmid (pPglΔB)); and (v) glycophages produced the same way, but has no glycans attached, in spite of its full plasmid and phagemid system, due to a mutation in the phagemid used (absence of glycans: No-GT).

As a result, while VCSM13, No-GT and GT-NS control groups gave low signal, immobilized glycophages detected with two antibodies gave significantly high and detectable signal (Fig. 4.19, A3). Therefore, indirect ELISA method was determined as the most suitable model (Fig. 4.19, B3).

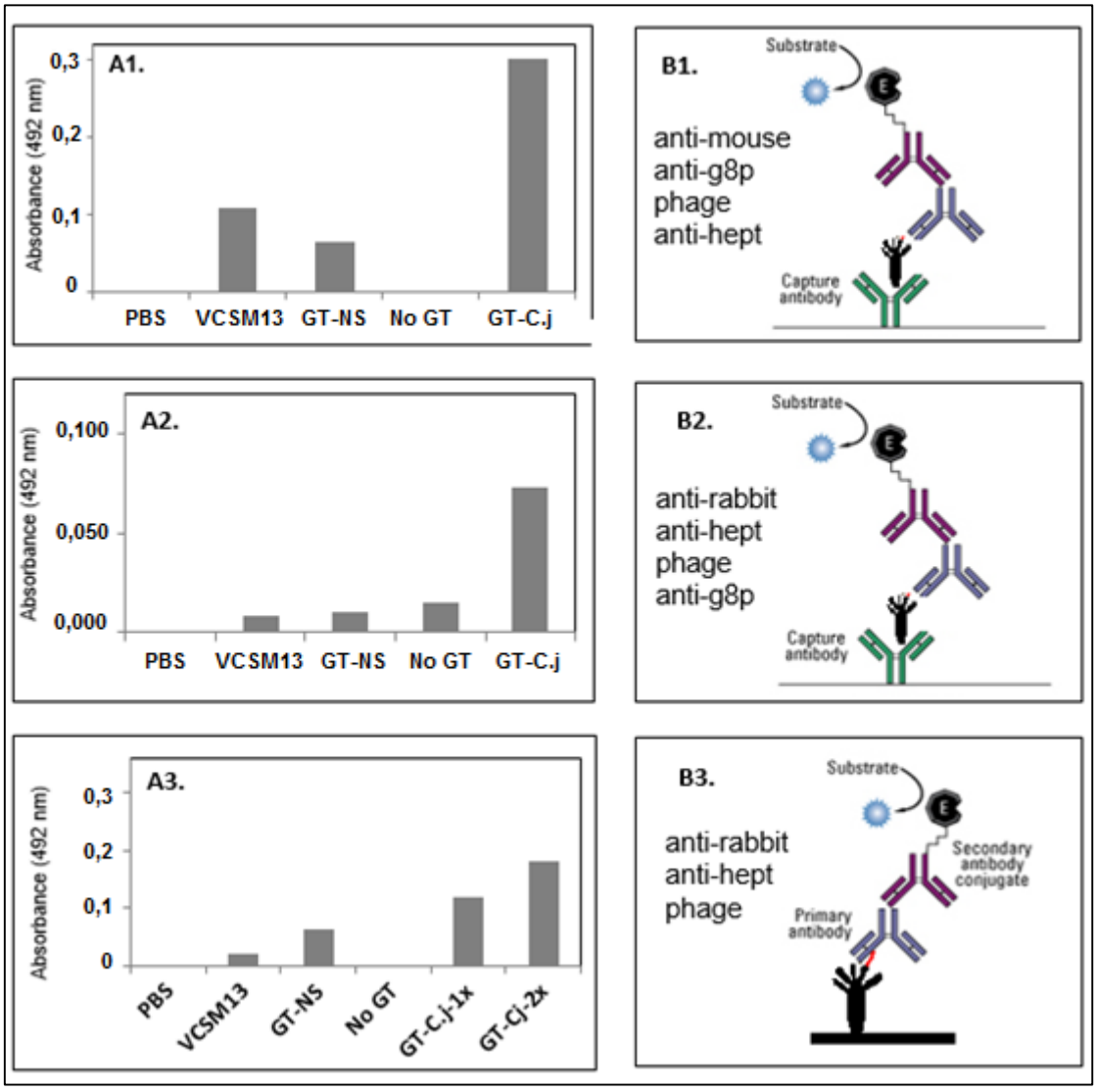

Figure 4.19 Comparison of glycophage-ELISA based on three diffrent methods. PBS: Phosphate Buffered Saline; VCSM13: Helper phage, GT-NS: Non-spesific glycophage, No-GT: Glycophage produced but with no glycans due to inactive PglB, GT-Cj: Phage carriying *C. jejuni* glycans (Glycophage).

4.4.2 Effect of Blocking Buffer Type on GlycoPhage ELISA Analysis

Once the antibody or protein antigens have been properly adsorbed onto the ELISA plate, the next critical step in creating a reliable immunoassay is the blocking of the plate. Proper blocking of the unoccupied areas of the ELISA plate wells will prevent nonspecific binding, reduce background signal, block nonspecific binding to adsorbed proteins, stabilize proteins adsorbed to plate for better interactions.

Using glycophage (pMG_4G_sP) and wild-type phage (VCSM13), glycophage-ELISA analysis blocking procedures were performed with two different blocking buffers, %2 BSA-PBS (bovine serum albumine) and %2 milk-PBS buffers. These are the two most commonly used buffers in ELISA methods and western blots. Immobilized plates treated with %2 BSA-PBS buffer gave significantly higher signal compared to when %2 milk-PBS blocking buffer is used. More importantly, the concentration difference between helper phage and glycophage is distinctly obvious for %2 BSA treated plates, which is especially critical at low dilution of phages.

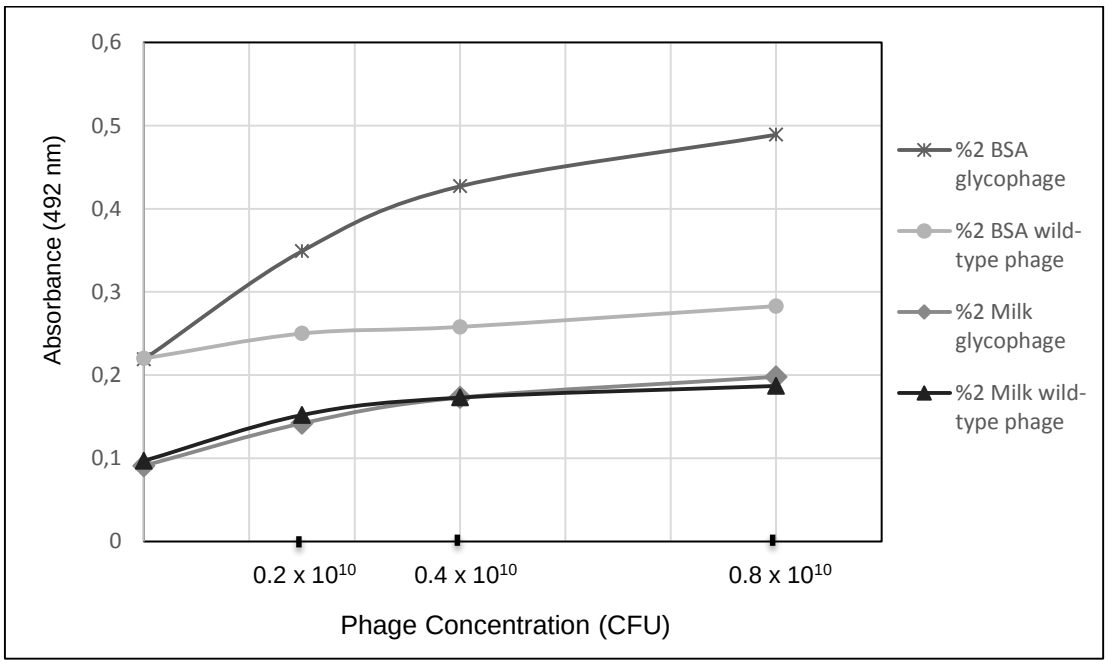

Figure. 4.20 Glycophage-ELISA analysis of glycophage (produced from *E. coli* TG1ΔwaaL host carrying pPglΔB plasmid and pMG4GsP phagemid) and wild-type phage (VCSM13) samples. After sample immobilization onto ELISA plates, the wells were blocked with different blocking buffers: %2 BSA-PBS or %2 milk-PBS.

5. CONCLUSION

The previously developed glycophage display system [19] was redesigned wihtin the scope of this thesis study, for the field of glycomics, utilizing tools of glycobiology, recombinant DNA technology, phage display system and the ELISA technique. The novelty of the approach used in this study lies in the *in vivo* production of glycosylated nano-particles (glycophages) in *E. coli*, and rapid precipitation-based purification of the well-defined glycophages from culture supernatant. The basic parameters for production, purification and immobilization of the newly synthesized glycophage particles were also optimized.

In the first stage of the study, the glycophage system [19] was redesigned for use in glycan array fabrication in several ways. Number of modifications were made to the original phagemid system in order to increase the efficiency and stability of glycan expression on the phage particles and to endow the ability to produce a diverse set of glycans from the original phagemid pBAD-MBP^{DQNAT}-g3p (pMGG) developed previously [19]. Firstly, additional acceptor sites were introduced for glycan attachment to MBP. This involved replacing MBP^{DQNAT} in pBAD-MBP^{DQNAT}-g3p with a version of MBP that was C-terminally modified with four tandem repeats of the bacterial glycan acceptor motif DQNAT, resulting in the phagemid pBAD-MBP^{4xDQNAT}-g3p (pMG$_4$G). Secondly, the bicistronic phagemid pBAD-MBP^{4xDQNAT}-g3p::PglB (pMG$_4$GP) that encodes both the MBP-g3p fusion and the *C. jejuni* PglB enzyme was generated, thereby affording inducible control over OST expression. Moreover, PglB is needed for transferring other recombinantly produced glycans (e.g. O-antigen polysaccharides) [18]. Hence, this bicistronic phagemid provides a copy of the PglB enzyme for future glycan library building. Thirdly, a truncated version of g3p in the phagemid was created, i.e., pBAD-MBP^{4xDQNAT}-g3p$_{tr}$::PglB (pMG$_4$G$_s$P). Fourthly, inactivated PglB (PglB$_{mut}$) versions of all the above phagemids were created (pMGGP$_{mut}$, pMG$_4$GP$_{mut}$, pMG$_4$G$_s$P$_{mut}$), to serve as negative controls. The newly constructed phagemids were confirmed by restriction digestion and DNA sequencing analyses.

In the second stage, the deletion of the *waaL* gene from the genome of *E. coli* TG1 to create *E. coli* TG1 Δ*waaL* host cell [169] was analysed and verified by FACS, before its use in glycophage production. The waaL O-antigen ligase in *E.*

coli transfers lipid-linked glycans onto lipid A and reduces protein glycosylation efficiency by depleting the pool of available substrates for PglB [18].

In the third stage, in order to increase the glycophage stability and production efficiency, basic parameters for glycophage production and purification were optimized, with respect to g3p size, detergents used in purification of glycophage samples, and induction conditions. Firstly, because display efficiency and fusion stability often decrease with protein size, possibly as a consequence of coat protein proteolysis, the overall size of the displayed fusion protein decreased by truncating g3p. Phage production by these cells was initiated by superinfecting cultures VCSM13 helper phage followed by induction of fusion protein expression. At the end of the induction phase, recombinant phage particles were recovered from these cells. The resulting phage titers from TG1 *waaL* cells expressing $MBP^{4xDQNAT}$-g3p or $MBP^{4xDQNAT}$-$g3p_{tr}$ were indistinguishable, indicating that the shortened g3p did not adversely affect phage production. Western blot analysis of phage preparations confirmed, with no degradation bands, that the truncated g3p fusions were superior for the next studies compared to full-length g3p. Secondly, six different purification conditions were investigated with glycophage ELISA analysis, and sarkosyl treated samples gave the higher and specific signal. Thirdly, cell growth and phage production capacity was improved via investigation of different induction conditions. The highest glycohage production conditions were obtained in the case where, OD_{600}=0.6 at the time of infection, $8x10^9$ CFU/mL of helper phage is used for infection and induction period is 16 h.

Lastly, “glycophage ELISA” method was improved for glycomics analysis and indirect ELISA method was choosen as the suitable ELISA type. Afterwards, inorder to obtain a more specific signal from ELISA analysis, blocking step was tested with two types of blocking buffers. Glycophage immobilized plates treated with %2 BSA-PBS buffer gave a significantly higher anti-glycan signal compared to the control group. The method can be continued to be devoloped with various other parameters in the future experiments, in order to increase the signal and its specificity.

The developed method introduces a facile, scalable production, and purification of glycans compatible with microarray patterning. The advantages of glycophage-based arrays include the low cost and scalability of phage/glycan production, which are biosynthetic processes involving the cultivation of recombinant *Escherichia coli* cells, and the ease with which glycophages can be recovered from the bacterial supernatant without laborious purification steps. For these reasons, glycophage arrays will become a useful tool for identifying and profiling glycan-binding-proteins (GBPs), including mammalian lectins (C-type lectins, galectins, and siglecs), plant lectins, antibodies, viral and bacterial lectins, and intact viruses. Further improvement of the developed technology is intended for use in the clinical research and diagnosis.

REFERENCES

1. Dube, D.H. and C.R. Bertozzi, *Glycans in cancer and inflammation. Potential for therapeutics and diagnostics.* Nature Reviews Drug Discovery, 4(6): p. 477-488, **2005**.
2. Kobata, A. and J. Amano, *Altered glycosylation of proteins produced by malignant cells, and application for the diagnosis and immunotherapyof tumours.* Immunology and Cell Biology, 83(4): p. 429-439, **2005**.
3. Li, M., L.J. Song, and X.Y. Qin, *Glycan changes: cancer metastasis and anti-cancer vaccines.* Journal of Biosciences, 35(4): p. 665-673, **2010**.
4. Lawson, V.A., S.J. Collins, C.L. Masters, and A.F. Hill, *Prion protein glycosylation.* Journal of Neurochemistry, 93(4): p. 793-801, **2005**.
5. Russelakis-Carneiro, M., G.P. Saborio, L. Anderes, and C. Soto, *Changes in the glycosylation pattern of prion protein in murine scrapie - Implications for the mechanism of neurodegeneration in prion diseases.* Journal of Biological Chemistry, 277(39): p. 36872-36877, **2002**.
6. Dunfee, R.L., E.R. Thomas, J.B. Wang, K. Kunstman, S.M. Wolinsky, and D. Gabuzda, *Loss of the N-linked glycosylation site at position 386 in the HIV envelope V4 region enhances macrophage tropism and is associated with dementia.* Virology, 367(1): p. 222-234, **2007**.
7. Kemal, K.S., B. Foley, H. Burger, K. Anastos, H. Minkoff, C. Kitchen, S.M. Philpott, W. Gao, E. Robison, S. Holman, C. Dehner, S. Beck, W.A. Meyer, A. Landay, A. Kovacs, J. Bremer, and B. Weiser, *HIV-1 in genital tract and plasma of women: Compartmentalization of viral sequences, coreceptor usage, and glycosylation.* Proceedings of the National Academy of Sciences of the United States of America, 100(22): p. 12972-12977, **2003**.
8. Nihlen, U., P. Montnemery, L.H. Lindholm, and C.G. Lofdahl, *Increased serum levels of carbohydrate-deficient transferrin in patients with chronic obstructive pulmonary disease.* Scandinavian Journal of Clinical & Laboratory Investigation, 61(5): p. 341-347, **2001**.
9. Freeze, H.H. and M. Aebi, *Altered glycan structures: the molecular basis of congenital disorders of glycosylation.* Current Opinion in Structural Biology, 15(5): p. 490-498, **2005**.
10. Wurm, D., G. Loffler, A. Lindinger, and L. Gortner, *Congenital disorders of glycosylation type Ia as a cause of mirror syndrome.* Journal of Perinatology, 27(12): p. 802-804, **2007**.
11. Wang, D.N., S.Y. Liu, B.J. Trummer, C. Deng, and A.L. Wang, *Carbohydrate microarrays for the recognition of cross-reactive molecular markers of microbes and host cells.* Nature Biotechnology, 20(3): p. 275-281, **2002**.
12. Oyelaran, O. and J.C. Gildersleeve, *Glycan arrays: recent advances and future challenges.* Current Opinion in Chemical Biology, 13(4): p. 406-413, **2009**.

13. Adams, E.W., D.M. Ratner, H.R. Bokesch, J.B. McMahon, B.R. O'Keefe, and P.H. Seeberger, *Oligosaccharide and glycoprotein Microarrays as tools in HIV glycobiology: Glycan-dependent gp120/protein interactions.* Chemistry & Biology, 11(6): p. 875-881, **2004**.

14. Oyelaran, O. and J.C. Gildersleeve, *Application of carbohydrate array technology to antigen discovery and vaccine development.* Expert Review of Vaccines, 6(6): p. 957-969, **2007**.

15. Wang, D.N., G.T. Carroll, N.J. Turro, J.T. Koberstein, P. Kovac, R. Saksena, R. Adamo, L.A. Herzenberg, L.A. Herzenberg, and L. Steinman, *Photogenerated glycan arrays identify immunogenic sugar moieties of Bacillus anthracis exosporium.* Proteomics, 7(2): p. 180-184, **2007**.

16. Szymanski, C.M., R.J. Yao, C.P. Ewing, T.J. Trust, and P. Guerry, *Evidence for a system of general protein glycosylation in Campylobacter jejuni.* Molecular Microbiology, 32(5): p. 1022-1030, **1999**.

17. Wacker, M., D. Linton, P.G. Hitchen, M. Nita-Lazar, S.M. Haslam, S.J. North, M. Panico, H.R. Morris, A. Dell, B.W. Wren, and M. Aebi, *N-linked glycosylation in Campylobacter jejuni and its functional transfer into E-coli.* Science, 298(5599): p. 1790-1793, **2002**.

18. Feldman, M.F., M. Wacker, M. Hernandez, P.G. Hitchen, C.L. Marolda, M. Kowarik, H.R. Morris, A. Dell, M.A. Valvano, and M. Aebi, *Engineering N-linked protein glycosylation with diverse O antigen lipopolysaccharide structures in Escherichia coli.* Proceedings of the National Academy of Sciences of the United States of America, 102(8): p. 3016-3021, **2005**.

19. Celik, E., A.C. Fisher, C. Guarino, T.J. Mansell, and M.P. DeLisa, *A filamentous phage display system for N-linked glycoproteins.* Protein Science, 19(10): p. 2006-2013, **2010**.

20. Apweiler, R., H. Hermjakob, and N. Sharon, *On the frequency of protein glycosylation, as deduced from analysis of the SWISS-PROT database.* Biochimica Et Biophysica Acta-General Subjects, 1473(1): p. 4-8, **1999**.

21. Zielinska, D.F., F. Gnad, K. Schropp, J.R. Wisniewski, and M. Mann, *Mapping N-Glycosylation Sites across Seven Evolutionarily Distant Species Reveals a Divergent Substrate Proteome Despite a Common Core Machinery.* Molecular Cell, 46(4): p. 542-548, **2012**.

22. Sethuraman, N. and T.A. Stadheim, *Challenges in therapeutic glycoprotein production.* Current Opinion in Biotechnology, 17(4): p. 341-346, **2006**.

23. Baker, J.L., E. Celik, and M.P. DeLisa, *Expanding the glycoengineering toolbox: the rise of bacterial N-linked protein glycosylation.* Trends in Biotechnology, 31(5): p. 49-59, **2013**.

24. Agard, N.J. and C.R. Bertozzi, *Chemical Approaches To Perturb, Profile, and Perceive Glycans.* Accounts of Chemical Research, 42(6): p. 788-797, **2009**.

25. Friedman, B.A., K. Vaddi, C. Preston, E. Mahon, J.R. Cataldo, and J.M. McPherson, *A comparison of the pharmacological properties of carbohydrate remodeled recombinant and placental-derived beta-*

glucocerebrosidase: Implications for clinical efficacy in treatment of Gaucher disease. Blood, 93(9): p. 2807-2816, **1999**.

26. Rothman, R.J., B. Perussia, D. Herlyn, and L. Warren, *ANTIBODY-DEPENDENT CYTOTOXICITY MEDIATED BY NATURAL-KILLER-CELLS IS ENHANCED BY CASTANOSPERMINE-INDUCED ALTERATIONS OF IGG GLYCOSYLATION.* Molecular Immunology, 26(12): p. 1113-1123, **1989**.

27. LaTemple, D.C., J.T. Abrams, S.Y. Zhang, and U. Galili, *Increased immunogenicity of tumor vaccines complexed with anti-Gal: Studies in knockout mice for alpha 1,3galactosyltransferase.* Cancer Research, 59(14): p. 3417-3423, **1999**.

28. Glover, K.J., E. Weerapana, M.M. Chen, and B. Imperiali, *Direct biochemical evidence for the utilization of UDP-bacillosamine by PglC, an essential glycosyl-1-phosphate transferase in the Campylobacter jejuni N-linked glycosylation pathway.* Biochemistry, 45(16): p. 5343-5350, **2006**.

29. Glover, K.J., E. Weerapana, and B. Imperiali, *In vitro assembly of the undecaprenylpyrophosphate-linked, heptasaccharide for prokaryotic N-linked glycosylation.* Proceedings of the National Academy of Sciences of the United States of America, 102(40): p. 14255-14259, **2005**.

30. Linton, D., N. Dorrell, P.G. Hitchen, S. Amber, A.V. Karlyshev, H.R. Morris, A. Dell, M.A. Valvano, M. Aebi, and B.W. Wren, *Functional analysis of the Campylobacter jejuni N-linked protein glycosylation pathway.* Molecular Microbiology, 55(6): p. 1695-1703, **2005**.

31. Olivier, N.B., M.M. Chen, J.R. Behr, and B. Imperiali, *In vitro biosynthesis of UDP-N,N '-diacetylbacillosamine by enzymes of the Campylobacter jejuni general protein glycosylation system.* Biochemistry, 45(45): p. 13659-13669, **2006**.

32. Jervis, A.J., J.A. Butler, A.J. Lawson, R. Langdon, B.W. Wren, and D. Linton, *Characterization of the Structurally Diverse N-Linked Glycans of Campylobacter Species.* Journal of Bacteriology, 194(9): p. 2355-2362, **2012**.

33. Nothaft, H. and C.M. Szymanski, *Protein glycosylation in bacteria: sweeter than ever.* Nature Reviews Microbiology, 8(11): p. 765-778, **2010**.

34. Young, N.M., J.R. Brisson, J. Kelly, D.C. Watson, L. Tessier, P.H. Lanthier, H.C. Jarrell, N. Cadotte, F.S. Michael, E. Aberg, and C.M. Szymanski, *Structure of the N-linked glycan present on multiple glycoproteins in the gram-negative bacterium, Campylobacter jejuni.* Journal of Biological Chemistry, 277(45): p. 42530-42539, **2002**.

35. Nothaft, H., X. Liu, D.J. McNally, J.J. Li, and C.M. Szymanski, *Study of free oligosaccharides derived from the bacterial N-glycosylation pathway.* Proceedings of the National Academy of Sciences of the United States of America, 106(35): p. 15019-15024, **2009**.

36. Alaimo, C., I. Catrein, L. Morf, C.L. Marolda, N. Callewaert, M.A. Valvano, M.F. Feldman, and M. Aebi, *Two distinct but interchangeable mechanisms*

for flipping of lipid-linked oligosaccharides. Embo Journal, 25(5): p. 967-976, **2006**.

37. Kelly, J., H. Jarrell, L. Millar, L. Tessier, L.M. Fiori, P.C. Lau, B. Allan, and C.M. Szymanski, *Biosynthesis of the N-linked glycan in Campylobacter jejuni and addition onto protein through Block transfer.* Journal of Bacteriology, 188(7): p. 2427-2434, **2006**.

38. Kowarik, M., N.M. Young, S. Numao, B.L. Schulz, I. Hug, N. Callewaert, D.C. Mills, D.C. Watson, M. Hernandez, J.F. Kelly, M. Wacker, and M. Aebi, *Definition of the bacterial N-glycosylation site consensus sequence.* Embo Journal, 25(9): p. 1957-1966, **2006**.

39. Fisher, A.C., C.H. Haitjema, C. Guarino, E. Celik, C.E. Endicott, C.A. Reading, J.H. Merritt, A.C. Ptak, S. Zhang, and M.P. DeLisa, *Production of Secretory and Extracellular N-Linked Glycoproteins in Escherichia coli.* Applied and Environmental Microbiology, 77(3): p. 871-881, **2011**.

40. Celik, E. and P. Calik, *Production of recombinant proteins by yeast cells.* Biotechnology Advances, 30(5): p. 1108-1118, **2012**.

41. Durr, C., H. Nothaft, C. Lizak, R. Glockshuber, and M. Aebi, *The Escherichia coli glycophage display system.* Glycobiology, 20(11): p. 1366-1372, **2010**.

42. H., N., *Outer membrane. In: Escherichia coli and Salmonella: cellular and molecular biology.*, in *Escherichia coli and Salmonella: cellular and molecular biology.* , C.I.R. Neidhardt F C, Ingraham J L, Lin E C C, Low K B Jr, Magasanik B, Reznikoff W S, Riley M, Schaechter M, Umbarger H E, Editor. American Society for Microbiology: Washington, D.C. p. 29–47, **1996**.

43. Whitfield, C. and M.A. Valvano, *BIOSYNTHESIS AND EXPRESSION OF CELL-SURFACE POLYSACCHARIDES IN GRAM-NEGATIVE BACTERIA.* Advances in Microbial Physiology, Vol 35, 35: p. 135-246, **1993**.

44. Caroff, M. and D. Karibian, *Structure of bacterial lipopolysaccharides.* Carbohydrate Research, 338(23): p. 2431-2447, **2003**.

45. Erridge, C., E. Bennett-Guerrero, and I.R. Poxton, *Structure and function of lipopolysaccharides.* Microbes and Infection, 4(8): p. 837-851, **2002**.

46. Moran, A.P., U. Zahringer, U. Seydel, D. Scholz, P. Stutz, and E.T. Rietschel, *STRUCTURAL-ANALYSIS OF THE LIPID-A COMPONENT OF CAMPYLOBACTER-JEJUNI CCUG 10936 (SEROTYPE O-2) LIPOPOLYSACCHARIDE - DESCRIPTION OF A LIPID-A CONTAINING A HYBRID BACKBONE OF 2-AMINO-2-DEOXY-D-GLUCOSE AND 2,3-DIAMINO-2,3-DIDEOXY-D-GLUCOSE.* European Journal of Biochemistry, 198(2): p. 459-469, **1991**.

47. Jannson, T., D.H. Kim, A. Kostrzewski, and I. Ternovskiy, *Soft computing and soft communications for synchronized data*, in *Applications and Science of Neural Networks, Fuzzy Systems, and Evolutionary Computation Ii*, B. Bosacchi, D.B. Fogel, and J.C. Bezdek, Editors. Spie-Int Soc Optical Engineering: Bellingham. p. 55-68, **1999**.

48. Palva, E.T. and P.H. Makela, *LIPOPOLYSACCHARIDE HETEROGENEITY IN SALMONELLA-TYPHIMURIUM ANALYZED BY SODIUM DODECYL SULFATE-POLYACRYLAMIDE GEL-ELECTROPHORESIS.* European Journal of Biochemistry, 107(1): p. 137-143, **1980**.

49. Aoki-Kinoshita, K.F., *An introduction to bioinformatics for glycomics research.* Plos Computational Biology, 4(5), **2008**.

50. Srivastava, S., *Move over proteomics, here comes glycomics.* Journal of Proteome Research, 7(5): p. 1799-1799, **2008**.

51. Campbell, M.P., L. Royle, C.M. Radcliffe, R.A. Dwek, and P.M. Rudd, *GlycoBase and autoGU: tools for HPLC-based glycan analysis.* Bioinformatics, 24(9): p. 1214-1216, **2008**.

52. Haslam, S.M., S.J. North, and A. Dell, *Mass spectrometric analysis of N- and O-glycosylation of tissues and cells.* Current Opinion in Structural Biology, 16(5): p. 584-591, **2006**.

53. Petrescu, A.J., T.D. Butters, G. Reinkensmeier, S. Petrescu, F.M. Platt, R.A. Dwek, and M.R. Wormald, *The solution NMR structure of glucosylated N-glycans involved in the early stages of glycoprotein biosynthesis and folding.* Embo Journal, 16(14): p. 4302-4310, **1997**.

54. Liu, Y., A.S. Palma, and T. Feizi, *Carbohydrate microarrays: key developments in glycobiology.* Biological Chemistry, 390(7): p. 647-656, **2009**.

55. Cook, G.M.W., *CELL-SURFACE CARBOHYDRATES - MOLECULES IN SEARCH OF A FUNCTION.* Journal of Cell Science: p. 45-70, **1986**.

56. Sears, P. and C.H. Wong, *Toward automated synthesis of oligosaccharides and glycoproteins.* Science, 291(5512): p. 2344-2350, **2001**.

57. de Paz, J. and P. Seeberger, *Recent Advances and Future Challenges in Glycan Microarray Technology*, in *Carbohydrate Microarrays*, Y. Chevolot, Editor. Humana Press. p. 1-12, **2012**.

58. Laurent, N., J. Voglmeir, and S.L. Flitsch, *Glycoarrays--tools for determining protein-carbohydrate interactions and glycoenzyme specificity.* Chem Commun (Camb), (37): p. 4400-12, **2008**.

59. Wang, D., *Carbohydrate Antigen Microarrays*, in *Carbohydrate Microarrays*, Y. Chevolot, Editor. Humana Press. p. 241-249, **2012**.

60. Ekins, R., F. Chu, and E. Biggart, *MULTISPOT, MULTIANALYTE, IMMUNOASSAY.* Annales De Biologie Clinique, 48(9): p. 655-666, **1990**.

61. Tang, P.W., H.C. Gool, M. Hardy, Y.C. Lee, and T. Feizl, *NOVEL-APPROACH TO THE STUDY OF THE ANTIGENICITIES AND RECEPTOR FUNCTIONS OF CARBOHYDRATE CHAINS OF GLYCOPROTEINS.* Biochemical and Biophysical Research Communications, 132(2): p. 474-480, **1985**.

62. Liang, R., L. Yan, J. Loebach, M. Ge, Y. Uozumi, K. Sekanina, N. Horan, J. Gildersleeve, C. Thompson, A. Smith, K. Biswas, W.C. Still, and D.

Kahne, *Parallel synthesis and screening of a solid phase carbohydrate library.* Science, 274(5292): p. 1520-1522, **1996**.

63. Roy, R., *Syntheses and some applications of chemically defined multivalent glycoconjugates.* Current Opinion in Structural Biology, 6(5): p. 692-702, **1996**.

64. Diskin, S., Z.Y. Cao, H. Leffler, and N. Panjwani, *The role of integrin glycosylation in galectin-8-mediated trabecular meshwork cell adhesion and spreading.* Glycobiology, 19(1): p. 29-37, **2009**.

65. Krarup, A., D.A. Mitchell, and R.B. Sim, *Recognition of acetylated oligosaccharides by human L-ficolin.* Immunology Letters, 118(2): p. 152-156, **2008**.

66. Zupancic, M.L., M. Frieman, D. Smith, R.A. Alvarez, R.D. Cummings, and B.P. Cormack, *Glycan microarray analysis of Candida glabrata adhesin ligand specificity.* Molecular Microbiology, 68(3): p. 547-559, **2008**.

67. Schallus, T., C. Jaeckh, K. Feher, A.S. Palma, Y. Liu, J.C. Simpson, M. Mackeen, G. Stier, T.J. Gibson, T. Feizi, T. Pieler, and C. Muhle-Goll, *Malectin: A novel carbohydrate-binding protein of the endoplasmic reticulum and a candidate player in the early steps of protein N-glycosylation.* Molecular Biology of the Cell, 19(8): p. 3404-3414, **2008**.

68. Li, Q., M.R. Anver, D.O. Butcher, and J.C. Gildersleeve, *Resolving conflicting data on expression of the Tn antigen and implications for clinical trials with cancer vaccines.* Mol Cancer Ther, 8(4): p. 971-9, **2009**.

69. Manimala, J.C., Z. Li, A. Jain, S. VedBrat, and J.C. Gildersleeve, *Carbohydrate array analysis of anti-Tn antibodies and lectins reveals unexpected specificities: implications for diagnostic and vaccine development.* Chembiochem, 6(12): p. 2229-41, **2005**.

70. Manimala, J.C., T.A. Roach, Z.T. Li, and J.C. Gildersleeve, *High-throughput carbohydrate microarray profiling of 27 antibodies demonstrates widespread specificity problems.* Glycobiology, 17(8): p. 17C-23C, **2007**.

71. Kamena, F., M. Tamborrini, X. Liu, Y.U. Kwon, F. Thompson, G. Pluschke, and P.H. Seeberger, *Synthetic GPI array to study antitoxic malaria response.* Nat Chem Biol, 4(4): p. 238-40, **2008**.

72. Parthasarathy, N., D. DeShazer, S.J. Peacock, V. Wuthiekanun, M.J. England, S.L. Norris, and D.M. Waag, *Application of polysaccharide microarray technology for the serodiagnosis of Burkholderia pseudomallei infection (melioidosis) in humans.* Journal of Carbohydrate Chemistry, 27(1): p. 32-40, **2008**.

73. Parthasarathy, N., R. Saksena, P. Kovac, D. DeShazer, S.J. Peacock, V. Wuthiekanun, H.S. Heine, A.M. Friedlander, C.K. Cote, S.L. Welkos, J.J. Adamovicz, S. Bavari, and D.M. Waag, *Application of carbohydrate microarray technology for the detection of Burkholderia pseudomallei, Bacillus anthracis and Francisella tularensis antibodies.* Carbohydrate Research, 343(16): p. 2783-2788, **2008**.

74. Blixt, O., J. Hoffmann, S. Svenson, and T. Norberg, *Pathogen specific carbohydrate antigen microarrays: a chip for detection of Salmonella O-antigen specific antibodies.* Glycoconjugate Journal, 25(1): p. 27-36, **2008**.

75. de Boer, A.R., C.H. Hokke, A.M. Deelder, and M. Wuhrer, *Serum antibody screening by surface plasmon resonance using a natural glycan microarray.* Glycoconjugate Journal, 25(1): p. 75-84, **2008**.

76. Wang, C.C., Y.L. Huang, C.T. Ren, C.W. Lin, J.T. Hung, J.C. Yu, A.L. Yu, C.Y. Wu, and C.H. Wong, *Glycan microarray of Globo H and related structures for quantitative analysis of breast cancer.* Proceedings of the National Academy of Sciences of the United States of America, 105(33): p. 11661-11666, **2008**.

77. Luppa, P.B., L.J. Sokoll, and D.W. Chan, *Immunosensors - principles and applications to clinical chemistry.* Clinica Chimica Acta, 314(1-2): p. 1-26, **2001**.

78. Zeng, X.Q., C.A.S. Andrade, M.D.L. Oliveira, and X.L. Sun, *Carbohydrate-protein interactions and their biosensing applications.* Analytical and Bioanalytical Chemistry, 402(10): p. 3161-3176, **2012**.

79. Kehoe, J.W. and B.K. Kay, *Filamentous phage display in the new millennium.* Chemical Reviews, 105(11): p. 4056-4072, **2005**.

80. Malys, N., D.Y. Chang, R.G. Baumann, D.M. Xie, and L.W. Black, *A bipartite bacteriophage T4 SOC and HOC randomized peptide display library: Detection and analysis of phage T4 terminase (gp17) and late sigma factor (gp55) interaction.* Journal of Molecular Biology, 319(2): p. 289-304, **2002**.

81. Smith, G.P., *FILAMENTOUS FUSION PHAGE - NOVEL EXPRESSION VECTORS THAT DISPLAY CLONED ANTIGENS ON THE VIRION SURFACE.* Science, 228(4705): p. 1315-1317, **1985**.

82. Hofschneider, P.H., *UNTERSUCHUNGEN UBER KLEINE E COLI K 12 BAKTERIOPHAGEN 1 UND 2 MITTEILUNG.* Zeitschrift Fur Naturforschung Part B-Chemie Biochemie Biophysik Biologie Und Verwandten Gebiete, B 18(3): p. 203-&, **1963**.

83. Loeb, T., *ISOLATION OF A BACTERIOPHAGE SPECIFIC FOR THE F+ AND HFR MATING TYPES OF ESCHERICHIA COLI K-12.* Science, 131(3404): p. 932-933, **1960**.

84. Messing, J., *CLONING IN M13-PHAGE OR HOW TO USE BIOLOGY AT ITS BEST.* Gene, 100: p. 3-12, **1991**.

85. Berkowitz, S.A. and L.A. Day, *TURBIDITY MEASUREMENTS IN AN ANALYTICAL ULTRA-CENTRIFUGE - DETERMINATIONS OF MASS PER LENGTH FOR FILAMENTOUS VIRUSES FD, XF, AND PF3.* Biochemistry, 19(12): p. 2696-2702, **1980**.

86. Marlovits, T.C., T. Kubori, A. Sukhan, D.R. Thomas, J.E. Galan, and V.M. Unger, *Structural insights into the assembly of the type III secretion needle complex.* Science, 306(5698): p. 1040-1042, **2004**.

87. Newman, J., H.L. Swinney, and L.A. Day, *Hydrodynamic Properties and Structure of Fd Virus.* Journal of Molecular Biology, 116(3): p. 593-603, **1977**.

88. Rakonjac, J., N.J. Bennett, J. Spagnuolo, D. Gagic, and M. Russel, *Filamentous Bacteriophage: Biology, Phage Display and Nanotechnology Applications.* Current Issues in Molecular Biology, 13(2): p. 51-75, **2011**.

89. Endemann, H. and P. Model, *LOCATION OF FILAMENTOUS PHAGE MINOR COAT PROTEINS IN PHAGE AND IN INFECTED-CELLS.* Journal of Molecular Biology, 250(4): p. 496-506, **1995**.

90. Grant, R.A., T.C. Lin, R.E. Webster, and W. Konigsberg, *Structure of filamentous bacteriophage: isolation, characterization, and localization of the minor coat proteins and orientation of the DNA.* Prog Clin Biol Res, 64: p. 413-28, **1981**.

91. Russel, M. and P. Model, *GENETIC-ANALYSIS OF THE FILAMENTOUS BACTERIOPHAGE PACKAGING SIGNAL AND OF THE PROTEINS THAT INTERACT WITH IT.* Journal of Virology, 63(8): p. 3284-3295, **1989**.

92. Gao, C.S., C.H. Lin, C.H.L. Lo, S. Mao, P. Wirsching, R.A. Lerner, and K.D. Janda, *Making chemistry selectable by linking it to infectivity.* Proceedings of the National Academy of Sciences of the United States of America, 94(22): p. 11777-11782, **1997**.

93. Gao, C.S., S.L. Mao, G. Kaufmann, P. Wirsching, R.A. Lerner, and K.D. Janda, *A method for the generation of combinatorial antibody libraries using pIX phage display.* Proceedings of the National Academy of Sciences of the United States of America, 99(20): p. 12612-12616, **2002**.

94. Huang, Y., C.Y. Chiang, S.K. Lee, Y. Gao, E.L. Hu, J. De Yoreo, and A.M. Belcher, *Programmable assembly of nanoarchitectures using genetically engineered viruses.* Nano Letters, 5(7): p. 1429-1434, **2005**.

95. Rakonjac, J., J.N. Feng, and P. Model, *Filamentous phage are released from the bacterial membrane by a two-step mechanism involving a short C-terminal fragment of pIII.* Journal of Molecular Biology, 289(5): p. 1253-1265, **1999**.

96. Rakonjac, J., G. Jovanovic, and P. Model, *Filamentous phage infection-mediated gene expression: construction and propagation of the gIII deletion mutant helper phage R408d3.* Gene, 198(1-2): p. 99-103, **1997**.

97. Boeke, J.D., P. Model, and N.D. Zinder, *EFFECTS OF BACTERIOPHAGE-F1 GENE-III PROTEIN ON THE HOST-CELL MEMBRANE.* Molecular & General Genetics, 186(2): p. 185-192, **1982**.

98. Holliger, P., L. Riechmann, and R.L. Williams, *Crystal structure of the two N-terminal domains of g3p from filamentous phage fd at 1.9 angstrom: Evidence for conformational lability.* Journal of Molecular Biology, 288(4): p. 649-657, **1999**.

99. Lubkowski, J., F. Hennecke, A. Pluckthun, and A. Wlodawer, *The structural basis of phage display elucidated by the crystal structure of the N-terminal domains of g3p.* Nature Structural Biology, 5(2): p. 140-147, **1998**.

100. Bennett, N.J. and J. Rakonjac, *Unlocking of the filamentous bacteriophage virion during infection is mediated by the C domain of pill.* Journal of Molecular Biology, 356(2): p. 266-273, **2006**.

101. Bennett, N.J., D. Gagic, A.J. Sutherland-Smith, and J. Rakonjac, *Characterization of a Dual-Function Domain That Mediates Membrane Insertion and Excision of Ff Filamentous Bacteriophage.* Journal of Molecular Biology, 411(5): p. 972-985, **2011**.

102. Tanaka, F. and C.F. Barbas, *Phage display selection of peptides possessing aldolase activity.* Chemical Communications, (8): p. 769-770, **2001**.

103. Berkowitz, S.A. and L.A. Day, *MASS, LENGTH, COMPOSITION AND STRUCTURE OF FILAMENTOUS BACTERIAL VIRUS FD.* Journal of Molecular Biology, 102(3): p. 531-547, **1976**.

104. Zenkin, N., T. Naryshkina, K. Kuznedelov, and K. Severinov, *The mechanism of DNA replication primer synthesis by RNA polymerase.* Nature, 439(7076): p. 617-620, **2006**.

105. Opalka, N., R. Beckmann, N. Boisset, M.N. Simon, M. Russel, and S.A. Darst, *Structure of the filamentous phage pIV multimer by cryo-electron microscopy.* Journal of Molecular Biology, 325(3): p. 461-470, **2003**.

106. Bass, S., R. Greene, and J.A. Wells, *HORMONE PHAGE - AN ENRICHMENT METHOD FOR VARIANT PROTEINS WITH ALTERED BINDING-PROPERTIES.* Proteins-Structure Function and Genetics, 8(4): p. 309-314, **1990**.

107. Breitling, F., S. Dubel, T. Seehaus, I. Klewinghaus, and M. Little, *A SURFACE EXPRESSION VECTOR FOR ANTIBODY SCREENING.* Gene, 104(2): p. 147-153, **1991**.

108. Marvin, D.A. and H. Hoffmannberling, *A FIBROUS DNA PHAGE (FD) AND A SPHERICAL RNA PHAGE (FR) SPECIFIC FOR MALE STRAINS OF E COLI .2. PHYSICAL CHARACTERISTICS.* Zeitschrift Fur Naturforschung Part B-Chemie Biochemie Biophysik Biologie Und Verwandten Gebiete, B 18(11): p. 884-&, **1963**.

109. Ran., D.D.-X.a.Z., *Application and Progress of Helper Phage in Phage Display[J].* Microbiology, 36(2): p. 0261-0266., **2009**.

110. Russel, M., S. Kidd, and M.R. Kelley, *AN IMPROVED FILAMENTOUS HELPER PHAGE FOR GENERATING SINGLE-STRANDED PLASMID DNA.* Gene, 45(3): p. 333-338, **1986**.

111. Vieira, J. and J. Messing, *PRODUCTION OF SINGLE-STRANDED PLASMID DNA.* Methods in Enzymology, 153: p. 3-11, **1987**.

112. Messing, J., B. Gronenborn, B. Mullerhill, and P.H. Hofschneider, *FILAMENTOUS COLIPHAGE M13 AS A CLONING VEHICLE - INSERTION OF A HINDII FRAGMENT OF LAC REGULATORY REGION IN M13 REPLICATIVE FORM INVITRO - (SINGLE-STRANDED-DNA PHAGE-BLUNT END LIGATION LACTOSE OPERON ALPHA-COMPLEMENTATION).* Proceedings of the National Academy of Sciences of the United States of America, 74(9): p. 3642-3646, **1977**.

113. Hyman, P., *Bacteriophages and Nanostructured Materials*, in *Advances in Applied Microbiology, Vol 78*, A.I. Laskin, S. Sariaslani, and G.M. Gadd, Editors. Elsevier Academic Press Inc: San Diego. p. 55-73, **2012**.

114. Gronwall, C. and S. Stahl, *Engineered affinity proteins-Generation and applications.* Journal of Biotechnology, 140(3-4): p. 254-269, **2009**.

115. Scott, J.K., S.F. Huang, B.P. Gangadhar, G.M. Samoriski, P. Clapp, R.A. Gross, R. Taussig, and A.V. Smrcka, *Evidence that a protein-protein interaction 'hot spot' on heterotrimeric G protein beta gamma subunits is used for recognition of a subclass of effectors.* Embo Journal, 20(4): p. 767-776, **2001**.

116. Seker, U.O.S. and H.V. Demir, *Material Binding Peptides for Nanotechnology.* Molecules, 16(2): p. 1426-1451, **2011**.

117. Fukuda, M.N., *Screening of Peptide-Displaying Phage Libraries to Identify Short Peptides Mimicking Carbohydrates*, in *Methods in Enzymology*, F. Minoru, Editor. Academic Press. p. 51-60, **2006**.

118. Oldenburg, K.R., D. Loganathan, I.J. Goldstein, P.G. Schultz, and M.A. Gallop, *PEPTIDE LIGANDS FOR A SUGAR-BINDING PROTEIN ISOLATED FROM A RANDOM PEPTIDE LIBRARY.* Proceedings of the National Academy of Sciences of the United States of America, 89(12): p. 5393-5397, **1992**.

119. Scott, J.K., D. Loganathan, R.B. Easley, X.F. Gong, and I.J. Goldstein, *A FAMILY OF CONCANAVALIN A-BINDING PEPTIDES FROM A HEXAPEPTIDE EPITOPE LIBRARY.* Proceedings of the National Academy of Sciences of the United States of America, 89(12): p. 5398-5402, **1992**.

120. Taki, T., D. Ishikawa, H. Hamasaki, and S. Handa, *Preparation of peptides which mimic glycosphingolipids by using phage peptide library and their modulation on beta-galactosidase activity.* Febs Letters, 418(1-2): p. 219-223, **1997**.

121. Kieber-Emmons, T., P. Luo, J.P. Qiu, T.Y. Chang, I.S. O, M. Blaszczyk-Thurin, and Z. Steplewski, *Vaccination with carbohydrate peptide mimotopes promotes anti-tumor responses.* Nature Biotechnology, 17(7): p. 660-665, **1999**.

122. Kozbor, D., *Cancer vaccine with mimotopes of tumor-associated carbohydrate antigens.* Immunologic Research, 46(1-3): p. 23-31, **2010**.

123. Monzavi-Karbassi, B., G. Cunto-Amesty, P. Luo, S. Shamloo, M. Blaszcyk-Thurin, and T. Kieber-Emmons, *Immunization with a carbohydrate mimicking peptide augments tumor-specific cellular responses.* International Immunology, 13(11): p. 1361-1371, **2001**.

124. Bua, A., V. Rosu, P. Molicotti, S.K. Das Gupta, N. Ahmed, S. Zanetti, and L.A. Sechi, *Phages specific for mycobacterial lipoarabinomannan help serodiagnosis of tuberculosis.* New Microbiologica, 32(3): p. 293-296, **2009**.

125. Gnanasekar, M., K.V.N. Rao, Y.X. He, P.K. Mishra, T.B. Nutman, P. Kaliraj, and K. Ramaswamy, *Novel phage display-based subtractive*

screening to identify vaccine candidates of Brugia malayi. Infection and Immunity, 72(8): p. 4707-4715, **2004**.

126. Hou, Y.C. and X.X. Gu, *Development of peptide mimotopes of lipooligosaccharide from nontypeable Haemophilus influenzae as vaccine candidates.* Journal of Immunology, 170(8): p. 4373-4379, **2003**.

127. Menendez, T., N.F. Santiago-Vispo, Y. Cruz-Leal, E. Coizeau, H. Garay, O. Reyes, Y. Batista, K. Cobas, T. Carmenate, G. Chinea, and G. Guillen, *Identification and characterization of phage-displayed peptide mimetics of Neisseria meningitidis serogroup B capsular polysaccharide.* International Journal of Medical Microbiology, 301(1): p. 16-25, **2011**.

128. Pincus, S.H., M.J. Smith, H.J. Jennings, J.B. Burritt, and P.M. Glee, *Peptides that mimic the group B streptococcal type III capsular polysaccharide antigen.* Journal of Immunology, 160(1): p. 293-298, **1998**.

129. Wu, Y., Q.B. Zhang, D. Sales, A.E. Bianco, and A. Craig, *Vaccination with peptide mimotopes produces antibodies recognizing bacterial capsular polysaccharides.* Vaccine, 28(39): p. 6425-6435, **2010**.

130. Kubota, T., T. Matsushita, R. Niwa, I. Kumagai, and K. Nakamura, *Novel Anti-Tn Single-Chain Fv-Fc Fusion Proteins Derived from Immunized Phage Library and Antibody Fc Domain.* Anticancer Research, 30(9): p. 3397-3405, **2010**.

131. Berdichevsky, Y., E. Ben-Zeev, R. Lamed, and I. Benhar, *Phage display of a cellulose binding domain from Clostridium thermocellum and its application as a tool for antibody engineering.* Journal of Immunological Methods, 228(1-2): p. 151-162, **1999**.

132. Haidaris, C.G., J. Malone, L.A. Sherill, J.M. Bliss, A.A. Gaspari, R.A. Insel, and M.A. Sullivan, *Recombinant human antibody single chain variable fragments reactive with Candida albicans surface antigens.* Journal of Immunological Methods, 257(1-2): p. 185-202, **2001**.

133. Goldman, E.R., M.P. Pazirandeh, J.M. Mauro, K.D. King, J.C. Frey, and G.P. Anderson, *Phage-displayed peptides as biosensor reagents.* Journal of Molecular Recognition, 13(6): p. 382-387, **2000**.

134. Stratmann, J., B. Strommenger, K. Stevenson, and G.F. Gerlach, *Development of a peptide-mediated capture PCR for detection of Mycobacterium avium subsp paratuberculosis in milk.* Journal of Clinical Microbiology, 40(11): p. 4244-4250, **2002**.

135. Knurr, J., O. Benedek, J. Heslop, R.B. Vinson, J.A. Boydston, J. McAndrew, J.F. Kearney, and C.L. Turnbough, *Peptide ligands that bind selectively to spores of Bacillus subtilis and closely related species.* Applied and Environmental Microbiology, 69(11): p. 6841-6847, **2003**.

136. Williams, D.D., O. Benedek, and C.L. Turnbough, *Species-specific peptide ligands for the detection of Bacillus anthracis spores.* Applied and Environmental Microbiology, 69(10): p. 6288-6293, **2003**.

137. Ide, T., S.H. Baik, T. Matsuba, and S. Harayama, *Identification by the phage-display technique of peptides that bind to H7 flagellin of Escherichia*

coli. Bioscience Biotechnology and Biochemistry, 67(6): p. 1335-1341, **2003**.

138. Kim, Y.G., C.S. Lee, W.J. Chung, E. Kim, D.S. Shin, J.H. Rhim, Y.S. Lee, B.G. Kim, and J.H. Chung, *Screening of LPS-specific peptides from a phage display library using epoxy beads.* Biochemical and Biophysical Research Communications, 329(1): p. 312-317, **2005**.

139. Bishop-Hurley, S.L., F.J. Schmidt, A.L. Erwin, and A.L. Smith, *Peptides selected for binding to a virulent strain of Haemophilus influenzae by phage display are bactericidal.* Antimicrobial Agents and Chemotherapy, 49(7): p. 2972-2978, **2005**.

140. Gasanov, U., C. Koina, K.W. Beagley, R.J. Aitken, and P.M. Hansbro, *Identification of the insulin-like growth factor II receptor as a novel receptor for binding and invasion by Listeria monocytogenes.* Infection and Immunity, 74(1): p. 566-577, **2006**.

141. Olsen, E.V., I.B. Sorokulova, V.A. Petrenko, I.H. Chen, J.M. Barbaree, and V.J. Vodyanoy, *Affinity-selected filamentous bacteriophage as a probe for acoustic wave biodetectors of Salmonella typhimurium.* Biosensors & Bioelectronics, 21(8): p. 1434-1442, **2006**.

142. Balasubramanian, S., I.B. Sorokulova, V.J. Vodyanoy, and A.L. Simonian, *Lytic phage as a specific and selective probe for detection of Staphylococcus aureus - A surface plasmon resonance spectroscopic study.* Biosensors & Bioelectronics, 22(6): p. 948-955, **2007**.

143. Domaille, D.W., J.H. Lee, and J.N. Cha, *High density DNA loading on the M13 bacteriophage provides access to colorimetric and fluorescent protein microarray biosensors.* Chemical Communications, 49(17): p. 1759-1761, **2013**.

144. Legendre, D. and J. Fastrez, *Construction and exploitation in model experiments of functional selection of a landscape library expressed from a phagemid.* Gene, 290(1-2): p. 203-215, **2002**.

145. Mount, J.D., T.I. Samoylov, N.E. Morrison, N.R. Cox, H.J. Baker, and V.A. Petrenko, *Cell targeted phagernid rescued by preselected landscape phage.* Gene, 341: p. 59-65, **2004**.

146. Romanov, V.I., D.B. Durand, and V.A. Petrenko, *Phage display selection of peptides that affect prostate carcinoma cells attachment and invasion.* Prostate, 47(4): p. 239-251, **2001**.

147. Samoylova, T.I., V.A. Petrenko, N.E. Morrison, L.P. Globa, H.J. Baker, and N.R. Cox, *Phage probes for malignant glial cells.* Molecular Cancer Therapeutics, 2(11): p. 1129-1137, **2003**.

148. Petrenko, V.A. and V.J. Vodyanoy, *Phage display for detection of biological threat agents.* Journal of Microbiological Methods, 53(2): p. 253-262, **2003**.

149. Bunde, R.L., E.J. Jarvi, and J.J. Rosentreter, *Piezoelectric quartz crystal biosensors.* Talanta, 46(6): p. 1223-1236, **1998**.

150. Cavic, B.A., G.L. Hayward, and M. Thompson, *Acoustic waves and the study of biochemical macromolecules and cells at the sensor-liquid interface.* Analyst, 124(10): p. 1405-1420, **1999**.

151. Kaspar, M., H. Stadler, T. Weiss, and C. Ziegler, *Thickness shear mode resonators ("mass-sensitive devices") in bioanalysis.* Fresenius Journal of Analytical Chemistry, 366(6-7): p. 602-610, **2000**.

152. O'Sullivan, C.K. and G.G. Guilbault, *Commercial quartz crystal microbalances - theory and applications.* Biosensors & Bioelectronics, 14(8-9): p. 663-670, **1999**.

153. Olsen, E.V., S.T. Pathirana, A.M. Samoylov, J.M. Barbaree, B.A. Chin, W.C. Neely, and V. Vodyanoy, *Specific and selective biosensor for Salmonella and its detection in the environment.* Journal of Microbiological Methods, 53(2): p. 273-285, **2003**.

154. Pathirana, S.T., J. Barbaree, B.A. Chin, M.G. Hartell, W.C. Neely, and V. Vodyanoy, *Rapid and sensitive biosensor for Salmonella.* Biosensors & Bioelectronics, 15(3-4): p. 135-141, **2000**.

155. Samoylova, T.I., B.Y. Ahmed, V. Vodyanoy, N.E. Morrison, A.M. Samoylov, L.P. Globa, H.J. Baker, and N.R. Cox, *Targeting peptides for microglia identified via phage display.* Journal of Neuroimmunology, 127(1-2): p. 13-21, **2002**.

156. Cekaite, L., O. Haug, O. Myklebost, M. Aldrin, B. Ostenstad, M. Holden, A. Frigessi, E. Hovig, and M. Sioud, *Analysis of the humoral immune response to immunoselected phage-displayed peptides by a microarray-based method.* Proteomics, 4(9): p. 2572-2582, **2004**.

157. Cekaite, L., E. Hovig, and H.H. Hauge, *Double-sided silicon strip detectors: new applications within genomics and proteomics.* Nuclear Instruments & Methods in Physics Research Section a-Accelerators Spectrometers Detectors and Associated Equipment, 527(1-2): p. 68-72, **2004**.

158. Arnaud, M.C., T. Gazarian, Y.P. Rodriguez, K. Gazarian, and V. Sakanyan, *Array assessment of phage-displayed peptide mimics of Human Immunodeficiency Virus type 1 gp41 immunodominant epitope: Binding to antibodies of infected individuals.* Proteomics, 4(7): p. 1959-1964, **2004**.

159. Zhong, L., X.J. Peng, G.E. Hidalgo, D.E. Doherty, A.J. Stromberg, and E.A. Hirschowitz, *Antibodies to HSP70 and HSP90 in serum in non-small cell lung cancer patients.* Cancer Detection and Prevention, 27(4): p. 285-290, **2003**.

160. Bi, Q., X.D. Cen, W.J. Wang, X.S. Zhao, X. Wang, T. Shen, and S.G. Zhu, *A protein microarray prepared with phage-displayed antibody clones.* Biosensors & Bioelectronics, 22(12): p. 3278-3282, **2007**.

161. Solis, D.J., S.R. Coyer, A.J. Garcia, and E. Delamarche, *Large-Scale Arrays of Aligned Single Viruses.* Advanced Materials, 22(1): p. 111-+, **2010**.

162. Dultsev, F.N., R.E. Speight, M.T. Florini, J.M. Blackburn, C. Abell, V.P. Ostanin, and D. Klenerman, *Direct and quantitative detection of bacteriophage by "Hearing" surface detachment using a quartz crystal microbalance.* Analytical Chemistry, 73(16): p. 3935-3939, **2001**.

163. Dwyer, J.J., M.A. Dwyer, and A.A. Kossiakoff, *High affinity RNase S-peptide variants obtained by phage display have a novel "hot-spot" of binding energy.* Biochemistry, 40(45): p. 13491-13500, **2001**.

164. Finucane, M.D. and D.N. Woolfson, *Core-directed protein design. II. Rescue of a multiply mutated and destabilized variant of ubiquitin.* Biochemistry, 38(36): p. 11613-11623, **1999**.

165. Lang, S., J. Xu, F. Stuart, R.M. Thomas, J.W. Vrijbloed, and J.A. Robinson, *Analysis of antibody A6 binding to the extracellular interferon gamma receptor alpha-chain by alanine-scanning mutagenesis and random mutagenesis with phage display.* Biochemistry, 39(51): p. 15674-15685, **2000**.

166. Ploug, M., S. Ostergaard, H. Gardsvoll, K. Kovalski, C. Holst-Hansen, A. Holm, L. Ossowski, and K. Dano, *Peptide-derived antagonists of the urokinase receptor. Affinity maturation by combinatorial chemistry, identification of functional epitopes, and inhibitory effect on cancer cell intravasation.* Biochemistry, 40(40): p. 12157-12168, **2001**.

167. Roberge, M., L. Santell, M.S. Dennis, C. Eigenbrot, M.A. Dwyer, and R.A. Lazarus, *A novel exosite on coagulation Factor VIIa and its molecular interactions with a new class of peptide inhibitors.* Biochemistry, 40(32): p. 9522-9531, **2001**.

168. Weber-Bornhauser, S., J. Eggenberger, I. Jelesarov, A. Bernard, C. Berger, and H.R. Bosshard, *Thermodynamics and kinetics of the reaction of a single-chain antibody fragment (scFv) with the leucine zipper domain of transcription factor GCN4.* Biochemistry, 37(37): p. 13011-13020, **1998**.

169. Çelik, E., Ollis, A.A., Lasanajak,Y., Fisher, A.C., Gur, G., Smith D.F., DeLisa, M.P. , *Glycoarrays with engineered phages displaying structurally diverse oligosaccharides enable high-throughput detection of glycan-protein interactions.* Biotechnology Journal, **2015,** DOI: 10.1002/biot.201400354.

170. Russell, J.F.S.a.D.W., *Molecular Cloning: A Laboratory Manual*. 3rd ed, ed. J.F.S.a.D.W. Russell. Vol. 1-3. USA: Cold Spring Harbor. 2100 **2001**.

171. Guzman, L.M., D. Belin, M.J. Carson, and J. Beckwith, *Tight regulation, modulation, and high-level expression by vectors containing the arabinose PBAD promoter.* J Bacteriol, 177(14): p. 4121-30, **1995**.

172. Jansson, P.E., B. Lindberg, G. Widmalm, and K. Leontein, *Structural studies of the Escherichia coli O78 O-antigen polysaccharide.* Carbohydr Res, 165(1): p. 87-92, **1987**.

173. Raetz, C.R. and C. Whitfield, *Lipopolysaccharide endotoxins.* Annual Review of Biochemistry, 71: p. 635-700, **2002**.

174. Bratkovic, T., *Progress in phage display: evolution of the technique and its application.* Cell Mol Life Sci, 67(5): p. 749-67, **2010**.

175. Stengele, I., P. Bross, X. Garces, J. Giray, and I. Rasched, *Dissection of functional domains in phage fd adsorption protein: Discrimination between attachment and penetration sites.* Journal of Molecular Biology, 212(1): p. 143-149, **1990**.

176. Larocca, D., K. Jensen-Pergakes, M.A. Burg, and A. Baird, *Receptor-targeted gene delivery using multivalent phagemid particles.* Mol Ther, 3(4): p. 476-84, **2001**.

177. Lowman, H.B., S.H. Bass, N. Simpson, and J.A. Wells, *Selecting high-affinity binding proteins by monovalent phage display.* Biochemistry, 30(45): p. 10832-8, **1991**.

APPENDIX A

BUFFERS AND STOCK SOLUTIONS

0.125 M (or 0.5 M) EDTA, pH 8.0	4.65 g (or 18.61 g) Ethylenediaminetetra acetic acid disodium salt dihydrate was was dissolved in 80 mL dH_2O. NaOH was added until EDTA was dissolved. The final pH was further adjusted to pH 8.0 and the final volume was adjusted to 100 mL. The buffer was autoclaved and stored at room temperature.
10 x TBE	108 g Tris base and 55 g boric acid was dissolved in 800 mL dH_2O and 40 mL of 0.5 M EDTA (pH 8.0) was added and volume was made up to 1 L.
1 M Tris-Cl, pH 8.0	12.1 g Tris base was dissolved in 80 mL dH_2O and the pH was adjusted to 8.0 by adding concentrated HCl. The volume was made up to 100 mL. The buffer was autoclaved and stored at room temperature
TE Buffer, pH 8.0	1 mL of 1M Tris-Cl (pH 8.0), 200 µL of 0.5 M EDTA (pH 8.0) was added to dH_2O and the volume was made up to 100 mL. The buffer was autoclaved and stored at room temperature.
RNaseA stock solution	RNaseA was dissolved at a concentration of 10 mg/mL in 50 mM potassium acetate (pH 5.5) and boiled for 10 min. Stored at -20 ˚ C.
6 x DNA gel-loading buffer	0.25% Bromophenol blue, 0.25% xylenecyanol FF, 40 % sucrose in dH_2O. Stored at room temperature.
3 M Sodium acetate, pH 5.2	24.6 g sodium acetate was dissolved in 80 mL dH_2O and the pH was adjusted to 5.2 with 3M acetic acid. The buffer was filter sterilized and stored at 2-8°C.

1.5 M Tris-HCl, pH 8.8	36.3 g Tris base was dissolved in 150 mL dH_2O and pH was adjusted to 8.8 with 6N HCl. The buffer was made up to 200 mL with dH_2O. The buffer was autoclaved and stored at 2-8°C.
0.5 M Tris-HCl, pH 6.8	12.1 g Tris base was dissolved in 150 mL dH_2O and pH was adjusted to 6.8 with 6N HCl. The buffer was made up to 200 mL with dH_2O. The buffer was autoclaved and stored at 2-8°C.
4 x Sample Loading Buffer for SDS-PAGE	200 mM Tris-HCl, pH 6.8; 40% glycerol; 6% SDS; 0.013% Bromophenol blue; 10% 2-mercaptoethanol. Distributed into microcentrifuge tubes and stored at -20°C.
5x SDS-PAGE Running Buffer	15 g Tris Base, 72 g glycine, 5 g SDS, dH2O to 1 liter. The buffer was stored at 2-8°C and diluted 1:5 with dH_2O prior to use.
Coomassie Staining Solution	0.25 g Coomassie Brilliant Blue R250, 45 mL methanol, 10 mL Acetic acid was added to 45 mL dH_2O.
Destaining Solution	180 mL methanol and 40 mL acetic acid was added to 180 mL dH_2O. Stored at room temperature.
10X Transfer buffer stock solution for Western blot	30.3 g Tris base and 144.1 g glycine was dissolved in dH_2O and the volume was made upto 1 liter. The buffer was stored at 2-8°C.
1X Transfer buffer for Western blot	100 mL 10X transfer buffer stock, 200 mL methanol, dH_2O to 1 liter. Prepared on the day of use and stored at 2-8°C.

10X TBS	12.11 g Tris-base, 87.66 g NaCl dissolved in 900 mL dH_2O and pH adjusted to 7.6. Stored at room temperature.
TBS-T solution	0.1% Tween-20 was added into 1xTBS solution. Prepared on the day of use.
TBS-T – Milk	5 % non-fat milk powder in TBS-T. Prepared on the day of use.
10xPBS	32 g NaCl, 0.8 g KCl, 5.76 g Na_2HPO_4, 0.96 g KH_2PO_4 dissolved in 300 mL dH_2O and the volume was made up to 400 mL with dH_2O.
PEG/NaCl	60 g 20% PEG 8000, 43.8 g 2.5 M NaCl dissolved in 200 mL dH_2O and volume was made up to 300 mL with dH_2O
5xM9	33 g Disodium phosphate, 15 g Monosodium phosphate, 2.5 g NaCl, 5 g Ammonium chloride dissolved in 800 mL dH_2O and volume was made up to 1 L.
PCR master mix	40 µL $dNTP_{mix}$ (25 µL each), 125 µL Thermopol buffer, 50 µL $MgSO_4$ was added to 1000 µL dH_2O.

APPENDIX B

GROWTH MEDIA

LB (Luria-Bertani)

10 g/L NaCl

10 g/L Tryptone

5 g/L Yeast extract

After adjusting pH to 7.0 with NaOH, the final volume is adjusted with distilled water. 20 g/L agar is added if solid medium is required. The medium is autoclaved and stored at room temperature. In media referred to as LB+Kanamycin, Kanamycin was added after sterilization when the medium has cooled to about 55°C, at a final concentration of 50 µg/mL from 50 mg/mL stock.

SOC

20 g/L Bacto-tryptone

5 g/L Yeast extract

0.5 g/L NaCl

0.19 g/L KCl

0.02 M Glucose

The pH was adjusted to 7.0 with 10N NaOH and the final volume adjusted with dH_20. 1M Glucose solution was autoclaved separately and added after sterilization. The medium was aliquoted into microcentrifuge tubes aseptically and stored at room temperature.

2 TY

16 g/L Tryp

10 g/L YE

5 g/L NaCl

M9 Minimal Medium

5xM9 salt solution (10 mL)

$MgSO_4$, 1M (100 µL)

$CaCl_2$, 1M (5 µL)

20% Glucose (1000 µL)

Thiamine, 50 mg/mL (50 µL)

Antibiotics as needed

YENB

7.5 g/L YE

8 g/L Nutrient Broth

Agar Solution

10 g/L agar

APPENDIX C

BACKBONE PLASMID MAP

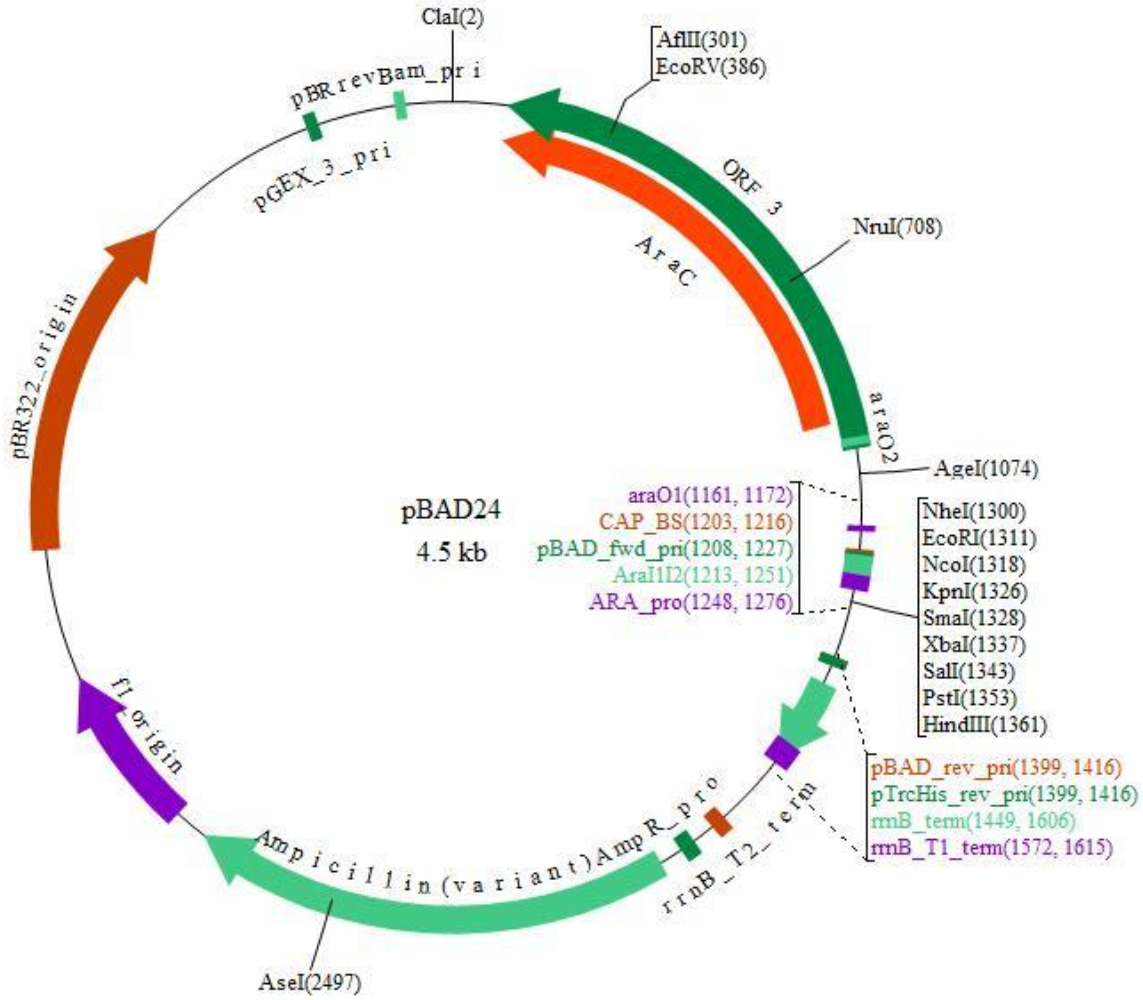

Figure C1. Plasmid map of pBAD24 [171]

APPENDIX D

MOLECULAR WEIGHT MARKERS

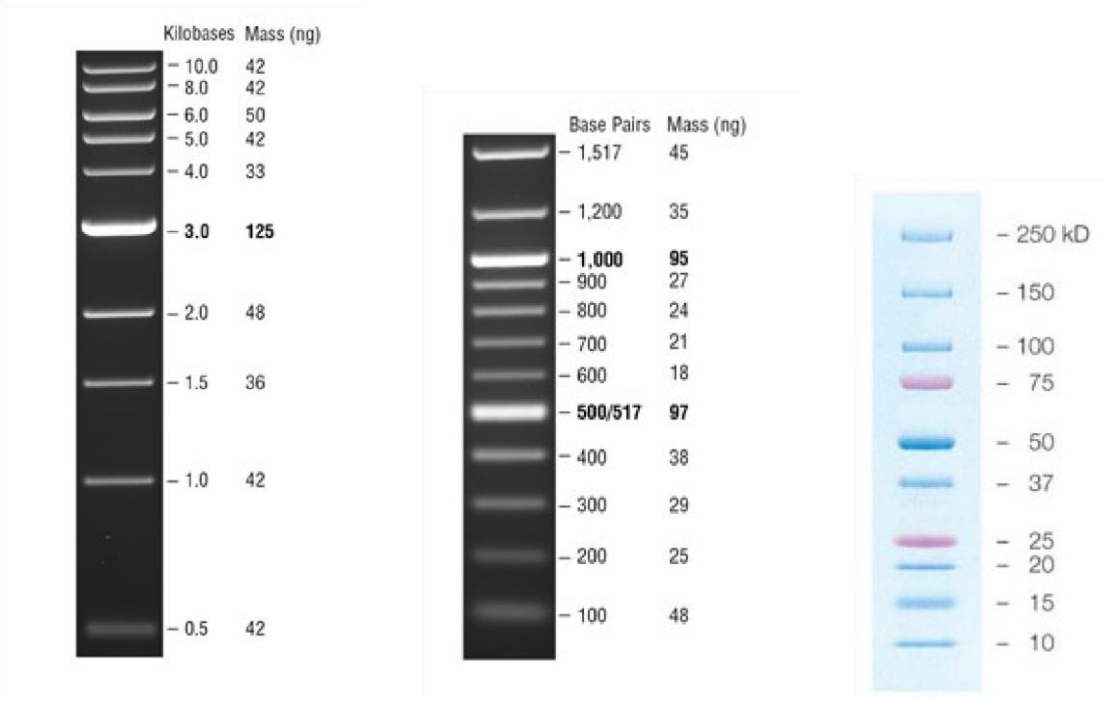

(a) (b) (c)

Figure D1. (a) 1 kb DNA Ladder, NEB **(b)** 100 bp DNA ladder, NEB **(c)** Precision Plus Protein™ Standards, BioRad.

APPENDIX E

PROPERTIES OF DESIGNED PRIMERS

Table E.1. Properties of the designed primers.

Name of Primer	Length (bp)	Gc (%)	T_m (°C)
MBPss-for-EcoRI	33	39.4 %	60.3 ºC
G3P-XmaI-Rev	42	42.9 %	64.2 ºC
XmaIRBSPglB	57	36.8 %	65.7 ºC
PglB-stop-SphI-R1	54	33.3%	64.0 ºC
PglB-stop-30bp-SphI-R2	60	48.3 %	70.3 ºC
MBP-GT-4x-Rev1	60	56.7 %	73.0 ºC
MBP-GT-4x-SalI-R2	69	56.5 %	73.9 ºC
trG3P-XhoI-For	63	63.5 %	75.3 ºC

The self-complimentary and dimer formation affinities of a representative primer is given below:

MBPss-for-EcoRI

Delta G -12.42 kcal/mole

Base Pairs 8

```
5'            CACCGAATTCATGAAAATAAAAACAGGTGCACG
                       ||||||||
3' GCACGTGGACAAAAATAAAAGTACTTAAGCCAC
```

APPENDIX F

CALIBRATION OF PROTEIN CONCENTRATION

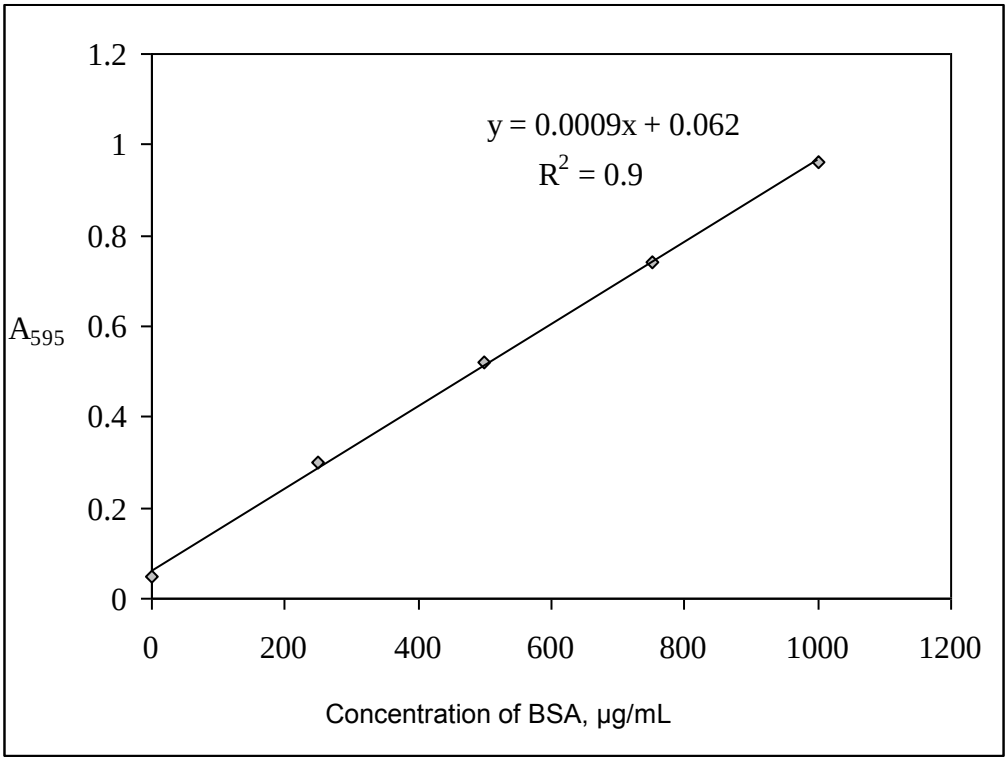

Figure F.1. Standard curve for Bradford Assay

$$Cp = \frac{A_{595} - 0.062}{9x10^{-4}} \text{ x Dilution Factor}$$

APPENDIX G

SDS-PAGE AND WESTERN BLOTTING PROTOCOLS

Gel electrophoresis

1. Add sample loading buffer to the samples (1:3) and heat at 95° C for 4 min, store on ice for 5 min, centrifuge and vortex.

2. Remove the comb slowly and clean the gel removing any excess with razor blade.

3. Wash the wells 3 times with tap water and distilled water, shaking out excess water in btw washes and soak paper towel to dry.

4. Assemble the gels onto the electrophoresis unit.

5. Fill the apparatus with 1x SDS-PAGE runnig buffer. Do not wet the electrodes. The space between the gels and the apparatus should be filled to the top, as well as the bottom of the apparatus to the point where the bottom of the gel is covered.

6. Load the samples and the prestained protein ladder into the wells with Pasteur pipette quickly and load the loading buffer into the unused wells as well, so that these lanes still visibly run. Make a note of each well and make individual gels identifiable from each other.

7. Close the lid by attaching the correct red/black power leads.

8. Run the gels at 20 mA for 1 mm gels and 25 mA for 1.5mm gels. This value needs to be multiplied by the number of gelds being run at the same time.

Blotting

1) Cut off stacking gel and nick top left-hand corner of resolving gel for orientation.

2) Transfer gel, while still attached to glass plate, into glass tray filled with at least 3 cm of 1x transfer buffer and peel off gently with a wet spatula, and keep for 15-20 min at RT to remove salts and SDS.

3) Cut membrane and 2 blotting papers to size, and cut one corner

4) Pre-wet PVDF or other hydrophobic membranes with methanol and transfer to the tray to equilibrate in transfer buffer for at least 10 min before blotting.

5) Put 2 sponges and 2 blotting papers into the tray to wet.

6) Open the cassette by releasing both latch tabs along the edge opposite the hinges. Place the opened cassette into the tray filled with transfer buffer and assemble the transfer stack so that the molecules will migrate toward the membrane. Make sure there are no bubbles in btw the gel and the membrane.

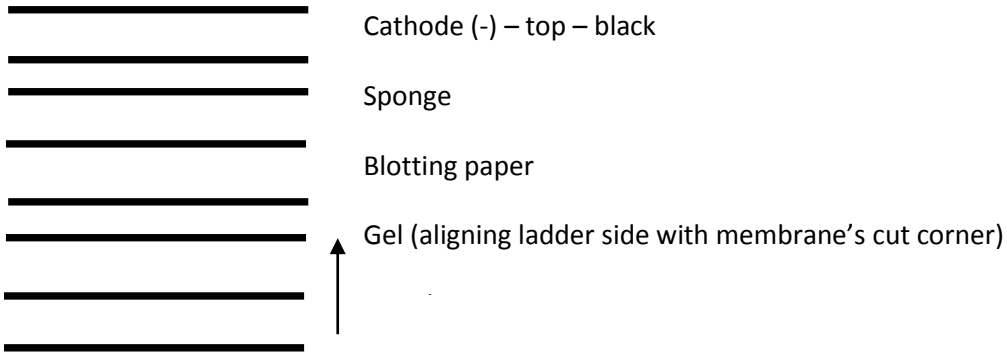

7) Close the cassette and press lightly to lock the tabs.

8) The cassette must be oriented so that the hinges face up so the black side of each cassette faces the black cathode panel.

9) Throw a magnetic stirrer inside. Inspect the buffer level, should be btw min-max lines.

10) Close the lid, turn on the stirrer and run the gel in cold room, at 50 V for 3 h, regardless of the number of gels.

Blocking, Antibody Incubation and Detection Using ECL Western Blotting Kit

1) Remove the membrane from cassette, put in a box, protein side facing up. Wash the membrane 2-3 times with TBS-T. Tween prevents non-specific binding of the Ab and optimizes the hybridization conditions.

2) Immerse the membrane in TBS-T-Milk for 1 hr, RT, shaking.

3) Wash 3 times (shaking 15 min, 5min, 5 min with fresh changes) with large volumes of TBS-T, at RT.

4) Transfer the membrane to a lid of 96-well microtiter plate or similar low volume container.

5) Dilute the primary antibody in TBS-T as 1:1 000

6) Incubate the membrane in the diluted primary Ab for o/n at 4 ˚C, on shaker platform.

7) Transfer the membrane into gel box and wash as in step 3.

8) Dilute the secondary antibody in TBS-T as 1:10 000

(Dilution factor should be determined empirically for each Ab as 1:1 000 - 1:10 000; more dilution will improve the linearity and increase the sensitivity).

9) Transfer the membrane back to the small container and incubate the membrane in the diluted secondary Ab for 1 hr at RT, on shaker platform.

10) Transfer the membrane into gel box and wash 3 times (10 min/wash) with fresh changes of large volumes of TBS-T buffer, at RT.

11) Mix the substrate components to prepare the chemiluminescent or immunocytochemical stain working solution. The final required volume is 0.125 mL/cm^2.

12) Place the membrane protein side-up on clear plastic wrap. Pipette the working substrate solution onto the membrane and wait for 5 min at room temperature.

15) Transfer the membrane to a new plastic wrap, protein side down. Wrap the membrane and take the picture.

CURRICULUM VITAE

Credentials

Name, Surname : Göksu Gür
Place of Birth : 25 April 1989, Ankara
Marital Status : Single
Email : goksugur89@gmail.com
Adress : Cayyolu, Park Cad., Atabilge Sitesi, 38/20, ANKARA

Education

High School : Ankara Atatürk Anadolu Lisesi (2003-2007)
BSc. : Ankara University Biology (2007-2012)
MSc. : Hacettepe University Bioengineering (2012-2014)
PhD. :

Foreign Languages

Advanced English.

Work Experience

Areas of Experience

- Visiting Researcher at Cornell University, School of Chemical and Biomoleculer Engineering (July-September, 2013).
- Visiting Researcher at Middle East Technical University, Department of Chemical Engineering, Industrial Engineering and Genetic Engineering Laboratory (January-March 2013; November 2014).
- Microbiology Laboratory, Biochemistry Laboratory, Animal Histology Laboratory, Cytology Laboratory, Microtechniques Laboratory, Plant Morphology Laboratory class experiments in Ankara University (2008-2012)

Projects and Budgets

- “Development of GlycoPhage Arrays as a novel high-throughput method for glycomics”, FP7-PEOPLE-2012-CIG, 1.10.2012-1.10.2016. (Scholar), Budget: 100 000 Euro.
- "GlikoFaj nanopartiküllerinin sentezini etkileyen parametrelerin incelenmesi”, (Project number: 014 D01 602 006), Hacettepe University Scientific Research Projects Coordination Unit, 13.3.2014– 15.9.2014, (Assistant researcher), Budget: 18 800 TL.

Publications

- Çelik, E., Ollis, A. A., Lasanajak, Y., Fisher, A. C., Gür, G., Smith, D. F. and DeLisa, M. P. (2015), Glycoarrays with engineered phages displaying structurally diverse oligosaccharides enable high-throughput detection of glycan–protein interactions. Biotechnology Journal. DOI: 10.1002/biot.201400354

Oral and Poster Prentation

- Çelik E., Gür G., DeLisa M.P. Engineering glycophages towards glycan microarrays. ESBES-IFIBiop-2014, Lille, France, poster presentation, 7-10/09/2014.